

The Significance of Defects in CFRP Bonded Honeycomb Structures  
and Non-Destructive Test Methods for Their Destruction

R. L Crocker, et al

Fulmer Research Institute  
Stoke Poges, England

May 1978

**DISTRIBUTION STATEMENT A**

Approved for public release;  
Distribution Unlimited

DEPARTMENT OF DEFENSE  
PLASTICS TECHNICAL EVALUATION CENTER  
ARRADCOM, DOVER, N. J. 07801

19960319 057

U.S. DEPARTMENT OF COMMERCE  
National Technical Information Service

**NTIS**

DTIC QUALITY INSPECTED 1

37541

A REPORT PREPARED BY  
FULMER RESEARCH INSTITUTE  
HOLLYBUSH HILL  
STOKE POGES, BUCKS.

N80-17158

Unclass  
93209

H2/24

(FRI-R736/4) THE SIGNIFICANCE OF DEFECTS IN  
CRFP BONDED HONEYCOMB STRUCTURES AND  
NON-DESTRUCTIVE TEST METHODS FOR THEIR  
DETECTION Final Report (Fulmer Research  
Inst. Ltd.) 114 p HC A06/MF A01

for

EUROPEAN SPACE AGENCY

Under Contract No. 2922/76/NL/PP(SC)

entitled

THE SIGNIFICANCE OF DEFECTS IN CFRP BONDED  
HONEYCOMB STRUCTURES AND NON-DESTRUCTIVE TEST

METHODS FOR THEIR DETECTION

by

R.L. Crocker\* and W.H. Bowyer\*

R736/4/May, 1978

REPRODUCED BY  
NATIONAL TECHNICAL  
INFORMATION SERVICE  
U.S. DEPARTMENT OF COMMERCE  
SPRINGFIELD, VA. 22161

European Space Agency

The work described in this report was done  
under E.S.A. contract. The responsibility  
for the contents resides with the author  
or organisation that prepared it.

\* Fulmer Research Institute, Stoke Poges, England.

E.S.A. Technical Manager : Mr. D. Eaton

NOTICE

THIS DOCUMENT HAS BEEN REPRODUCED  
FROM THE BEST COPY FURNISHED US BY  
THE SPONSORING AGENCY. ALTHOUGH IT  
IS RECOGNIZED THAT CERTAIN PORTIONS  
ARE ILLEGIBLE, IT IS BEING RELEASED  
IN THE INTEREST OF MAKING AVAILABLE  
AS MUCH INFORMATION AS POSSIBLE.

FULMER RESEARCH INSTITUTE LIMITED

THE SIGNIFICANCE OF DEFECTS IN CFRP BONDED  
HONEYCOMB STRUCTURES AND NON DESTRUCTIVE  
TEST METHODS FOR THEIR DETECTION

by

R.L. Crocker and W.H. Bowyer

FINAL REPORT

R736/4/May 1978

Contract No. 2922/76/NL/PP (SC)

SYNOPSIS

Carbon Fibre Reinforced Plastic (CFRP) skinned aluminium honeycomb sandwich materials are becoming well established in the aerospace industry. These materials exhibit high specific strength and high specific stiffness. The types of structure for which they are suitable are those which require a large stiffness to mass ratio such as side-walls, solar arrays, antenna dishes etc. Whilst a great deal is known about the behaviour of these materials there are certain areas where neither theoretical nor physical studies have so far been successfully undertaken. One of these is the problem of defects within the material and their effect on its properties. Lack of this information hampers the spacecraft designer in making a reasonable estimate of the practical properties of the materials at his disposal with the consequent risk of structural over-design.

A study has been undertaken at Fulmer Research Institute in conjunction with ESTEC to identify the defects that occur in CFRP/Al sandwich materials and to assess the significance of these defects

in terms of overall mechanical properties. A range of defects have been considered and all have been shown to have significant effects on laminate strength.

Available non-destructive test methods have been reviewed and evaluated using specimens containing deliberately introduced defects. It has been recommended that the optimum NDT practice which is presently available involves a combination of visual examination, roller probe coupled ultrasonics and X-radiography.

The performance of other techniques including holographic interferometry, laser speckle pattern interferometry and thermography is discussed.

## CONTENTS

	<u>Page No.</u>
1. <u>INTRODUCTION</u>	1
2. <u>SURVEY OF DEFECTS OCCURRING IN CFRP SANDWICH PANELS</u>	4
2.1 Defects Occurring During Preparation of Prepreg	4
2.2 Defects Occurring During Laminating	5
2.3 Integration of Skins and Cores	7
3. <u>SURVEY OF NDT METHODS WHICH HAVE BEEN APPLIED TO CFRP/ALUMINIUM SANDWICH PANELS</u>	7
3.1 Visual Examination	7
3.2 Coin Tap Testing	8
3.3 Radiography	8
3.4 Ultrasonics	9
3.4.1 General	9
3.4.2 Direct Contact	9
3.4.3 Soft Tipped Probes	9
3.4.4 Air-Coupled Resonance	10
3.4.5 Roller-Probe Coupling	10
3.4.6 Fokker Bond Tester	11
3.4.7 Acoustic Flaw Detector	12
3.5 Thermography	13
3.6 Holographic Interferometry	13
3.7 Laser Speckle Interferometry	15
3.8 Acoustic Emission Monitoring	16
4. <u>DEFINITION AND MANUFACTURE OF SPECIMENS</u>	17
4.1 Availability of Materials and Manufacturing Facilities	17
4.2 Mechanical Testing Requirements	18
4.3 Selection of Specimen Types and Defect Plans	18
4.4 Manufacturing Procedures	25
5. <u>TESTING PROCEDURES AND OBSERVATIONS ON TEST METHODS</u>	25
5.1 Non-Destructive Testing	25
5.1.1 Summary of Methods Employed	25
5.1.2 Visual Examination	27
5.1.3 "Coin-Tap" Testing	27
5.1.4 Radiography	27
5.1.5 Ultrasonics	27
5.1.5.1 Direct Contact	27
5.1.5.2 Soft Tipped Probes	28
5.1.5.3 Air Coupled Resonance	28
5.1.5.4 Roller Probe/Discriminator	28
5.1.5.5 Fokker Bond Tester	29
5.1.5.6 Acoustic Flaw Detector	29
5.1.6 Thermography	30
5.1.7 Holographic Interferometry	30
5.1.8 Speckle Pattern Interferometry	31
5.1.9 Acoustic Emission	32
5.2 Mechanical Testing	34
5.2.1 Flexural Testing	34
5.2.2 Vibration Testing	35

Contents Continued:

	<u>Page No.</u>
<b>6. <u>RESULTS</u></b>	38
6.1 NDT Results	38
6.1.1 Defect Types and Methods of Detection	38
6.2 Mechanical Test Results	46
6.2.1 Flat Specimens	46
6.2.1.1 0/90/90/0 Lay-up Specimens	46
6.2.1.2 0/60/120 Lay-up Specimens	46
6.2.1.3 Observations on Failure Mode	49
6.2.1.4 Acoustic Emission from Flexural Tests	50
6.2.2 Bicurved Specimens	51
6.2.2.1 Vibration Testing Results	51
6.2.2.2 Observations on the Vibration Tests	56
<b>7. <u>DISCUSSION</u></b>	56
7.1 Flexural Testing	56
7.2 Acoustic Emission from Flexural Tests	60
7.3 Vibration Testing	63
7.4 Non-Destructive Testing	67
<b>8. <u>SUMMARY AND CONCLUSIONS</u></b>	74
<b><u>REFERENCES</u></b>	
<b><u>FIGURES 1 - 21</u></b>	
<b><u>APPENDIX</u></b>	

## 1. INTRODUCTION

CFRP is being increasingly selected for spacecraft components because of its high specific strength and specific stiffness, and its high resistance to distortion under the influence of temperature gradients during thermal cycling.

In order to realise the potential offered by the high specific stiffness, it is desirable to reduce design safety factors to a minimum; however this increases risk of failure due to material or manufacturing defects. At present, knowledge of the effects of defects on performance is very limited and reliable non-destructive testing procedures have not been established. It is necessary therefore to examine the types of defect which occur in CFRP, to determine their effect on service performance and to devise means of detecting them.

Spacecraft components in which CFRP has displaced the more conventional materials include struts, booms, pressure vessels, side-walls, pallet floor panels and antenna dishes.

Struts, pressure vessels and booms are manufactured using techniques of pultrusion and/or filament winding. These are outside the scope of this project and are not considered further.

Side-walls, pallet floor panels and antenna dishes employ a sandwich construction where face skins of CFRP are bonded to aluminium honeycomb cores. The high structural efficiency of this type of construction enables very thin face skins to be employed. Ideal designs often involve the use of skins which are so thin that it is beyond present technology to produce them. The compromise is to produce skins which are as thin as technology permits and adjust the core thickness accordingly.

CFRP is normally produced in the form of prepeg (preimpregnated resin/fibre sheets). These sheets are produced by flattening tows or bundles of parallel fibres and introducing these between two films of resin. Thus the fibres are unidirectionally oriented in the prepeg. Furthermore as the final fibre distribution is produced from a number of bundles, there is the possibility of a non-uniform fibre distribution across the width of the prepeg sheet, possibly giving rise to completely fibre free regions. It is because of this

problem that it is not feasible to manufacture very thin sheets of CFRP from prepreg, and even if it was, the highly anisotropic nature of such sheets would severely limit their usefulness. This anisotropy arises because the ratio of modulus or strength in and transverse to the fibre direction is about 25. Thus multi-ply lay-ups must be used, not only to reduce anisotropy but also to facilitate manufacture.

When multiple ply lay-ups are used, coupling effects between strains in the individual plies must be considered. These may lead to shear deformation under the action of in-plane stresses, bending under the influence of in-plane stresses and twisting caused by bending stresses. These strain interactions are complex but have been explained in terms of classical laminate theory by Tsai<sup>(1)</sup>. Laminates designed to be free from these distortions are termed balanced laminates. The general rules for balancing of laminates are as follows<sup>(2)</sup>:

- (i) To avoid shear distortions due to in-plane stresses, an equally thick ply at  $-\theta$  to the direction of stressing must balance every ply at  $+\theta$ . By this means each lamina is prevented from undergoing shear deformation by its bond to the next lamina. The net result is zero average shear strain in the laminate.
- (ii) To avoid bending and twisting due to in-plane stresses the laminate should have mid-plane symmetry. That is to say that for each lamina above the plane, there is another lamina below with identical angle of orientation, distance from the mid-plane and mechanical properties.
- (iii) To avoid twisting under bending stresses it is necessary to have mid-plane anti-symmetry. For example a 4-ply laminate must have a lay-up sequence  $\theta, -\theta, \theta, -\theta$ .

Conditions (ii) and (iii) are clearly in conflict. Whilst it is possible to minimise the effects described in (ii) and (iii) by using a large number of plies, this solution is not feasible for thin laminates.

The  $0^\circ, 90^\circ$  laminating sequences are special cases as far

as resistance to twisting during bending is concerned. All the criteria (i) to (iii) above are therefore satisfied by the cross-ply series 0/90/0; 0/90/90/0 etc., and the choice between an odd number and an even number of plies for this type must be determined by the level of anisotropy which may be tolerated. A lower level anisotropy than the 0°, 90° sequence may be achieved using the 0°/60°/120° sequence. This is balanced with respect to bending stresses but not with respect to in-plane stresses. If two 0°/60°/120° skins are used in a sandwich construction and effective coupling is obtained through the honeycomb core, it is feasible to have a structure which is balanced with respect to in-plane stresses making use of skins which are themselves balanced with respect to bending stresses, (0°/60°/120°/honeycomb/120°/60°/0°).

Since the minimum thickness of prepreg which is available is 0.05 mm, the minimum thickness for 0°/90°/90°/0°, and 0°/60°/120° are respectively 0.2 and 0.15 mm. The adoption of designs using skins of these thicknesses will provide useful weight savings over competitive materials. However, there are a number of types of defect which occur in this form of sandwich construction. These are associated with the difficulties of producing and handling thin prepgres, with the lay-up procedure itself, with the handling of cured skins, with the bonding of skins to cores and with the bonding in of inserts to be used as fixing points. Unless the significance of these defect types is known then the designer cannot optimise the strength/weight ratio of the material to be used, whilst maintaining sufficient safety margins.

In the research programme reported, both flat and bicurved sandwich panels using 0°, 90°, 90°, 0°, and 0°, 60°, 120° skins have been studied.

Surveys of the defects which are known to occur in such panels (Section 2) and both established and novel non-destructive test methods for their detection have been undertaken (Section 3). These have been used to define a test programme in which panels containing deliberately produced defects have been made and subjected to examination for the defects, both during and after manufacture. A wide range of defect types have been investigated and a range of

NDT methods have been used in their examination. The effectiveness of the various NDT methods has been compared.

Following the non-destructive examination, destructive four point bend tests have been carried out on specimens cut from the flat panels to determine their mechanical strengths. During destructive testing each specimen was monitored for acoustic emissions in an attempt to relate the presence of defects in specimens to acoustic emissions occurring before the fracture events. Statistical methods have been used to assess the significance of the effects of defects on mechanical strength.

The bicurved specimens have been subjected to vibration testing at ESTEC, in an attempt to promote controlled growth of defects and to monitor acoustic emissions associated with that growth.

## 2. SURVEY OF DEFECTS OCCURRING IN CFRP SANDWICH PANELS

### 2.1 Defects Occurring During Preparation of Prepreg

Prepreg producers experience many problems in the production of prepreg, and these are intensified when the prepreg is thin or when type I rather than type II fibres are used. For this reason very thin prepregs (less than 100  $\mu\text{m}$ ) in type I fibre are difficult to obtain on a regular basis.

The production of prepreg sheet requires that tows of roughly circular cross section, containing 3000 or more fibres, be flattened to the desired thickness. This flattening operation and the need to align a large number of flattened tows leads to three main types of defect, these are Gaps, Misorientations and Contamination.

Gaps, up to 1 mm wide occur due to separation of groups of fibres within the tows during flattening and incomplete butting of flattened tows. End to end butts within the same sheet of prepreg are avoided. Since gaps occur parallel to the fibres they have little effect on the strength or stiffness of single plies in the fibre direction, but the resin rich zone associated with a gap is a preferred site for the formation of voids and the nucleation of cracks. Voids occur as a result of air or vapour entrapment during later stages of processing, these may act as crack nuclei themselves, (for instance

during outgassing), but cracks may also occur as a result of shrinkage stresses in the resin. Such cracks will only assume significance if they occur close to end-to-end joints in the same or in adjacent plies where their growth would result in loss of stress transfer along fibres.

Fibre misorientations occur due to fibres being "picked up" on processing equipment or on the fingers of operatives. The result may be fibres laying across the main direction in the prepreg when they are released. The effects of fibres being misoriented in this way is likely to be very small on the individual ply, but the disturbance in the thickness direction may have a significant effect on adjacent plies.

Contamination of the prepreg may occur due to foreign bodies (dust, metallic particles), grease (from fingers), or solvents coming into contact with the surface. Whilst precautions are always taken to avoid these events, they do occur; in particular, small particles of fibre debris from guides on processing equipment often adhere to the prepreg. The effects of the contaminants may be to disturb the lay-up of the fibres in the thickness direction, to reduce the bonding within and between plies, to induce voids (if solvent) or to cut fibres (if sharp).

## 2.2 Defects Occurring During Laminating

Prepreg sheets are stored between backing sheets which protect them from damage or contamination. In order to build up a laminate, several sheets of prepreg may be used in one ply. This involves cutting the prepgres to shape, carefully removing backing sheets, laying the prepreg onto the mould and manually adjusting it to take up the shape of the mould. Both end-to-end and side-to-side joints between prepreg sheets are necessary. When end-to-end joints are made a decision has to be taken as to whether butts or overlaps should be used. Whilst butt joints do not disturb the profile of the laminate they depend on adjacent layers for stress transfer along the fibres, and incomplete butting leads to an extensive fibre free zone and a discontinuity of strength in the fibre direction. Clearly if parallel plies on either side of the joint are not used this method may not be tolerated. The disadvantage of an overlap joint is

that it disturbs the profile of the sheet and kinks the adjacent layers. In addition, extensive resin fillets are formed at the ends of the overlaps which are themselves crack nucleation sites.

The main defects which arise as a result of handling of prepgs during the laminating stage and during the curing stage are Gaps, Defective Joints, Misorientation, Contamination, Poor Bonding, Resin Undercure and Resin Overcure.

Gaps in the prepg layers inevitably arise when the shape to be moulded is not flat, these gaps are the same in effect as those described in 2.1 above.

Defective joints may be overlapped edge joints (rather than butted) which lead to local high fibre (low resin) concentrations and distortions of the adjacent plies and resin rich regions in the interlaminar zone close to the overlap. Very slight tensile strength loss may be expected due to distortion of fibres in these zones but the major effect, if there is one, would be to nucleate interlaminar cracks which would be likely to reduce flexural or compressive strengths. End to end joints are always a problem for the reasons given above. In sandwich panels, end butt joints are not satisfactory because insufficient plies are available to transfer the stress across the join. Overlaps must therefore be used and they should be long enough to give reliable stress transfer. The resin rich fillets at the ends of the butts are undesirable but there is no way of preventing them.

Misorientations occur due to errors in the lay-up sequence, they result in drastic changes in strength and tendencies to distortion. They should not occur but it is essential to check.

A major source of contamination at this stage is the inclusion of small areas of backing sheet which tears away when the main part is removed. These small strips of backing sheet are often undetected and are the more damaging since they tend to occur near edges where joints are to be made. Minor sources of contamination include foreign bodies, grease, solvents etc. and air bubbles which frequently occur if the prepg is too "tacky" so that it tends to fold and ripple when its position is adjusted relative to the lower layer.

- 7 -

Poor bonding may occur as a result of air entrapment between layers in the laminate or as a result of using prepgs which are too "dry" (low resin content). This defect is likely to lead to poor flexural or compressive strength due to a lack of resistance to buckling. Resin undercure or overcure rarely occurs and should be checked for on a test coupon. The usual resins are tolerant to a wide variation in cure schedule.

### 2.3 Integration of Skins and Cores

Skins are bonded to cores on the mould in a single operation using film adhesive and curing under pressure (vacuum bag). Cores are preformed in aluminium honeycomb, and potting resin is used to fill cells where attachments have to be made to the finished panel. The defects which arise at this stage include Crushed Core, Misplaced Potting, Mechanical Damage to Skins and Incomplete Skin to Core Bonds.

The crushed core defect occurs as a result of mechanical damage to the core. The skins may bond to the crushed region, in which case the surface profile is disturbed or, if the crushing is deep, bonding may be incomplete with the result that one skin is unbonded over the damaged region. This could lead to reductions in compressive and flexural strengths.

Misplaced potting occurs due to bad workmanship and leads to problems in later stages of manufacture using the panels. Mechanical damage such as splits or dents occur in skins during handling. Splits are usually repaired or cause rejection of the skin. Dents often persist through into the finished panel leading to incomplete bonding.

Incomplete bonding between skin and core may result from damage to either member or to the film adhesive itself or to the inclusion of backing sheet at the interface. Whatever the cause the effect is believed to be the same.

## 3. SURVEY OF NDT METHODS WHICH HAVE BEEN APPLIED TO CFRP/ALUMINIUM SANDWICH PANELS

Manufacturers and suppliers of the equipment used in this study are listed in the Appendix.

### 3.1 Visual Examination

Visual examination of CFRP/Al honeycomb structures gives a rapid and simple indication of the presence of many defect types. This is particularly so when the structures under examination are

small, thus ensuring detailed inspection of the whole surface, and when very thin face skins are employed. The technique is subjective but is extremely sensitive to many defect types, particularly when the relationship between the observer's angle of view, the source of illumination and the orientation of the specimen are continuously variable.

It is most unlikely that any CFRP laminate or CFRP/Al honeycomb panel could be manufactured without considerable incidental visual inspection and many defects are certain to be visually detected before any specialised techniques are employed.

### 3.2 "Coin Tap" Testing

"Coin Tap" testing is the technique most commonly used (and trusted) by workers in CFRP laminates and honeycomb sandwich panels. It is essentially a resonance technique whereby the natural pitch and timbre of sound resulting from tapping one area is compared with that resulting from other surrounding areas. The technique therefore detects changes in the resonance frequency and, by implication, any defect which causes such changes. In CFRP laminates and sandwich structures these defects are likely to be delaminations, in the laminates, and in the case of thin face skins, debonds between skins and core.

The subjectivity of this test is an inverse function of operator experience and a coin tap test can efficiently detect many defects before more sophisticated techniques are employed.

### 3.3 Radiography

X-ray radiography is a well established NDT technique utilising the differential absorption of energy by different materials. For use in conjunction with CFRP and CFRP/Aluminium honeycomb structures only very low voltage X-rays are required. This ensures the production of mainly long wavelength (soft) X-rays which are of low enough energy to be absorbed by the molecularly light carbon.

A range of voltages is available in most X-ray production equipment, and it was found that to examine the CFRP skins alone, a voltage of 7kV was satisfactory and to examine the honeycomb core

50kV was adequate. When using 50kV, no detail of the CFRP is revealed as the harder X-rays suffer negligible absorbtion.

Both photographic contact techniques and direct viewing with a fluorescent screen can be used to examine the honeycomb, but when 7kV is used only photographic techniques are possible.

### 3.4 Ultrasonics

#### 3.4.1 General

Considerable effort has been directed towards the development of ultrasonic test methods which do not rely on the use of liquid couplants between probes and specimens. There are several techniques for achieving this. In addition there are several techniques used to test bonded structures. Whilst many of these rely on similar principles, there is sufficient variation to merit separate evaluation of several techniques.

All ultrasonic techniques involve the insertion of ultrasonic energy into a specimen and the monitoring of the energy either transmitted through, or reflected from inside, the specimen. It is the way in which the energy is inserted and monitored which produces the variations in technique.

#### 3.4.2 Direct Contact

It was not possible to develop any system that would give reliable reproducible ultrasonic coupling to either CFRP or CFRP honeycomb using direct contact probes and liquid or gel coupling media.

#### 3.4.3 Soft Tipped Probes

Ultrasound of frequency 0.5 - 1.0 MHz is introduced to the specimen using a soft tipped transducer, the tip being formed from polymer. This causes the specimen to vibrate in resonant modes and the vibrations are picked up by a second soft-tipped transducer a few mm away on the same side of the specimen. The signals from this transducer are processed and fed to a cathode ray oscilloscope which provides an amplitude versus time display. Any variations in this display are indicative of the presence of flaws.

#### 3.4.4 Air-Coupled Resonance

Two 30 mm diameter transducers are used spaced 125 mm apart with the bonded honeycomb panel between them (i.e. in the through transmission configuration). The probes are tuned separately to give optimum resonance and pick up conditions. The beam of ultrasound covers an area of 2000 mm<sup>2</sup>.

It is possible to use focussing probes to improve resolution but this technique is still under development.

#### 3.4.5 Roller-Probe Coupling

A system of roller probes has been developed which incorporates a transmitting transducer mounted on the non-rotating axle of an oil-filled rubber tyre. This provides a reliable and reproducible ultrasonic coupling to the specimen surface. The system operates in transmission; either through-transmission with transmitter and receiver directly opposed through the specimen or transverse transmission with transmitter and receiver on the same side of the specimen a few centimetres apart.

In either configuration the rollers are lightly spring loaded to maintain an even contact pressure and the surface of the specimen can be rapidly examined in a series of passes across the surface. With suitable jigging a C scan system could be constructed.

An important and unusual feature of this system is incorporated in the received signal processing equipment. Instead of the receiver output being fed straight to a conventional attenuator/amplifier combination, a narrow band tunable amplifier (or discriminator) is inserted. This effectively filters out all frequencies except that to which it is tuned, this it amplifies and the output then goes to a conventional amplification and display unit.

The oscillating crystal of an ultrasonic transducer necessarily emits many frequencies, even when in resonance. The discriminator selects just one of these frequencies and examines the variation of received intensity as the probes are scanned across the specimen. Thus many spurious resonance and interference effects are eliminated and the resolution of the system greatly enhanced.

### 3.4.6 Fokker Bond Tester

The Fokker Bond Tester (F.B.T.) is a non-destructive test instrument which exploits the mass-spring-mass behaviour model of a bonded structure to provide information about the cohesive properties of the bonding. A mass-spring-mass system has inherent properties of resonance and impedance, and it is these that are measured by the F.B.T. A piezo-electric transducer (normally a single cylindrical undamped barium titanate crystal) is swept through its natural resonance frequency in the radial direction. When these oscillations are coupled to the specimen they exert, on it rapidly fluctuating loads of a very low magnitude and high frequency.

When a mass, the test specimen, is coupled to this transducer, then the resonant frequency and the impedance change. In practice if the mass is small only an impedance change is seen. The F.B.T. has two scales; the A scale is a cathode-ray-tube (CRT) display and shows any frequency shift, the B scale is an ammeter and indicates the amplitude of the resonance vibration, a measure of the impedance.

The main function of the bond tester is to examine the cohesive properties of the cured resin and to detect the porosity level in the resin. Fokker reported that porosity in the resin is the main bonding defect. They use Redux Phenolic resin which requires seven atmosphere's pressure to prevent porosity in the cured resin. If the pressure in any region is lower than this, the region is likely to be porous. By careful calibration and the preparation of correlation curves, it is possible to obtain reliable quantitative information about bond quality. For example, in the case of two simple skins bonded together, calibration is carried out by centering the resonance frequency peak on the CRT oscilloscope, which displays amplitude versus frequency, when the probe is positioned on a single unbonded skin. When the probe is placed over a well bonded region, the resonance frequency peak shifts to the right or left. The direction of the shift depends on whether the lower skin is vibrating in or out of phase with the upper sheet, this in turn depends on the particular probe being used. For convenience this shift is measured in Bond Tester units but these, of course,

represent certain fractions or multiples of kHz. The A scale, the CRT, displays different shifts depending on the bond quality between the skins, and the correlation of these shift values and the results of destructive mechanical tests enables correlation graphs to be compiled.

When testing CFRP sandwich materials the B scale is more sensitive than the A scale because the coupled mass of the light Aluminium honeycomb core and the skins is small, and there is only a very small frequency shifting effect.

It is possible to set limits on both the A and B scale indications. Thus an audible or visible rejection signal can be given. The whole apparatus can be automated.

Various transducers are available to examine different materials: the frequency range is 50 kHz - 1 MHz. Multi-layer structures can be examined but care must be taken in defective bond location because the tester averages over good and bad bonds. Consequently both sides should be examined. The resolution of the instrument is a function of the probe diameter; defects of two thirds of this dimension can be detected. The smallest probe available has a diameter of less than 6 mm.

#### 3.4.7 Acoustic Flaw Detector

This instrument relies for its operation upon the detection of changes in mechanical impedance of the test specimen coupled to the flaw detector probe.

This probe comprises two piezo-electric transducers. One of these is the transmitter and an audio frequency sinusoidal signal is fed to it. The vibrations are transmitted to the specimen and the second transducer measures the amplitude of these vibrations and the phase of the received signal relative to the transmitted signal. Defects in structures manifest themselves as changes in the amplitude and phase displays.

The Harmonic Bond Tester is an instrument which operates on the same principles as the Acoustic Flaw Detector using two transducers which require no liquid couplant to the specimen. The

Harmonic Bond Tester works well on metallic bonded structures.

### 3.5 Thermography

The EMI Thermoscan system comprises an infra-red camera and Cathode Ray Tube (CRT) display unit. The system senses temperature by measuring the energy of infra-red photons. Thus when inspecting a surface, information about the temperature at any point is displayed in terms of intensity on the CRT display.

The camera contains a  $200 \mu\text{m} \times 200 \mu\text{m}$  square detector element which is scanned across the field of view using a lens and mirrors system. This size of element permits a theoretical limit of resolution of 2.2 mm. This is the size of object point required to produce one picture point of image at near focus. However, to achieve full contrast response, it is necessary to have about three picture points and this raises the limit of resolution to approximately 6 mm (the size of the honeycomb cells).

When inspecting CFRP/Al panels and CFRP skins the viewed surface is designated the front, and the other surface the back. To visualise any structure within the specimen the effect of thermal conductance is utilised. The back surface is heated as uniformly as possible and is considered to have a constant temperature across its area. Heat is conducted through the specimen at a rate which is a function of the thermal conductance between any two perpendicularly opposed points on the two skins. Thus the temperature at any point on the front surface is a function of the thermal conductance perpendicularly between it and the back surface. The camera detects the temperature distribution on the front surface. Any variations in temperature are displayed as intensity variations on the CRT; whether in the A scan or C scan mode, both of which are available, as is an isometric mode. The relevance of this to the CFRP/Al honeycomb is the perturbations of thermal conductance caused by defects either in the honeycomb core or the face skins. These should give rise to local variations in front surface temperature which will be visualised by the system.

### 3.6 Holographic Interferometry

A hologram is a complete recording of the visual information

available from an object, both intensity variations and phase relationships being recorded simultaneously. Consequently an ideal holographic image of an object is visually indistinguishable from the object itself.

The output from the laser is divided into two beams, designated "reference" and "illumination" beams. The reference beam is routed via an aperture and beam spreader direct to the photographic plate. The illumination beam also passes through an aperture and beam spreader and is then incident on the object. Light is reflected from the object onto a photographic plate. Thus the plate receives light directly from the laser source and light reflected from the object.

The radiation from a laser is practically monochromatic and the coherence length is practically infinite. Thus, assuming the object is fixed rigidly such that any movement that does occur is much less than one wavelength of the illumination, the interference pattern, formed by the two beams arriving at the glass plate, is stable.

In practice the photographic plate is shielded and then exposed using a shutter mechanism, thus recording the interference pattern over a short time interval. This pattern records intensity and phase variations from the object and after processing will reconstruct exactly the object in its original position. It is the phase information which produces the well known "3D" and "parallax" effects of holography.

In order to extend the usefulness of the holographic technique a process of holographic interferometry has been developed.

When the holographic image is reconstructed it is situated precisely where the object was when the hologram was formed. If the system is extremely stable, then the image of an object can be formed exactly on the object itself.

In this situation the observer's eye receives reflected laser light from the object and light diffracted by the hologram

forming the image. Assuming no movement of the object has occurred, these two light sources are in phase and constructive interference occurs. However, if the object moves towards or away from the plate by a half wavelength (or odd integral number of half wavelengths), then the diffracted light will be in antiphase with the object-reflected light. This will cause destructive interference with consequent zero perceived intensity.

In practice this lateral whole body movement rarely occurs and instead a system of fringes caused by successive displacements of half wavelengths is seen across the specimen. The spacing of the fringes indicates the rate of change of displacement from the original specimen position. Further if a "no-fringe" position is found and the movement of fringes is monitored as the specimen is deformed, then absolute strain measurements can be made.

For use with CFRP/Al honeycomb it was envisaged that defects would cause local deviations in expansion coefficients such that if the specimen was heated, differential expansion around the defects would be visualised in the resulting fringe patterns. This is discussed further in Chapter 5.

### 3.7 Laser Speckle Interferometry

A team at Loughborough University of Technology have synergised the properties of laser light and the capabilities of high speed electronics to produce an instrument which is primarily designed to provide an NDT technique enabling inspection of strain, and by implication, stress fields in real time, using standard specimens and service stress conditions (in contrast to, say, photo-elasticity which seeks to provide the same information but which requires perspex, planar specimens).

When a scattering surface is illuminated with the coherent light from a laser a speckle pattern is observed, (usually described by observers as a "graininess" of the object). These speckles can be recorded as individual interferograms by interfering them with an unscattered reference beam on the face of a vidicon television tube. This pattern is stored digitally in either a solid state or floppy disc electronic memory. This "single frame" is then played back

through a television monitor.

Having recorded a frame, the camera continues to provide a digital image of the speckle pattern and this is then combined on the screen of the monitor simultaneously with the recorded frame. The two signals are subtracted with the result that if the object does not move in any way then the simple speckle pattern is seen. As the object moves however, the subtraction of the unchanging stored speckle pattern and the changing real time speckle pattern results in the formation of fringes on the monitor screen. The variation of intensity of the fringes is sinusoidal and the separation of two adjacent like fringes represents an object surface displacement of  $\frac{\lambda}{2}$ , where  $\lambda$  is the wavelength of the laser illumination.

At positions of high strain the fringes are closely packed, conversely at low strain areas the fringes are widely spaced. The relative spacing of fringes across the surface of a specimen visualises the variation in strain. It was envisaged that defects in CFRP/Al sandwich panels would cause local differential expansion which would cause disturbances in the overall fringe patterns. This is discussed further in Chapter 5.

### 3.8 Acoustic Emission Monitoring

Whilst the methods discussed in the previous sections often allow the detection and identification of defects in a structure, they give little indication of their significance. Acoustic emission (AE) on the other hand is a technique which may indicate the significance of a defect without identifying its nature. This latter technique is not truly non-destructive in that it depends on damage occurring close to a defect for its detection. However, proof tests are carried out on structures before they are put into service and acoustic emissions occurring during these tests may be monitored very easily. If no emissions occur it can be concluded that however many defects are present in the structure and whatever their type, they have not resulted in damage during proof testing. If emissions are detected, it is a certain indication that strain energy release has occurred and this almost invariably means damage has occurred. Repeated proof testing indicates whether

or not damage is cumulative and likely to cause failure or is merely causing a reduction in the stress concentration associated with a defect so that its growth is stopped. The monitoring of acoustic emissions has been shown to be the most sensitive method available for detecting damage occurring during proof testing of many materials and triangulation techniques allow damage sites to be located. These properties of the AE method identify it as an invaluable tool in proof testing and also in studies of the significance of defects. (It is possible to subject specimens containing a range of known defects to a gradually increasing uniform stress, thus the stress levels at which the individual defects become active may be determined and the character (amplitude and frequency content) of the emissions associated with the particular defect type may be assessed.)

4. DEFINITION AND MANUFACTURE OF SPECIMENS

4.1 Availability of Materials and Manufacturing Facilities

All materials were supplied by Ciba-Geigy, Bonded Structures Division, Duxford, Cambridge, England. Specimens were manufactured by Ciba-Geigy at Duxford and members of the staff of the Bonded Structures Division were available to give advice and take part in discussions at all stages of the work.

It was anticipated by Ciba-Geigy that it would be difficult to obtain supplies of very thin prepreg in type I fibre. An early decision was taken therefore to carry out the major part of the work using type II fibre, and to carry out selected tests towards the end of the programme using type I to examine critical defects only. In the event, type I fibre became available towards the end of the work but in view of delays which had occurred at early stages, a decision had been taken to complete the work using type II only. No other materials problems were experienced.

The prepgs used were all of type II carbon fibre in Fibredux 914 resin and they were all 50  $\mu\text{m}$  thick, the film adhesive used was Redux 319, the potting compound was Redux 253. The aluminium honeycomb was 11.5 mm thick having a cell size of 6.5 mm and a density of  $54.4 \text{ kg/m}^3$ .

During the currency of the programme a 600 mm x 600 mm flat platten and vacuum bag autoclave facilities were available for our use and specimens were therefore designed for manufacture using these. For curved specimens an aluminium mould of 450 mm diameter and a radius of curvature of 457 mm was used. The mould surface was machined and polished to a highly reflecting finish.

#### 4.2 Mechanical Testing Requirements

For mechanical testing of flat specimens, four point bending is considered to be most satisfactory since in these tests the whole specimen surfaces between the centre rollers are uniformly strained (top in compression, bottom in tension). Thus defects appearing anywhere close to these surfaces and between the centre rollers have equal opportunities to influence strength and the failure mechanism.

A series of preliminary experiments using available four point bend test equipment resulted in the selection of rollers having a 22.6 mm diameter and separations of 360 mm and 120 mm between outer and inner rollers respectively. A specimen length of 380 mm and width of 25.4 mm was required in order to ensure that failure occurred between the rollers rather than under one of them. Reproducibility of maximum bending moment measurements was adequate to justify no more than triplicate testing.

The ideal way of testing bicurved specimens is on a vibrating table making use of g forces to apply stresses. The vibrational test facility at ESTEC was made available for these tests and the only requirement on the specimens was that they should be capable of being fixed to the vibrating table. This was achieved using the specimen design and adapting fixture shown in Figure 1.

#### 4.3 Selection of Specimen Types and Defect Plans

Failure in sandwich panels almost invariably occurs on the compressive face in flexure tests because the compressive strength of laminates is invariably lower than tensile strength. For this reason every panel used in this work had one nominally perfect skin and one

skin (the compressive surface) containing deliberately introduced defects. A decision was taken to examine all the defect types mentioned in Section 2 except resin undercure or overcure and misorientation of plies. To have examined these would have involved the use of three whole laminates which was not feasible, and it was felt that cure schedules and lay-up procedures may be adequately monitored and checked.

In each flat panel it was necessary to have a number of nominally perfect control specimens for comparison purposes and to introduce defects at as many levels of severity as possible. In addition defects had to occur at the same level of severity in the centre spans in each of three flexure specimens taken from the same panel.

It was not possible to manufacture nominally perfect bicurved specimens for comparison purposes within the limits of time and finance on the present contract and tests on panels containing selected defects only were carried out.

Two  $0^\circ$ ,  $90^\circ$ ,  $90^\circ$ ,  $0^\circ$  flat panels A and B were manufactured to contain the defects listed below:

Panel A

- (i) Air bubbles in part of the laminate caused by careless lay-up.
- (ii) An "end to end" joint butted instead of overlapped in the third ply.
- (iii) An "end to end" overlap joint incorporating a piece of prepreg backing sheet, 75 mm x 30 mm in the third ply.
- (iv) A 3 mm wide side to side butt joint between prepreg sheets in the first ply.

Panel B

- (i) Prepreg splits in the  $0^\circ$  plies (1 and 4) in part of the laminate, effected by removal of 1 - 2 mm width of tow at approximately 15 mm intervals.
- (ii) Contamination of plies 1 and 3 in part of the laminate with drops of methyl chloride (solvent).

(iii) Incorporation of pieces of prepreg backing sheet 75 mm x 30 mm between plies 1 and 2 and between plies 3 and 4.

The positions of the defects in and between the individual plies are given in Figures 2 and 4, and the specimen cutting plans are given in Figures 3 and 5. The panels were both 600 mm x 600 mm, the maximum size available in the autoclave.

One 0°, 60°, 120° panel C, was manufactured containing the following defects:

Panel C

- (i) Prepreg splits in plies 1 and 3 in part of the laminate, effected by removal of 1 - 2 mm width of tow at approximately 15 mm intervals.
- (ii) An "end to end" joint butted instead of overlapped in the second ply.
- (iii) An "end to end" overlap joint incorporating a piece of prepreg backing sheet 75 mm x 30 mm in the second ply.
- (iv) A piece of backing sheet 75 mm x 30 mm incorporated between plies 2 and 3.
- (v) An area of core was crushed using a hammer to depress the cell walls by about 1 mm. This was considered to be the maximum level of accidental damage which would be tolerated in the core prior to bonding.
- (vi) A piece of film adhesive backing sheet about 90 mm x 30 mm was incorporated between the C.F.R.P. skin and the core.
- (vii) A quantity of Redux 253 encapsulating compound was incorporated in the core. This does not represent a defect since it is standard procedure to reinforce the core in regions where components are to be secured. However, it is necessary to check the locations of these reinforcements.

The positions of the defects are given in Figure 6 and the specimen cutting plan is given in Figure 7.

The size of the panel was 600 mm x 600 mm.

Skin to core defects (v to vii) were concentrated in this panel rather than in A and B because it was felt that the unbalanced nature of the skins would make  $0^\circ$ ,  $60^\circ$ ,  $120^\circ$  panels more sensitive to these particular defect types than the  $0^\circ$ ,  $90^\circ$ ,  $90^\circ$ ,  $0^\circ$  panels.

Each specimen in Figures 3, 5 and 7 are identified by a number and the panel identity (A, B or C). A list relating specimen number to defect type is given in Table I below.

TABLE 1

<u>Defect</u>	<u>Specimens containing defect in test region (between loading points in four point bending test rig)</u>
Air Bubbles in plies 2 and 4 in part of the laminate	16A, 17A
An "end-to-end" joint butted instead of overlapped in the third ply	21A, 22A, 23A
An "end-to-end" joint incorporating a piece of prepreg backing sheet, 75 mm x 30 mm in the third ply	4A, 5A, 6A
A 3 mm wide "side to side" butt joint in the 1st and 4th plies ( $0^\circ$ )	18A, 19A, 20A
An "end-to-end" overlap joint in the third ply	1A, 2A, 3A
Nominally perfect, but cut at $45^\circ$ to fibre directions	7A, 8A
Nominally perfect	9A, 10A, 11A, 12A, 13A, 14A, 15A
<hr/>	
Prepreg splits in plies 1 and 4 ( $0^\circ$ ) in part of the laminate	1B, 2B, 3B, 4B
Contamination of plies 1 and 3 in part of the laminate with drops of Methyl Chloride (solvent)	10B, 11B, 12B

Table 1 cont.

<u>Defect</u>	<u>Specimens containing defect in test region (between loading points in four point bending test rig)</u>
Incorporation of pieces of prepreg backing sheet 75 mm x 30 mm between plies 1 and 2 and between plies 3 and 4	18B, 19B, 20B
An "end-to-end" overlap joint in ply 4 contained in specimens cut at 45° to the fibre direction	6B, 7B, 8B
A "side to side" butt gap in layers 2 and 3 contained in specimens cut at 45° to the fibre directions	6B, 7B, 8B
A "side to side" butt gap containing a few strands of glass fibre contamination in ply 3	13B, 14B
A "side to side" butt gap in plies 2 and 3	15B, 16B, 17B,
Nominally perfect	2B
<hr/>	
Prepreg gaps 1-2mm wide and approximately 15 mm apart in plies 1 and 3 in part of the laminate	15C, 16C, 17C
An "end-to-end" joint butted instead of overlapped in the second ply	1C, 2C, 3C
A good "end-to-end" overlap joint in the second ply	4C, 5C, 6C
An "end-to-end" overlap joint incorporating a piece of prepreg backing sheet 75 mm x 30 mm in the second ply	7C, 8C, 9C
An area of crushed core to a depth of approximately 1 mm	13C, 14C
A piece of film adhesive backing sheet 90 mm x 30 mm between ply 1 and the core	10C, 11C, 12C

Table 1 cont.

<u>Defect</u>	<u>Specimens containing defect in test region (between loading points in four point bending test rig)</u>
A piece of prepreg backing sheet 75 mm x 30 mm between plies 2 and 3	20C, 21C, 22C
A quantity of Redux 253 encapsulating compound incorporated into the core	18C, 19C
Nominally perfect	23C, 24C, 25C, 26C

Two  $0^\circ$ ,  $90^\circ$ ,  $90^\circ$ ,  $0^\circ$  and two  $0^\circ$ ,  $60^\circ$ ,  $120^\circ$  bicurved panels were made, these contain the defects listed below:

Dish 1 ( $0^\circ$ ,  $90^\circ$ ,  $90^\circ$ ,  $0^\circ$ )

- (i) Four areas containing potting compound.
- (ii) Two pieces of film adhesive backing sheet 75 mm long and 3 mm wide included in the skin to core bond line.
- (iii) A skin to core debond produced by a hole in the film adhesive.

The positions of these defects are shown in Figure 8.

Dish 2 ( $0^\circ$ ,  $60^\circ$ ,  $120^\circ$ )

- (i) Two pieces of film adhesive backing sheet 6 mm x 75 mm included in the skin to core bond.
- (ii) Three areas of crushed core, 1 mm, 2 mm and 3 mm deep respectively.
- (iii) A skin to core debond produced by a hole in the film adhesive.

The positions of these defects are shown in Figure 9.

Dish 3 ( $0^\circ$ ,  $90^\circ$ ,  $90^\circ$ ,  $0^\circ$ )

- (i) A side to side overlap joint 3 mm wide.
- (ii) 2 mm wide prepreg gaps in layers 2 and 3 causing a resin rich zone at their intersection.
- (iii) Two pieces of backing sheet 75 mm x 3 mm oriented in a radial direction placed between plies 1 and 2 and 3 and 4.
- (iv) Two pieces of backing sheet 75 mm x 3 mm oriented in a circumferential direction between plies 1 and 2 and 3 and 4.

The positions of these defects are given in Figure 10.

Dish 4 ( $0^\circ$ ,  $60^\circ$ ,  $120^\circ$ )

- (i) 2 mm wide prepreg gaps in layers 1 and 2 causing a resin rich zone at their intersection.
- (ii) Two pieces of backing sheet 50 mm x 4 mm oriented in a radial direction between plies 1 and 2 and 2 and 3.
- (iii) Two pieces of backing sheet 75 mm x 4 mm oriented in a circumferential direction between plies 1 and 2 and 2 and 3.

(iv) A single piece of backing sheet 75 mm x 5 mm oriented in a radial direction between plies 2 and 3.

The positions of these defects are given in Figure 11.

The chord diameter of the bicurved panels was 300 mm and the radius of curvature 457 mm.

#### 4.4. Manufacturing Procedures

Laminates were made by hand lay-up on the moulds. The nominally perfect skins were made using the standard Ciba-Geigy practice. The defective skins were made using normal procedures except in regions where defects were introduced by the methods described in 4.3 above.

Laminates were cured using a vacuum bag/autoclave technique at a temperature of 170°C and pressure of 100 lb/in<sup>2</sup> for one hour followed by post curing for four hours at 190°C.

All defective skins were carefully inspected before bonding to one side of its aluminium core. A nominally perfect skin was bonded to the other side. Redux 319 fibre adhesive was used and curing was carried out at 170°C and 30 lb/in<sup>2</sup> for one hour using the vacuum bag/autoclave technique.

### 5. TESTING PROCEDURES AND OBSERVATIONS ON TEST METHODS

#### 5.1 Non-Destructive Testing

##### 5.1.1 Summary of Methods Employed

It was not possible to examine every skin and every panel using every non-destructive method. Table 2 below indicates which techniques were used on each skin and each panel. Where individual techniques have not been used, symbol 0 indicates not available.

TABLE 2

Panel Designation	Skin/ Panel	Ultrasonics											
		Visual	Coin Tap	Radiography		Direct Contact	Soft Tipped Probes	Air Coupled	Roller Probes	Fokker Bond Tester	Thermography	Holographic Interferometry	Speckle Pattern Interferometry
Panel A	Skin Panel	X X	X X	X O	X X	O O	O O	O O	X X	O X	X X	O O	O O
Panel B	Skin Panel	X X	X X	X O	O X	O O	O O	O O	O O	O X	X X	O O	O O
Panel C	Skin Panel	X X	X X	O O	O X	X X	O O	O O	X X	O X	X X	O X	O O
Dish 1	Skin Panel	X X	X X	O X	O X	O O	O O	O O	O O	O X	O O	X O	O O
Dish 2	Skin Panel	X X	X X	O X	O X	O O	O O	O O	O O	O X	O O	X O	O O
Dish 3	Skin Panel	X X	X X	O X	O X	O O	O O	O O	O O	O X	O O	X O	O O
Dish 4	Skin Panel	X X	X X	O X	O X	O O	O O	O O	O X	O X	O O	X O	O O
Flat Panel Sample				X		X						X	

### 5.1.2 Visual Examination

The laminated CFRP skins, the completed flat panels and the completed dished specimens were all subject to careful visual examination, both with the unaided eye and a X10 magnifying glass. The resolution of defects was greatly enhanced by using a bright light source at a low angle of incidence to the surfaces of the skins and panels.

### 5.1.3 "Coin Tap" Testing

All the specimens were subjected to this test many times during the investigation. In conjunction with visual examination this test was applied as a preliminary to other tests.

### 5.1.4 Radiography

The flat skins were inspected using 7kV x-rays and a contact technique where the skin was placed in direct contact with a film pack. The film pack was simply x-ray sensitive photographic film sealed in a light tight envelope. By situating the specimen and film pack in contact, maximum resolution is achieved because the x-ray source is not point-like in practice and separation of specimen and film causes umbra effects.

Samples of flat bonded honeycomb panels were inspected using a range of low energy x-rays, from 5kV to 25 kV.

The bicurved honeycomb dishes were examined with medium energy x-rays (50kV) using both the direct contact technique described above and a proprietary fluorescent screen apparatus to visualise the specimen directly.

Portions of the dishes were examined using low energy x-rays as described above.

### 5.1.5 Ultrasonics

#### 5.1.5.1 Direct Contact

As stated in 3.4.2 it was not possible to obtain reliable coupling using hard faced conventional ultrasonic probes. Various coupling fluids were investigated ranging from proprietary ultrasonic coupling fluids to Swarfega solvent but, none proved

practical in examining the panels. All produced contamination of the CFRP surface and consequently the technique was not considered viable in this application.

#### 5.1.5.2 Soft Tipped Probes

These were used both in transverse and through transmission configurations. No major problems arose and good coupling was obtained with consequent location of defects as shown in the results tables. However, to examine a large area of panel would prove time consuming as the probes required to be lifted from the surface rather than slid to be repositioned, otherwise rapid probe wear would result.

#### 5.1.5.3 Air Coupled Resonance

A major problem with this technique in its present state is the mounting of the probes. These have to be accurately aligned on a common axis and thus require a substantial jig upon which to mount them. This precludes examination of large areas of CFRP/Al honeycomb panel.

The transducers actually used in this project were non-focussing and irradiated an area of approximately  $2,000 \text{ mm}^2$ , the resolution could not be expected to be significantly smaller than this.

Consequently, in its present form this apparatus has limited application. However, when equipped with focussing transducers the resolution and power density improvement may render the technique easier to apply whilst retaining its inherent potential advantages of speed and non-contact testing.

#### 5.1.5.4 Roller Probe/Discriminator

The flat skins and the flat bonded panels were examined using this technique, as were the bicurved bonded panels. The probes were mounted in stands and the specimen traversed relative to them. This ensured maintainance of alignment of the probes whilst allowing unrestricted specimen movement.

Transverse transmission proved impossible with the particular apparatus available, because of attenuation, and

consequently all results were in the through-transmission configuration.

Using the discriminator a frequency of 18 kHz was selected and the attenuation adjusted to give a peak on the CRT. As the specimen was traversed a lowering of this peak, on attenuation, indicated the presence of a flaw. In order to increase resolution, traversing along the honeycomb cell walls was found desirable. In this way the normal variation of the signal, caused by the honeycomb, was kept to a minimum and effects caused by defects were more positively identified.

#### 5.1.5.5 Fokker Bond Tester

The flat bonded panels were examined with a Fokker Bond Tester (FBT).

With the probe positioned on a nominally perfect area of panel the B scale indicator was set to a value of 80 in FBT units. Proprietary Fokker Coupling fluid was used to couple the transducer to the specimen.

The probe was then repositioned at several points on both sides of the specimen surface. Firm pressure and a liberal supply of coupling fluid were required to produce consistent and reproducible results. The undulatory nature of the surface, a result of the combination of thin skins and honeycomb core, caused the variability in reading from any particular point. It was considered that this problem would diminish with increasing skin thickness but with the specimens used in this project the coupling problem was not satisfactorily overcome.

#### 5.1.5.6 Acoustic Flaw Detector

The major practical requirement for the operation of the Acoustic Flaw Detector was the maintenance of a constant light pressure on the probe to maintain uniform coupling with the specimen. This was achieved using a long counter-balanced lever, which gave reproducible coupling whilst the panels were scanned beneath the probe.

#### 5.1.6 Thermography

The honeycomb cells in the CFRP/Al panels give rise to a regular variation of thermal conductance and this feature was resolvable with the Thermoscan, the points on the front surface in contact with the cell walls were up to  $\frac{1}{3}^{\circ}$  C warmer than points over the interior of the cells.

This regular variation proved beneficial in locating defects in the CFRP/Al panels as any defect tended to perturb the regular honeycomb pattern, this deviation giving added contrast to the defect area. When the back surface temperature was sufficiently uniform then linear defects of width less than 2 mm were readily resolvable, provided they were considerably longer than 6 mm in length ( $> 12$  mm).

The overriding difficulty in all work with the Thermoscan was the provision of a uniform temperature on the back face of the panels and skins. The detector can differentiate temperatures separated by  $\frac{1}{3}^{\circ}$  C and its most useful range when working with CFRP/Al was a full scale (of intensity in C scan, or peak amplitude in A scan) of  $2^{\circ}$ C. This meant that even slight variations in temperature across the back face masked any perturbing effects caused by defects within the material.

A solution was found which utilised a vertical flat panel heater and a 150 mm air gap to act as a thermal diffuser. The air gap and specimen were shielded to avoid draughts and convection currents. This system gave satisfactorily uniform heating on both the flat panels and the dished specimens. This system was not available before the skins were bonded to form panels and so information on single skins is not as reliable as that on the composite panels.

#### 5.1.7 Holographic Interferometry

In any form of holographic technique the major practical consideration is one of spatial stability of the system. If there is any movement greater than a small fraction of a wavelength of the laser light, then the hologram produced will be poor or non-existent.

Having produced a hologram, in order to perform interferometry the system must again be extremely stable. To obtain useful data from the specimen it must be deformed but in such a way that no vibration or large movements occur. This was achieved in this case by gentle heating.

The dished specimens were held adequately rigidly by using heavy steel support stands. Good holograms and interference patterns were produced with an even distribution across the specimen indicating good stability. The flat panels proved extremely difficult to support, tending to act as edge supported membranes, thus producing acceptable fringes around the edges but not across the central area. This problem was not resolved in the time available.

The defects were expected to be detectable because of the differential thermal expansion they caused in relation to surrounding areas. This would disturb the regularity of the interference fringes thus visualising the defect.

The fringes were photographed using a 35 mm camera viewing through the hologram onto the front surface of the object. Care had to be taken to ensure that the fringes were formed in this surface as an in-plane movement of the hologram would cause fringes in front of this surface which the eye could accommodate and detect but the camera could not.

The fringe pattern could be varied by adjusting the angle of incidence of the illumination beam using micrometer screw threads on one of the plane mirrors. This meant the optimum fringe conditions for visualising a defect in any position could be realised.

#### 5.1.8 Speckle Pattern Interferometry

Both the theory and the equipment of this technique are innovative and at the time of preparation of this project only a laboratory facility and the first prototype commercial instrument were available for test. The method was examined for this project because of its potential advantages over other NDT methods.

The principle of operation as described in Section 3.7 allows examination of specimens in real time. This is a distinct advantage over holographic interferometry as no photographic processing is involved. Specimen stability is extremely important as in any interferometric technique, and this was achieved by rigidly mounting a specimen of CFRP/Al honeycomb in a heavy steel support. The major drawback with the present equipment is that the specimen size is severely limited because the equipment is not developed to its full capability. The maximum specimen size capability is only 100 mm square.

In view of this none of the prepared specimens was examined in detail. However, a 100 mm square CFRP/Al honeycomb panel was examined and defects were detected. The specimen was strained by gentle heating and perturbations in the regular fringe patterns were seen. These are caused by differential expansion of the defect, and the disturbance and creation of fringes was extremely sensitive to slight changes in strain; a finger placed lightly on the specimen and then removed left a detectable fringe disturbance for several seconds.

When fully developed this will provide a sensitive and rapid method of inspecting CFRP/Al honeycomb panels.

#### 5.1.9 Acoustic Emission

Acoustic emissions are stress waves on the surface of an object created by release of strain energy within the body. This stress wave distorts a transducer (piezo-electric in this project) which produces an electrical output signal corresponding in frequency and amplitude to the stress wave (with due consideration for response time and distortion of the stress wave input due to the transducer characteristics). If the voltage produced by the stress wave is above a predetermined level then an event is said to have occurred and a count recorded.

Two sets of equipment were available for acoustic emission studies in this project; a Dunegan Endevco 3000 series and a Surrey University Signal Processor.

The Dunegan Endevco equipment was used with a single transducer in the "sum" mode, giving the total number of counts above the threshold level that had occurred since the start of any test.

The Surrey University equipment contained an amplitude sorter and an interlock system allowing two signals to be processed simultaneously. The amplitude sorter divided the incoming signal into four channels, the selection of channel being a function of the signal amplitude; channel 4 corresponding to  $10 \mu\text{m}$  at the transducer, channel 3 to  $100 \mu\text{V}$ , channel 2 to  $1000 \mu\text{V}$  and channel 1 to  $1 \text{mV}$ . The counts in each channel were summed and routed through a digital to analogue converter which drove a pen or U.V. chart recorder, normally giving total counts versus elapsed time. A range of  $10^4$  of amplitude is thus recorded.

The distribution of counts within each amplitude level gives information on the strain energy release mechanisms occurring in the specimen.  $(\text{Amplitude})^2$  is a measure of energy and hence a range of  $10^8$  in energy is differentiated with this equipment. Present research is investigating the relationship between failure mechanism types and amplitude characteristics.

The interlock system was designed to allow detection of signals from a localised area only. A "guard-channel" on the Surrey equipment had provision for four transducers. If any one of these detected a signal it immediately inhibited the signal transducer on the "signal-channel" output for a variable amount of time. This "dead time" is adjusted so that a signal passing under the guard transducer causes the signal transducer to be inhibited long enough for the pulse to pass under it. Thus signals originating outside an area defined by the points midway between the signal and any guard transducers are not recorded by the signal transducer, although they are counted on the guard transducer channel. Essentially the system allows the statement that any emissions recorded on the signal channel are real events in the material and not spurious noise or fretting occurring at the specimen mounts or in associated apparatus.

The flexural tests were monitored with the Surrey equipment only. The signal transducer was mounted close to the centre of the specimen (within the centre rollers) and a guard transducer midway between each centre and outer roller. This arrangement meant that only signals from an area within the central rollers would be registered on the signal channel. These signals were amplified and amplitude sorted, the total count from each of the four amplitude levels being recorded on a 4 channel pen recorder, versus elapsed time. A load versus time recording was made simultaneously.

The vibration tests required the simultaneous use of both the Surrey and the Dunegan Endevco equipment. The Surrey equipment was used with one guard transducer in this application so that a measure of defect location was possible; emissions originating close to one transducer would inhibit the other, thus inspection of output revealed the approximate location of a defect. In this case the four amplitude levels of output of each transducer were converted to an analogue voltage and recorded on a U.V. chart recorder.

The Dunegan Endevco equipment was operated in the "sum" mode giving total count of events detected. This output was converted to an analogue voltage and recorded on the U.V. chart recorder.

Thus nine channels of acoustic emission data were recorded versus time.

## 5.2 Mechanical Testing

### 5.2.1 Flexural Testing

The preliminary investigations reported in 4.2 determined a specimen configuration suitable for four-point bend testing.

An Instron Type II-DM was used with a 5000 N load cell mounted in the crosshead. The experimental arrangement is shown in Figure 12. The load was applied to the central rolls via a ball and socket mount to ensure an even distribution on the specimen. PTFE pressure pads were inserted under each roll to reduce further

the tendency of the material to crush under them.

The tests were monitored for acoustic emissions by placing three transducers on each specimen as shown in Figure 12. As reported in 5.1.13, this arrangement causes the signal transducer to record only emissions originating within the central rollers. The signals were processed by the Surrey amplitude sorting equipment and then counted and recorded on a four channel chart recorder.

The specimens were oriented such that the deliberate defects were incorporated in the compressive face for reasons outlined in 4.3. The specimens were photographed before and after testing to facilitate examination of fracture mode.

The load versus time recording was used to calculate the fracture load of each specimen and from this the fracture stress was calculated.

The fracture stresses of the specimens containing the various defects were examined using the t-distribution statistical procedure for small samples. The defect type groups were examined for distribution of fracture stress and then the groups compared to look for significant differences between defect groups and the control specimens.

#### 5.2.2 Vibration Testing

A programme of vibration testing was devised and executed using the 7 tonne electromagnetic vibrator facility at ESTEC, and the mounting arrangement shown in Figure 1.

The programme was designed to cause failure of the specimens by subjecting them to stresses induced by g forces, initially on their own mass and finally with the addition of extra mass, in the Z-axis mode of vibration.

Continuous monitoring with acoustic emission equipment was considered to be the most satisfactory technique for the detection of defect activity.

Accelerometers were positioned on the rims and the centres

34. of the dish specimens in addition to control accelerometers on the mounting adaptor. The rim-mounted accelerometers enabled the resonant frequency of the dishes to be determined as a frequency sweep at constant input g, as monitored at the dish centre and on the adaptor, caused variation of the g level on the rim. The position of resonance is the frequency at which the rim g level is a maximum. The ratio of rim g to input g gives an amplification factor which at non-resonant frequencies is close to unity but at resonance may be considerably larger (>4).

Three acoustic emission transducers were bonded to the dishes, as close as possible to the central load spreading plate and symmetrically around it to reduce vibrational stresses on the transducers and the transducer/skin bond to a minimum. Two transducers were connected to the amplitude sorting equipment and one to the Dunegan Endevco equipment as described in Section 5.1.13 above. The sensitivity of the three channels was adjusted so that only signals originating from certain areas on the dish were registered by each transducer, thus allowing identification of which defects were operating.

Test runs on the vibrator alone revealed the presence of significant amounts of energy within the operating frequency band of the acoustic emission equipment. It was considered that the wide-band noise from the hydraulic bearings was responsible for this. Consequently only counts on the two highest amplitude levels of the amplitude sorting equipment were considered as real events within the test material. The Dunegan Endevco gain setting was adjusted to correspond to the second highest level of the amplitude sorter so that only events of that amplitude or greater were recorded.

A preliminary test was performed on each dish which involved a frequency sweep from 5 to 200 Hz at 1g to locate the resonant frequency. A frequency well away from resonance was then chosen for the start of the testing. The testing was done in three phases.

Phase 1 The test programme for this phase is shown in Figure 13. Having found the resonant frequency at a low g level in preliminary tests, further tests were performed at a non-resonant frequency. This enabled controlled g levels throughout the dish as it behaved as a rigid body at non-resonant frequencies.

Tests were performed at increasing input g levels to the limit of the system. Similar tests were then performed at the indicated resonant frequency in order to increase the stress exerted on the rim of the dish. At resonance the amplitude and acceleration of the rim rises and increases the stress experienced by the dish. .37.

Degradation of the dish was monitored electronically by the acoustic emission equipment and physically by a shift in the resonant frequency. Resonance is found by sweeping the input frequency and inspecting the rim accelerometer outputs, which rise to a maximum at resonance. A sweep before and after a programme of tests will thus indicate a resonance shift.

The resonant frequency is a function of the mass and stiffness of the dish. If a defect grows then it changes the stiffness of the dish thus changing the resonant frequency.

Phase 2. In order to raise the stress exerted on a dish for a given acceleration, an annular mass of 985 g was attached around the rim. A frequency sweep was undertaken to locate the resonant frequency followed by testing at constant g levels and a fixed non-resonant frequency. Finally tests were performed at the resonant frequency.

Phase 3. The annular mass was divided into three 60° segments, attached to the rim with a separation of 60°. This configuration caused higher amplitudes at the rim. Slight differences in the masses caused segments of the dish to vibrate out of phase with others thus raising further the strain, and hence stress, experienced by the dish.

Tests at non-resonant and resonant frequencies were performed at various input levels. The final tests consisted of a slow frequency sweep, 1 octave/minute, across a frequency band containing the resonant frequency. Around the resonant frequency the acceleration of the dish rim is a rapidly changing function of frequency (for a fixed input level). The rim acceleration changes considerably over a few Hz change in frequency. Consequently when testing at a constant input level the exact resonant frequency may not be selected. By sweeping across a frequency region containing the resonant frequency, then the maximum acceleration must occur. This mode of testing resulted in g levels at the dish rim considerably above the input acceleration limit of the apparatus.

6. RESULTS

6.1 N.D.T. Results

6.1.1 Defect Types and Methods of Detection

Observations on ease of application of the various NDT methods are included in Section 5 above.

The results are summarised in Tables 3 and 4 and presented in more detail in Tables 5 to 11.

TABLE 3 Summary of NDT Results for Built in Defects in Laminated CFRP skins

Reference Table	5	6	7	8
Defect	Vapour and Solvent Contamination	Overlap and Butted Overlap Joint	Prepreg Splits	Backing Sheet Contamination
NDT Method	Front	Rear	Front	Rear
Visual	ND	D	D	D
Coin Tap	ND	ND	ND	ND
Radiography	ND	D	D	D
Direct Contact	ND	ND	ND	ND
Soft Tipped Probes	ND	ND	ND	D
Air Coupled	ND	ND	ND	NA
Roller Probes	ND	D	D	D
Fokker Bond Tester	ND	ND	ND	D
Thermography	ND	ND	ND	PD
Acoustic Flaw Detector	ND	ND	ND	D

Front - defect in face towards the detector

ND positive identification  
 PD indication of a defect but not positive identification  
 ND not detectable  
 NA not attempted

TABLE 4 Summary of NDT Results for Built-in Defects in Bonded Honeycomb Panels

Reference Table	5	6	7	8	9	10	9	11
Defect	Vapour and Solvent Contamination	Overlap and Butted Overlap Joint	Prepreg Splits	Backing Sheet Contamination in Laminate	Backing Sheet Contamination Between Skin and Core	Encapsulation Compound	Debonding Between Skin and Core	Crushed or Damaged Core
NDT Method	Front	Rear	Front	Rear	Front	Rear	Front	Rear
Visual	ND	ND	PD	ND	D	ND	PD	PD
Coin Tap	ND	ND	ND	ND	ND	ND	ND	ND
Radiography	ND	ND	ND	ND	ND	ND	D	ND
Direct Contact	ND	ND	ND	ND	ND	ND	ND	D
Soft Tipped Probes	ND	ND	ND	D	D	ND	PD	PD
AIR Coupled	ND	ND	ND	ND	ND	ND	D	ND
Roller Probes	ND	ND	ND	PD	ND	D	D	D
Fokker Bond Tester	ND	ND	ND	PD	ND	D	PD	D
Thermography	ND	ND	ND	D	ND	D	D	D
Holographic Interferometry	ND	NA	ND	NA	D	NA	D	NA
Speckle Pattern Interferometry	NA	NA	NA	NA	NA	NA	NA	NA

Front = defect in face towards the detector

Rear = defect in face away from the detector

D positive identification

PD indication of a defect but not positive identification

ND not detectable

NA not attempted

TABLE 5

Defect Type NDT Method	Solvent and Vapour Contamination
All Methods	Not detected by any of the methods studied in this project

TABLE 6

Defect Type NDT Method	Good Overlap and Butted Joints in Prepreg Plies	
	Laminate Only	Bonded Sandwich Panel
Visual	Overlap joints visible in thin skins. Butt joints visible only if adjacent to a good overlap	Detected in some cases if in outer ply. Many deliberate joints not detectable.
Coin Tap	Undetected	Undetected
Radiography	Positive identification of both overlap and butted jointed areas	Undetected - Masking effects in bonded panels
Ultrasonics		
Liquid Coupled Soft Tipped Probes	Undetected	Undetected
Air Coupled Roller Probes	Undetected Detection of good overlap but difficulty with butted joints	Undetected Undetected
FBT AFD	Undetected Undetected	Undetected Undetected
Thermography	Undetected	Undetected
Holographic Interferometry	Undetected	Undetected

TABLE 7

NDT method	Defect Type	Prepreg Splits and Resin Rich Areas	
		Laminate only	Bonded panel
Visual		Positive identification	Positive identification if in outer ply.
Coin tap		Undetected	Undetected
Radiography		Positive identification	Undetected - masking effects in bonded panels
Ultrasonics			
Liquid coupled	Undetected		Undetected
Soft tipped probes	Positive detection		Positive detection from front surface. Undetected from reverse
Air coupled	Undetected		Undetected
Roller Probes	Positive identification especially of extensive area		Indication of a defect from front, not from rear Not positive identification
F.B.T.	Undetected		Undetected
A.F.D.	Undetected		Undetected
Thermography	Undetected		Detection from front surface but not from reverse
Holographic Interferometry	Not attempted		Undetected

TABLE 8

Defect Type NDT method	Prepreg Backing Sheet Contamination and Delamination in CFRP Face Skins	
	Laminate only	Bonded Sandwich Panel
Visual	Positive identification as raised bubble on laminate surface	Delamination between any plies results in surface-visible effects. From front side only
Coin tap	Positive identification. Distinct variation in pitch from tapping	Positive identification on front surface only
Radiography	Positive identification. Light areas on radiograph	Undetected. Masking effects in bonded panels
Ultrasonics		
Liquid coupled	Detected but variable coupling produces unreliable response	As 'laminate only'
Soft tipped probes	Detected attenuation in through-transmission	As 'laminate only'
Air coupled	Undetected	Undetected
Roller probes	Positive identification	Positive identification
F.B.T.	Positive identification	Positive identification from front only
A.F.D.	Positive identification	
Thermography	Positive identification	Detection from both sides but poor resolution
Holographic Interferometry	Not attempted	Positive identification from front surface. Not attempted from reverse

TABLE 9

Defect Type NDT method	Prepreg Backing Contamination and Debonding(Adhesive Hole) Between Face Skin and Honeycomb Core
Visual	Positive identification from front surface. Undetected from reverse
Coin tap	Positive identification from front surface. Undetected from reverse
Radiography	Undetected. Masking effect of bonded panels
Ultrasonics	
Liquid coupled	Partial detection but variable coupling produces unreliable response
Soft tipped probes	Not attempted
Air coupled	Undetected
Roller probes	Positive identification from both sides of the panel
F.B.T.	Positive detection from both sides of the panel
A.F.D.	Positive identification from front of panel. Undetected from reverse
Thermography	Positive identification
Holographic Interferometry	Positive identification from front surface. Not attempted from reverse
Speckle pattern Interferometry	Detected from front surface. Not attempted from reverse

TABLE 10

Defect Type NDT method	Encapsulation Compound in the Honeycomb Core
All methods examined	All methods investigated in this project located the areas containing encapsulation compound

TABLE 11

Defect Type NDT method	Crushed or Damaged Honeycomb Core
Visual	Detected from the front surface of the thin skinned specimens. Undetected from reverse
Coin tap	Positive identification, particularly if the damage causes a debond between skin and core. Undetected from reverse
Radiography	Positive identification of any abnormality in the honeycomb core using medium (50kV) or low (10kV) voltages
Ultrasonics	
Liquid coupled	Detection if debonding caused by damage
Soft tipped probes	Positive detection
Air coupled	Detection if damaged area greater than 2000 mm <sup>2</sup>
Roller probes	Detection in all cases
F.B.T.	Detection if debond caused by damage
A.F.D.	Not attempted
Thermography	Detection from both sides of the panel
Holographic Interferometry	Detection from front surface. Not attempted from reverse
Speckle pattern Interferometry	Detection from front surface. Not attempted from reverse

## 6.2 Mechanical Test Results

### 6.2.1 Flat Specimens

#### 6.2.1.1 0/90/90/0 Lay-up Specimens

The results of the 4-point bend flexural tests are shown in Table 12. The fracture stresses within each defect type group are from a normal population of that group. Statistical t-tests at the 0.05 level (95%) were performed between the defect groups and the control sample group. These showed:-

1. There is no significant difference between the fracture stresses of specimens containing prepreg gaps and splits, good overlap joints and solvent and vapour contamination.
2. There is a significant difference between the fracture stress of the control specimens and that of the specimens contained in 1 above.
3. The defective specimens included in 1 above have an average fracture stress 14% lower than that of the control specimens.
4. Specimens containing butted overlap joints have a lower mean fracture stress than those in 1 but statistical procedures were not justified with two specimens only.
5. The backing sheet contamination defects, both interlaminar and between the skin and core, cause a drastic reduction in fracture strength, (or more precisely failure load as none of the specimens suffered skin fracture, failure being defined as buckling of the core).

#### 6.2.1.2 0/60/120 Lay-up Specimens

The results of the 4-point bend flexural tests are shown in Table 13. The small number of specimens of this type precludes statistical analysis, but the following observations may be made from the data:-

TABLE 12: 0/90/90/0 SPECIMENS. 4-POINT BEND FLEXURAL TESTS

Defect Type	Specimen Number	Orientation	Failure Mode	Fracture Stress GPa	Sample Mean and Standard Deviation GPa	Flexural Modulus GPa	Sample Mean and Standard Deviation GPa
Control	9A	Fibres 11 & 1 to beam axis	Compressive failure of upper face skin	2.85	$\sigma = 0.36$	5.86	$\sigma = 0.36$
	10A	"	"	3.17		5.97	
	11A	"	"	2.55		6.21	
	12A	"	"	3.73		6.14	
	13A	"	"	3.17		6.08	
	14A	"	"	2.99		5.77	
	15A	"	"	3.08		4.80	
Prepreg gaps and splits	1B	"	Tensile failure of lower skin	2.14	$\sigma = 0.29$	4.60	$\sigma = 0.53$
	2B	"	Compressive failure of upper skin	2.63		4.46	
	3B	"	"	2.28		5.80	
	4B	"	"	2.85		5.43	
	15B	"	"	2.71		5.58	
	16B	"	"	2.64		5.86	
	17B	"	"	3.16		5.95	
	18A	"	"	2.55		6.19	
	19A	"	"	2.54		5.79	
	20A	"	"	2.43		5.65	
Butted overlap joints	21A	"	"	2.34	2.18	6.40	6.09
	22A			2.02	$\sigma = 0.16$	5.78	$\sigma = 30$
Good overlap joints	13B	"	"	2.81	$\sigma = 0.23$	5.84	$\sigma = 0.20$
	14B	"	"	2.41		6.26	
	1A	"	"	2.77		6.21	
	2A	"	"	2.40		6.44	
	3A	"	"	2.98		6.03	
Solvent & vapour contamination	10B	"	"	2.39	$\sigma = 0.18$	6.16	$\sigma = 0.20$
	11B	"	"	2.94		5.82	
	12B	"	"	2.65		5.62	
	16A	"	"	2.75		6.07	
	17A	"	"	2.72		5.68	
Backing sheet contamination overlap joint	4A	"	No failure of skin. Aluminium honeycomb failure by backing.			5.30 4.70	5.00
	5A	"					
	6A	"					
Backing sheet contamination causing delamination	18B	"	"			4.63	4.85
	19B	"	"				
	20B	"	"			5.07	
Prepreg gaps, bubbles	6B	Fibre direction 45° to beam axis	Compressive failure of upper face skin.	1.47	$\sigma = 0.19$	1.06	1.24
	7A			-			
	8A			1.22		1.36	
	7B			1.29		1.34	
	8B			1.73		1.19	

TABLE 13. 0/60/120 SPECIMENS. 4-POINT BEND FLEXURAL TESTS

Defect Type	Specimen Number	Failure Mode	Fracture Stress GPa	Sample Mean and Standard Deviation GPa	Flexural Modulus GPa	Sample Mean and Standard Deviation GPa
Control	23C	Compressive failure of upper face skin	1.91	1.57	3.09	3.17
	24C	"	1.55		3.15	
	25C	"	1.38		3.19	
	26C	"	1.45		3.25	
Butted overlap joints	1C	"	1.45	1.39	3.52	3.31
	2C	"	1.41		3.17	
	3C	"	1.32		3.26	
Good	4C	"	1.89	1.78	3.27	3.20
	5C	"	1.74		3.34	
	6C	"	1.70		3.01	
Prepreg gaps	16C	"	1.68	1.58	3.23	3.17
	17C	"	1.48		3.11	
Air bubbles & Solvent contamination	18C	"	1.78	2.0	3.05	3.24
	19C	"	2.22		3.43	
Crushed Core	13C	"	1.53	1.64	1.38	2.38
	14C	"	1.84		3.23	
	15C	"	1.55		2.54	
Backing sheet contamination in overlap joint	7C	No failure of skin.	0.76	0.73	0.38	0.452
	8C	Aluminium honeycomb failure by buckling	0.69		0.59	
	9C		-		-	
Backing sheet contamination between core & skin	10C	"	-		0.703	0.35
	11C	"	-		0.116	
	12C	"	-		0.23	
Backing sheet contamination inter-laminate	20C	"	0.948	1.01	1.02	1.05
	21C	"	1.03		1.07	
	22C	"	1.05		1.06	

49.

1. Four groups of defective specimens, namely those with good overlap joints, air bubbles and solvent contamination, prepreg gaps and crushed core have mean fracture strengths in excess of that of the control specimens. This implies that these defects are not detrimental to the fracture strength in this lay-up configuration.
2. The specimens containing butted instead of overlapped joints have mean fracture strength below that of the control but it is not possible to assess with confidence to what degree this is the case.
3. The groups of specimens containing backing sheet contamination all have significantly reduced fracture strength. The failure mode of these specimens is unlike any other group as no fracture of the skin occurred, failure being defined by crushing of the core.

#### 6.2.1.3 Observations on Failure Mode

All control specimens and defective specimens, except one, containing defects other than backing sheet contamination, failed through compressive failure of the top skin. The failures occurred suddenly and up to the time of failure the specimens showed no visible sign of degradation.

The failed CFRP skins contain crack lines which lie along the fibre directions for all the specimen configurations, i.e. 0/90/90/0 specimens with axis along the 0 direction and 45° direction, and 0/60/120 specimens (Figures 14, 15, 16). The skins failed in a brittle manner and crack propagation was along the principal axes of the skins.

The skin to core adhesive layer also suffered brittle fracture but the core showed little or no damage either just before or after failure. In some cases there was evidence of slight wrinkling of the cell walls indicating a shear stress along the specimens long axis but this was slight. In cases where this did occur the effect was greatest at the point of failure.

The crack line across the specimens was not straight but consisted of a series of steps. The average crack line was approximately straight across the width however, even in the case of the 0/60/120 specimens.

Microscopic examination of sections of failed specimens showed in some cases complete failure of all plies leaving a fracture surface perpendicular to the plane of the skin, Figure 17 and some cases extensive delamination, Figure 18. It was not possible to correlate failure modes with the defect types as time available did not permit mounting and sectioning of all the specimens.

The specimens containing backing sheet contamination showed buckling of the skin on the compressive face, with no fracture. The tests were stopped when the aluminium core failed. In all cases the core deformed continuously until failure, at which point the cell walls in compression collapsed forming a discontinuity, Figure 19.

#### 6.2.1.4 Acoustic Emission from Flexural Tests

For specimens within a group containing the same defect type, the acoustic emission data were similar. Typical graphs of total count versus deflection and load are shown in Figures 21a to 21m.

For clarity the three highest amplitude levels only are shown, L1 representing the highest amplitude. Thus counts on the L1 channel represent events  $10^6$  times more energetic than those on L3.

The control specimens of both lay-up types (Figure 21a and 21h) showed little activity until immediately prior to fracture and in both cases the highest numbers of counts were on L2 and L3. Only at the point of failure did high amplitude counts occur on L1. The emission on L1 appeared as a large instantaneous burst.

The good and butted overlap joints of each lay-up type (Figures 21b, c, i, j) exhibited similar characteristics. Low amplitude emissions occurred at lower deflections than in the controls. The onset of emissions was earlier in the good overlap joints than in butted joints and the presence of rich no counts

were recorded on L1 until fracture. The emissions tended to occur in large bursts separated by periods of quiescence.

The emission behaviour of specimens containing side to side butt gaps and prepreg gaps (Figures 21d and 21k) were similar. That is to say low amplitude emissions occurred in a large number of small steps and high amplitude emissions were not present until the point of failure.

Figure 21f illustrates the typical emission from a specimen containing a backing sheet contamination defect. There are high counts on the low amplitude levels, L2 and L3, and a very low count on L1. This corresponds to the observations during testing where buckling of the skin accompanied by deformation of the honeycomb core but negligible fibre breakage occurred.

The behaviour of the specimens containing encapsulation compound (Figure 21l) was characterised by the rise in small increments of the L3 count indicating activity of low energy processes.

The crushed core defect, (Figure 21m), shows progressive damage on L1 and L2 in the early stages of the test followed by a large burst of energy at failure.

The 0/90/90/0 specimen oriented at 45° to the fibre axes showed no activity until at a relatively large deflection. At this point there was a large burst of activity on L2 and L3 but none on L1 (Figure 21g).

#### 6.2.2 Bicurved Specimens

##### 6.2.2.1 Vibration Testing Results

The results of the vibration tests on the four bicurved dish specimens are shown in Tables 14, 15, 16, 17.

One of the dishes, Dish 2, failed as a result of catastrophic growth of defects, whilst three of the dishes suffered premature termination of testing through failure of peripheral components. However, in all cases high g levels were imposed on the dishes before testing was terminated.

TABLE 14

Dish 1.

Resonant Frequency 325 Hz

<u>Phase</u>	<u>Test No.</u>	<u>Input Level</u>	<u>Frequency</u>	<u>Comments</u>
1	1-14	1-70	100	No A.E.
	15	40	325	Test at resonance. No A.E.
	16	70	325	" " " "
2				Not tested
3	17	20	120-300	Slow sweep at oct/min. Rim loading mass became detached at 174z causing severe damage to dish. Tests terminated. No A.E. from defects.

A.E. = Acoustic Emission.

TABLE 15

Dish 2

Resonant Frequency 430 Hz

<u>Phase</u>	<u>Test No.</u>	<u>Input Level</u>	<u>Frequency</u> <u>Hz</u>	<u>Comments</u>
1	1-8	1-70	100	No A.E.
	9	20	430	Test of resonance. No. A.E.
	10	50	430	Test at resonance No A.E.
2	1-6	1-15	100	No A.E.
	7	20	100	A.E. event from defect L
	8	25	100	No A.E.
	9	30	100	No A.E.
	10	40	100	A.E. event from defect J
	11	5g	35-2000	Sweep at 2 oct/min.
	12	20	180	No A.E.
	13	30, 40, 50, 60	180	A.E. from defects L & J. Events occur as input acceleration level is raised, No failure occurred and A.E. activity ceased after several seconds at 70g.

TABLE 15 (Cont'd)

<u>Phase</u>	<u>Test No.</u>	<u>Input Level</u> g	<u>Frequency</u> Hz	<u>Comments</u>
3	14	10	50-2000	Sweep at 2 oct/min to locate a frequency band which contained the resonance frequency.
	15	60	120-180	Slow sweep at 1 oct/min. The dish failed at resonance, frequency 132 Hz. A.E. from L & J. Failure caused by two radial cracks through defects L & J.

TABLE 16

Dish 3

Resonant Frequency (Phase 3) 127 Hz

<u>Phase</u>	<u>Test No.</u>	<u>Input Level</u>	<u>Frequency</u>	<u>Comments</u>
1				Specimen not available.
2				Specimen not tested.
3	1	5	50-500	Sweep at 2 oct/min.
	2	100-300	20g	Sweep at 1 oct/min. A.E. Event simultaneously on all channels.
	3	120-300	50g	Sweep at 1 oct/min. A.E. activity on all channels. Load spreader/dish bond failed at 127 Hz. A.E. events apparently associated with this. Tests terminated

TABLE 17

Dish 4

Resonant Frequency (Phase 3) 162 Hz

<u>Phase</u>	<u>Test No.</u>	<u>Input Level</u>	<u>Frequency</u>	<u>Comments</u>
1				Specimen not available.
2	1	1	5-2000	Sweep at 2 oct/min to find resonance frequency.
	2	10	400	No A.E.
	3	20	400	A.E. event. Source located at defect U (Fig. 11).
	4	40	400	" " " " " " "
	5	50	400	" " " " " " "
	6	60	400	A.E. activity. Events more frequent and persistant.
3	7	10	50-2000	Sweep at 2 oct/min.
	8	150-300	50g	Slow sweep at 1 oct/min. At 162 Hz two transducers became detached from the CFRP skin causing severe damage. Tests terminated.

Dishes 1 and 2 were available for Phase 1 testing and both experienced high g levels at their resonant frequency; 70g at 325 Hz in the case of Dish 1, 50g at 430 Hz for Dish 2. No acoustic emission was recorded.

Dishes 1 to 4 were available for Phase 2 and 3 and it was considered more efficient to fully complete tests on one dish before mounting another.

Phase 2 produced defect activity in Dishes 2 and 4, detected as bursts of acoustic emission, whilst Dishes 1 and 3 were not tested.

Dishes 1, 2, 3 and 4 were tested in Phase 3.

Dish 1 Tests were terminated when a segment of loading mass mounted on the rim of the dish, became detached, causing severe damage to sandwich material in that area.

Dish 2 Acoustic emission was detected and the active defects located in the dish during Phase 2. Dish failure resulted from growth of cracks through the active defects, (Figure 20). The cracks extended from the load spreading plate radially to the rim, separated by 120° and each passing through a crushed core defect which had caused debonding of the skin and core. The honeycomb was split along the path of the crack. The failure occurred at 132 Hz and an input level of 60g. However the amplitude amplification factor at resonance resulted in a level of 260g being recorded at the rim at failure. At this frequency the mode of vibration caused a 240° segment of the dish to be in antiphase with the remaining 120° segment, the resulting large amplitude causing stresses severe enough to fracture the honeycomb material.

Dish 3 During the course of testing, the adhesive bond between the load spreader plates and the CFRP skins failed catastrophically. No acoustic emission was detected from the defects in the dish and testing was terminated.

Dish 4 A defect was active during Phase 2 testing and this was identified as backing sheet contamination within the skin. However no catastrophic failure had occurred and a level of 50g was

selected for the input during a sweep through resonance. This caused detachment of two of the three acoustic emission transducers which resulted in severe damage to the CFRP skin and termination of the tests.

#### 6.2.2.2 Observations on the Vibration Tests

Throughout the testing only three active defects were detected, and in each case these were in the severe category in which a debond of skin and core or a delamination in a face skin had occurred. Further, the acoustic emission associated with these defects revealed a characteristic behaviour. During any test where activity was detected the emissions occurred in a burst in the form of a slow initial emission rate which rose to a maximum and then emission stopped. The length of the burst was a function of the input level, lasting several seconds in tests at the beginning of Phase 2 and rising to several tens of seconds at high levels at the end of Phase 2.

However having stopped, no further emissions occurred until a higher input g level, i.e. higher stresses, was selected. Thus the results of these tests suggests that a defect which is active at a particular stress level is eventually accommodated by the surrounding material and activity stops. Not until higher stresses are imposed does activity re-occur. Only in the case of Dish 2 were stresses imposed which were large enough to cause continuous and rapid growth of the defective areas, resulting in a loss of stiffness of the honeycomb material and subsequent large scale failure.

## 7. DISCUSSION

### 7.1 Flexural Testing

Both the flexural modulus and the ultimate fracture stress were found from the 4-point flexural testing programme. The comparison of these parameters enables a distinction to be made between the localised and average effect of the different defect types. The flexural modulus defines the behaviour of a specimen subjected to loads less than the fracture load and is thus an

average over the whole specimen. The fracture stress however is defined as an event at either the weakest point or the point of highest stress concentration. By comparison with nominally perfect specimens an indication is obtained of the extent to which the material is weakened by the various defect types.

Tables 12 and 13 indicate that the only defects which caused significant modification to the flexural modulus were contamination by backing sheet and crushed core. The reason for this is that this group of defects modified the deformation mode. The defects extended across the full specimen width and caused local increases in compliance. The crushed core defect caused a local reduction in thickness, and the contamination within plies or at the skin/core boundary allowed the onset of buckling to occur at very low compressive loads. Had it been that these defects were small compared with the specimen width, it is likely that they would have been supported by surrounding material and their effect would have been much less marked.

Butted end-to-end joints extended across the full specimen width and the fact that they did not cause a reduction in modulus indicates that efficient stress transfer across the joint has been effected by the adjacent layer. The stress transfer length and therefore the area in which strain intensification occurred was small compared with the total surface area under test and therefore the effect of localised strain intensification on the measured modulus has not been detected.

The disturbance to the direction of fibres close to an overlap joint and the associated resin rich zones, and the presence of solvent and vapour contamination may all lead to localised strain intensification but the magnitude of this effect has been small compared with the total strain imposed. The presence of prepreg splits effectively reduces the number of fibres carrying load and since the splits correspond to the absence of a very small proportion of the fibres and the effect on modulus is small.

When localised strain intensification occurs due to the presence of a defect, the area close to the defect reaches its

fracture strain at a lower applied stress than the rest of the specimen. It is to be expected therefore that the defects causing the highest strain intensification in specimens should act as fracture initiation sites and that even defects showing little or no effect on modulus would cause significant reductions in ultimate strength. Thus if the defects which have been deliberately introduced to the specimens, are more severe than those which occur naturally they should cause reductions in ultimate bending moment of the specimens. Tables 12 and 13 show that this has been the case. The severe defects which influenced the flexural modulus, backing sheet contamination and crushed core, had a marked effect on ultimate bending moment. The backing sheet contamination resulted in failure of the defective skins to support compressive loads with a resulting fall in ultimate bending moment. Damage to the core by crushing results in fibre bending at the defect edge and in severe cases, debonding between skin and core, both of which cause significant reduction of the fracture stress, either through stress intensification or buckling of the compressive debonded skin.

The remaining (less severe) defects were shown to have caused a statistically significant reduction in ultimate bending moment but the relative effect of the various types does not emerge from the statistics. It is only possible to calculate therefore that members of this group of defects behaved similarly and on average they caused a 14% reduction in ultimate bending moment.

It is interesting to note that both overlapped and end-to-end butted joints in the prepreg had an effect on ultimate bending moment. This is an important consequence, for although there is probably adequate stress transfer in tensile situations, for which overlapped joints are required, there is also a geometrical consideration at the joint. The overlapped zones contain buckled fibres and resin fillets both of which are deleterious in compression, whilst the butted joint cannot provide adequate stress transfer along the fibres of the jointed ply, consequently localised overstrain is inevitable. Thus in both

cases there are processes which exacerbate the stress in the compression skin and cause premature failure. Thus it is not correct to assume a conventionally overlapped joint is equivalent to a continuous ply in terms of mechanical properties. This is discussed further in Section 7.2.

59

The reduction of ultimate bending moment is only apparent in the 0/90/90/0 specimens. Although not enough 0/60/120 specimens were available to enable statistical significance tests to be performed, inspection of the data indicated that the less severe defects have no effect on the fracture stress. This contrast in behaviour of the two lay up types is not understood and further work is required to investigate and confirm this result.

No account was taken of the effect of moisture in the present tests. Experiments in the United States have shown (private comm.) that moisture migrates to defect sites and precipitates causing degradation of the honeycomb core and the skin/core bond. The interaction of this and outgassing is unknown as is the effect, if any, on the fatigue performance of the sandwich.

Two important points must be made from a consideration of these data. The first is that all the defect types have been effective in reducing the fracture stress in these specimens. The fact that they fall into two different populations is probably a reflection of the fact that one group was very large compared with specimen width whilst the other group was small. It is essential therefore if a quantitative assessment of the effect of defects is to be obtained, that a fracture mechanics approach should be taken, which relates defect size, specimen size and critical stress level for defect growth.

The second point is that whilst certain defects had insignificant effect on flexural modulus there is no doubt from the fracture stress data that they acted as strain intensifiers. They might therefore be expected to act as preferred sites for fatigue failure and their effects upon fatigue performance should be examined.

## 7.2 Acoustic Emission from Flexural Tests

The observations on the control specimens, Figures 21a and h indicated that no failure events occurred until 90% and 60% respectively of the ultimate fracture stress had been applied. This was in contrast to the behaviour of defective specimens. The fact that the acoustic emission (A.E.) behaviour within specimen groups which contained the same defect type were similar and that each group had a different signature indicate that A.E. may be very valuable in qualification testing of structures when it is in the hands of an experienced operator.

In general, defective specimens generated emissions early in the test procedure and a characteristic was that the emissions tended to occur as bursts of activity followed by periods of no activity. The bursts of activity were usually in the low energy channels which indicated resin cracking and delamination type processes, until the final fracture stress was approached when activity was recorded in the high energy channels. This was presumably due to fibre failures and massive delamination events. The bursts of activity early in life are due to development of cracks in the vicinity of defects and the following periods of low activity indicate that these crack growth events have successfully redistributed stresses in the region of the defect and reduced strain concentrations. The cracks have thus become stable at the applied stress levels. Work by Fuwa Bursell and Harris <sup>(3)</sup> on unidirectional CFRP showed that A.E. was generated on loading a tensile specimen but there was no A.E. on unloading. Subsequent loading to the previous maximum load produced much less A.E. and after less than ten cycles no further A.E. was produced, unless the maximum load level was raised. Their results indicated that if a specimen is never reloaded above 94% of the maximum load reached on the first cycle, no new damage will occur and the material will in effect be below a "fatigue limit". Although there are major differences in material properties between the unidirectional CFRP and the honeycomb sandwich panels, the face skins of the sandwich experience compressive and tensile stress in flexural tests and it is reasonable that damage accommodation occurs in the same

manner. This further emphasises the requirement for work which would examine the critical defect size above which damage could not be accommodated for a given stress level thus causing continuous defect growth.

It should be noted (compare Figure 21a to g with Figure h to m) that A.E. observations were similar on 0/90/90/0 and 0/60/120 specimens containing the same defect type. This is to be expected but conflicts slightly with the unexpected observation that the 0/60/120 specimens did not appear to have lower fracture stresses than the nominally defect free specimens.

In Figure 21f it is observed that specimens containing backing sheet contamination defects are the ones which generate emissions earliest in the testing. This is because they are the most severe type and is consistent with the observation that this group had reduced flexural moduli.

Figures 21a, b, i and j compare the behaviour of overlap and butted end-to-end joints. Both generate emissions much earlier in testing than the control which concurs with the observations in 7.1 but it is interesting to note that the overlapped joints were active much earlier than the butted joints. This suggests that the kinking of fibres at overlaps and the resin rich fillets are more severe defects than a straight end-to-end joint. It would appear that resin cracking in the region of the overlap occurs at a lower load than it would in an end-to-end joint. This would tend to destroy stress transfer at the overlap and thereby render it redundant. It is not surprising therefore that the overlap specimens were no stronger than the butted specimens and that both were less strong than the controls.

The results on specimens containing prepreg gaps indicate resin cracking occurred to a much higher degree than in end-to-end jointed specimens, (note scaling factors), this was not expected and is not clearly understood. It does appear however, that whenever resin rich zones occur whether they are connected with joints or merely with a reduced fibre concentration cracking occurs at lower stress and ultimate bending moments are reduced.

Solvent contamination, (Figure 21e), led to a high rate of emission at low applied load and these specimens also had low strain to failure values. This suggests that the contamination has led to interlaminar crack growth, (because the defects were interlaminar), through the major part of the test, and to premature failure.

Specimens containing encapsulation compound showed similar behaviour to the controls, Figure 21f. This result is expected since there are no defects which lead to high local strain concentration. Similarly with the crushed core defect, Figure 21m, the strain concentrations again appear small, in this case. However the local strain intensification caused by a crushed core defect is probably extremely dependent on the depth and area of crushing with respect to the effects of fibre kinking and skin/core debonding described in Section 7.1. It may be concluded that the low levels of activity seen in both these defect types at deflections of 0.5 cm to 0.9 cm are due to the slight strain concentrations at the areas where the specimens change stiffness, i.e..the edges of the encapsulation compound or crushed core.

Figure 21g shows the behaviour of 0/90/90/0 specimens cut so that the fibre directions were at  $\pm 45^\circ$  to the specimen axis. The A.E. behaviour was similar to the controls up to 1 cm deflection but beyond this they were interesting. A burst of emissions at approximately 1 cm deflection was followed by a relatively quiet period up to failure at 2 cm deflection. Control specimens failed at 1.2 cm deflection. It seems likely that the bursts in the  $45^\circ$  specimen were due to relaxation of shear stresses by resin cracking or delamination but no direct observations of this were made. It seems unlikely however that a 2 cm deflection could have been sustained before failure unless some stress redistribution had occurred. The significance of this to real structures is not that high levels of emission are likely to occur at the deflection which would correspond to failure of a 0/90/90/0 specimen cut parallel to a fibre direction, but that if

large scale stress redistribution occurs below the nominal failure load it should be accompanied by these high levels of emission.

Whilst the A.E. method does not constitute a non-destructive test most structures have to pass a qualification proof test. These experiments have indicated that monitoring of A.E. during proof tests can provide information on whether or not defects are present.

The use of reloading may, through observation of the emission phenomenon described above indicate whether or not defects continue to be active after a first load cycle. If emission stops after a number of cycles then it is unlikely that further defect growth will occur unless the previous maximum load is exceeded. Further work is required to determine the similarity in behaviour of CFRP and CFRP/Al honeycomb but because the skins of the sandwich material experience tensile and compressive stresses it is reasonable to postulate similar behaviour. Other work (Reference 4) has stated the CFRP does not show true fatigue behaviour, however in defective material there may well be a critical size for each defect type, which, above a given stress level, causes continuous growth and therefore premature failure under conditions of cyclic loading.

### 7.3 Vibration Testing

The aims of the vibration testing programme, to cause failure of the dishes containing deliberate defects and to record the acoustic emission (A.E.) from any defect growth, were partially met. Section 6.2.2.1 shows that only one dish failed as a result of defect activity whilst the other three had pre-shortened tests because of the failure of attachments to the dishes, of various components.

The primary observation on the test results is that with the specimens used in this project it was extremely difficult to impose stress/strain intensities high enough to cause any defect

growth. Phase 1 testing, in which stress was generated by the g forces acting only on the dish mass itself, produced no acoustic activity, indicating no defect growth. Phase 2 testing involved greater stresses on the dishes through the use of annular masses on the dish rims but although valuable A.E. data was accrued indicating some defect activity, no failure occurred. Failures occurred in Phase 3 but only in one case as a result of defect growth. The other failures, although providing interesting information, did not involve any of the inbuilt defects. However it should be noted that all phases involved g levels at the operational limit of the vibration equipment.

As reported in Section 6.2.2.1, Dish 2 failed when two radial cracks were formed, each passing through a defect. The defects involved were areas of crushed core and acoustic energy was emitted from their vicinity during much of Phase 2 and 3 testing. Defect L, the area of core crushed by 3 mm, caused debonding between the skin and core and one of the cracks passed centrally through this area.

A sweep at 2 oct/min at the beginning of Phase 3 indicated a resonant frequency of 190 Hz. After a series of tests at increasing g levels up to 60 g a further sweep showed that the resonant frequency had fallen to 155 Hz. This lowering of resonant frequency corresponded to a reduction of the overall stiffness of the dish. Growth of defects was the most likely cause of this but there was no visible evidence of degradation of the dish until fracture, however A.E. detected, emanating from the two defects and is discussed later.

At failure, as the resonant frequency was approached, the amplitudes of the three rim-loaded segments of the dish were over one centimetre. When two of the segments vibrated in antiphase with the third, large strains were imposed which caused rapid and catastrophic growth of the defects. It is interesting to note the different behaviour of the two crushed core areas involved. Defect L, crushed to 3 mm depth caused a debond between skin and core and a crack propagated across the

centre of the debonded area (Figure 20). However Defect J, crushed core to a depth of 1 mm, did not cause a debond and the crack associated with it propagated along the radial edge of the crushed core area. This result concurs with the observations on this type of defect in Section 7.2, that both debonding across the defect and stress intensification at the edges can be important. Further, Dish 2 contained a deliberately debonded area, Defect M, effected by a film adhesive hole, which generated no emissions. Although at an equivalent radial distance to Defects J and L this defect was smaller in area and had no core discontinuity at its edge. Thus the crushed core area having caused a debond, became more deleterious than an initially debonded area. This is concluded to be a combination of the reduced stiffness of the crushed core and the stress intensification at the edges.

The A.E. associated with the defect growth showed the discontinuous characteristics described in Section 6.2.2.2. These results are in good agreement with those found in the flexural testing and discussed in Section 7.2, where, at a particular stress level, when a defect grows it redistributes local excessive strain and eventually is accommodated by the surrounding material. This process occurred consistently until the failure of Dish 2, which indicated that for the defects involved a critical stress level was reached at which accommodation did not occur rapidly enough to prevent catastrophic crack growth.

The fact that the backing sheet contamination defect in Dish 4, the only other defect to generate emissions, did not cause failure indicates that the critical stress level was not reached. Although one of the severe defects, its shape was very different to that of the crushed core areas. It is reasonable to suggest that shape plays a part in the effectiveness of the defect, particularly when considering the maximum stress a component can tolerate. The emissions were similar in form to those from Dish 2 and the same accommodation processes were involved. The important point to be drawn from this behaviour is that both the flexural and vibration modes of testing indicate

662  
that defects are important but in order to quantify the effect a fracture mechanics approach is required. The fact that defects in Dish 2 caused failure and those in the other dishes did not, further indicates that parameters such as critical stress level and critical size need defining for defects in bulk specimens.

The failures of sub-system attachments to Dishes 1, 3 and 4 were both undesirable and unexpected as far as defect investigation was concerned. However, the various methods of attachment are commonly found on service components and the fact that acoustic emission was recorded from the degrading attachment points, and that its source could be identified is a useful result for qualification testing. Three different types of failure occurred; the bonded (Hottinger accelerometer adhesive) and bolted rim segment breaking away from the rim of Dish 1, the redux bonded (Ciba Geigy 410) aluminium load spreading plates becoming detached from Dish 3, and the bonded (Hottinger) transducers lifting from the surface of Dish 4. These types of failures can all be regarded as possibilities in service, and although A.E. was recorded prior to failure, high g levels near the resonant frequency in Phase 3 were required before these events occurred. The importance of these emissions is, in common with the inbuilt material defects, that if there is activity during testing then emissions are generated and the activity can thus be detected.

The results of the vibration test programme show correlation with the flexural testing both in the context of the present project and in indications of the requirement for further work. The more severe defects of backing sheet contamination and crushed core have proved most deleterious but both modes of testing have pointed to the need to determine quantitatively the size, configuration and stress level, and the relationships between them, for defects to grow continuously rather than be accommodated. The acoustic emission evidence suggests that any failure processes, whether from defects or peripheral components, can be monitored and its source identified.

Evidence from this project and elsewhere, Section 7.1, leads to the observation that if a defect, does not produce emissions at a particular stress, whether or not it has done so in past testing, there is little likelihood that it will become active at that, or any lower, stress level. This is particularly important in aerospace projects where stress is accurately predictable. If in qualification testing, the stress levels imposed are higher than those to be encountered during service and the specimen is found to be acoustically quiet then the evidence indicates that no defect growth will occur.

#### 7.4 Non-Destructive Testing

The survey of non-destructive test methods for use in locating and identifying defects in CFRP/Al sandwich materials has revealed two categories into which all defects fall. These correspond to the categories established in the test programme and are broadly the severe group (backing sheet contamination, crushed core debonds and delaminations) and the less severe group (prepreg gaps and splits, end-to-end joints, overlap joints, vapour and solvent contamination). It should be stressed however that in terms of NDT, the categories arise as a result of ease of detection and this is not simply related to their size. In the case of the mechanical test results the categories may well have emerged because the defect types in the severe group occupied the full specimen width whilst those in the less severe group did not.

Before undertaking a detailed discussion of the test methods examined it should be stressed that in order to minimise cost it is desirable to conduct tests as early in the manufacturing process as possible. This allows defective structural elements to be discarded before they are integrated into otherwise perfect structure.

In order to evaluate the NDT techniques examined, criteria of practicability, effectiveness and availability must be considered. It is inevitable that the optimum solution for examination of complex structures will be a combination of methods

and a compromise between these criteria.

The traditional methods of visual examination and coin-tap testing undoubtedly form the optimum initial test procedures. They will inevitably occur at all stages of manufacture and many defects will be located and identified before any more sophisticated techniques are used. Visual inspection is performed during lay-up of a skin and whilst it is still on its mould after curing. This gives a very early indication of any major defects, before any handling has occurred. Coin-tap testing will locate debonds and delaminations both in the skins and the integrated sandwich panels. Although not as objective as more advanced techniques these methods certainly fulfil the requirements of practicability and availability. Furthermore a skilled operator can be highly effective in defect location using these simple methods.

The most reliable technique after examination of visual and coin-tap testing unbonded skins is low voltage contact radiography. This method allows all skin defects except solvent or vapour contamination to be located and identified (See Table 4). This method provides the greatest amount of information, in addition to ease of interpretation, of any of the methods used on the unbonded skins. The disadvantages of the method however, are the severe difficulty in dealing with curved skins and the need to handle all skins, curved or flat, before any examination can occur. Unfortunately the effectiveness of the technique, extremely high on flat unbonded skins, is not transferred to the bonded panels because of the masking effects of two separated skins and adhesive layers.

The honeycomb core can be examined using higher energy x-rays after integration with the skins but because the x-ray source is effectively point-like, the depth of the honeycomb cells causes shadowing, the severity of which increases with distance away from the perpendicular between the source and specimen. However irregularities and inclusions in the core,

particularly encapsulation compound, can be located quickly and accurately, especially if a direct viewing cabinet can be used.

Overall the radiographic technique has the advantages of extremely high effectiveness in locating the less severe defects in the skins and damage to the aluminium core, combined with relative abundance of generation equipment. It does, however, have the disadvantages that all specimens need to be handled before inspection, curved skins are difficult to examine, either on or off the mould and, using higher energies in integrated panels, only core defects can be found but not debonds or skin defects. The low voltage technique is not at all effective on the bonded panels.

Where radiography is not feasible, two ultrasonic test methods can be considered as suitable alternatives. The first is the roller probe/discriminator technique. The roller probes provide good, consistent coupling of ultrasonic energy whilst allowing free movement of both transmitting and receiving transducers across the specimen surface. The probes themselves are not innovative as devices, although several (proprietary) novel materials and features were incorporated in those used in this project. The technique is further greatly enhanced by the frequency discriminator, which is the innovative element of this ultrasonic method, which simplifies the output information to the extent that this becomes an efficient simple and accurate method for locating and identifying all types of defect except solvent and vapour contamination.

The method has the advantages of being commercially developed and consequently test instruments, both probes and discriminator readily are available. The technique can be used in through-transmission or transverse-transmission so that skins can be examined whilst still on the mould and both skins and panels can be scanned quickly. The effectiveness is high, with detection and identification capability for all defects except solvent and vapour contamination.

The only real disadvantage of the method is evident when it is compared to radiography of flat skins. The radiographs provide easily interpretable data and "hard copy" of the information in what is essentially the C-scan mode, whereas the ultrasonic method relies on the oscilloscope A-scan display for information presentation unless special scanning jigs are constructed. Thus the effectiveness of the ultrasonic technique is more reliant on operator skill.

The second ultrasonic technique is the Fokker Bond Tester, which is a well-known and well-established instrument. Only severe defects (backing sheet contamination and crushed core) were reliably detected in this project but it is recognised that many users consider detection of these defect types sufficient for their purpose. Further, because the instrument uses a single transducer, skins can be examined whilst still on the mould, eliminating handling problems. One of the significant advantages of this method is the wide availability both of the actual instruments and of skilled and experienced operators.

The instrument suffers from the same disadvantages as other direct contact techniques in that energy coupling is a problem. Copicus amounts of coupling fluid are required to produce acceptable results. To avoid couplant ingress, the skins are sometimes covered with a coating of thin plastic film, but this carries a risk of damage as it is removed. Further the surfaces of panels are rarely flat owing to the depression of the skin at the centre of each honeycomb and it is the resulting inconsistency in coupling which makes defect identification particularly difficult.

In the hands of experienced operators the effectiveness of the roller probe/discriminator method and the Fokker Bond Tester are probably comparable but there is no doubt that the former is more efficient in fault location and identification, and additionally there is no risk of contamination by coupling fluid.

The other ultrasonic techniques studied in this survey; soft tipped probes, direct contact and air coupled, all had serious disadvantages when compared to either the roller

probe method or the Fokker Bond Tester. The air coupled technique is still under development and is discussed later. The soft tipped probes detected prepreg splits in addition to the more severe defects of backing sheet contamination and crushed core. However examination of large areas is slow and laborious when compared to the roller probes and consequently the latter technique is preferred. Direct contact ultrasonics is extremely difficult to use successfully on the integrated panels as described in Section 5.1.5 and in common with Fokker Bond Tester always produces a potential source of contamination by acoustic couplant. Consequently this technique is not recommended as an alternative to either the roller probes or the Fokker Bond Tester.

It has been shown that the use of four of these techniques; visual, coin-tap, radiography and either roller probe/discriminator ultrasonics or a Fokker Bond Tester will locate and identify all the defects defined in this project with the exception of solvent and vapour contamination.

If radiography is not feasible then the use of roller probe/discriminator ultrasonics is the most satisfactory alternative, used initially in the transverse-transmission mode on the skins whilst they are still on their moulds and subsequently in through transmission on the integrated panels.

Solvent and vapour contamination cannot be detected by any of the NDT techniques investigated, Section 6.1, however it may be possible to detect the presence of pre-cure vapour contamination. If an interply volume of vapour is expelled during the pressure cure then damage could result in the form of split prepreg and fibre buckling at the edges of the contaminated area. Both these residual damage effects could be located by radiography.

The non-contact techniques of thermography, holographic interferometry and speckle pattern interferometry are extremely

attractive in principle, offering large area examination which in many cases means that a whole component can be in the field of view whilst being strained. However serious problems arose during the survey, which tended to detract from these advantages.

Thermography is a sensitive technique for the detection of surface temperature variation. Unfortunately it is extremely difficult to provide a rear face temperature which is so uniform that variations in front face temperature, caused by defects, are larger than those caused by a non-uniform heat source. Variable output across the heat source area, variable source to specimen distance and convection currents all exacerbate this problem.

Further the limit of spatial resolution is of the same order as the size of many of the defects likely to occur in CFRP and CFRP/Al honeycomb. The defects that were detected in this survey were prepreg splits, backing sheet contamination, crushed core and encapsulation compound. However these were in known positions and could be "searched for" and it is considered that even under the best heating conditions attained, defects present whose location was not known beforehand would probably remain undetected, either because they could not be resolved or because of non-uniform background effects.

Although not attempted in this project it may be possible to use the heat of a still-warm platter or mould, immediately after cure, to provide a uniform temperature on the skin's rear surface, and to permit examination before any handling.

Holographic interferometry is an elegant NDT technique but good quality holograms need to be produced from the specimen. As described in Section 5.1.12 this requires an extremely stable specimen, having maximum movements much less than a wavelength of the illumination. This stability can be obtained although often only with great difficulty. Considerable time is involved in the production and processing of the

holographic plates before any indication of stability is obtained.

Once a good hologram of the specimen is available a further problem arises. Only those defects which cause differential expansion of the surface, on heating, will disturb the interference fringes. In practice these were found to be the more severe defects only, crushed core, backing sheet contamination and debonded areas. Although these are the most serious defects the less severe types have been shown in the flexural testing, to be significant, and therefore require location.

The advantage of this process over thermography is that it is less sensitive to non-uniform heating and consequently more complex components can be examined. However the technique is restricted to detecting only the more severe defects; if this is sufficient then the ability to examine simultaneously the whole front surface of a large component is very useful.

When considering the three criteria of practicability, effectiveness and availability these two techniques show serious drawbacks. However the advantages of non-contact, whole specimen examination, where only the detection of defects such as debonding is required may render them quite attractive. It must be concluded though, that they cannot be recommended as general defect location and identification techniques for use with CFRP and CFRP/Al sandwich composites.

Two techniques examined in the survey are still under development. These are laser speckle interferometry and air coupled ultrasonics. Both offer the same advantages as thermography and holographic interferometry in that they are non-contact methods and in the case of the laser speckle technique, whole body viewing may well become available. Both techniques offer potential advantages of real-time examination with the consequent capability for rapid adjustments to obtain optimum defect detection conditions.

The speckle pattern interferometric technique described in Section 3.7 may obviously be subject to the same stability problems of conventional holography, but because the interference fringes are formed "live", instantaneous indication of instability is given and adjustments can be made. At present the specimen is strained by heating to produce fringes and this may mean that only the more severe type of defects can be detected, as in the case of holographic interferometry.

Air-coupled ultrasonics at present is a little used method but development of higher energy density at the specimen will improve this situation. The development of focusing transducers and higher operating powers is well advanced and these should improve the detection ability of the method in this application. This coupled with the advantage of non-contact, real-time examination could make the method an attractive alternative to the various contact techniques. At the present time the unfocussed ultrasonic beam renders the resolution of the technique very low and only defects covering relatively large areas can be detected. Consequently at the moment this technique does not appear useful in this application but further developments may well alter this situation.

8. SUMMARY AND CONCLUSIONS

(1) The effects of defects on ultimate strength are more marked than they are on modulus. This is because localised strain concentrations associated with defects are averaged over a large specimen volume when modulus determinations are made. Failure is initiated at points of concentrated strain associated with defects in both nominally sound and defective specimens.

In the nominally defective specimen the defect size or type is such that the strain concentration for a given stress is more severe than the general levels associated with intrinsic defects in the material. Thus failure is initiated at the nominated defect at a lower stress than it would otherwise be.

(2) In this work only defects which extended across the full specimen width caused measurable reduction in flexural moduli. These were contamination of the skin by inclusion of backing sheet, contamination of the skin core boundary by backing sheet and regions of crushed core. The remaining smaller defects did not affect modulus and this difference in behaviour may simply be a reflection of different defect size rather than defect type.

(3) All defect types examined led to reductions in ultimate flexural strength but reductions associated with the large defects were very much more marked than those associated with small defects. There is thus a marked effect of defect size and in order to obtain a quantitative estimate of the effects of defects it will be necessary to adopt a fracture mechanics approach in which critical defect sizes for given states of stress and particular defect types are determined.

(4) End-to-end joints in prepreg lead to reductions in ultimate strength whether or not they are overlapped. This is because in the butted case localised strain intensification occurs due to lack of continuity of stress transfer and in the overlapped case distorted fibres and resin rich fillets give rise to localised strain intensification and cracking.

(5) Crushed core defect leads to both a local reduction in thickness and localised buckling of the skin. The resulting strain intensification under load can lead to delamination and early failure. Similarly the presence of potting compound in a core can lead to a local decrease in compliance which causes strain intensification at its edges and can also cause early failure.

(6) In this work no attempt has been made to measure the effects of moisture or cyclic loading on the effects of defects. It is well known that moisture migrates to defect sites and the strain intensification which occurs at defects is likely to

assist in the development of fatigue damage. These factors are worthy of further consideration.

(7) The acoustic emission behaviour of all nominally perfect specimens were similar to each other but distinctly different from all specimens containing defects. It was a characteristic of the nominally perfect specimens that no significant emissions were detected until immediately before failure.

The behaviour of specimens containing defects was consistent within groups containing the same defect type but different between groups. All defect types caused the generation of emissions early in the loading history and the distinction between types was in terms of the energy of the emissions and the general specimen strain at which they were detected.

(8) The acoustic emissions which were detected at low load levels corresponded to the growth of resin cracks in interlaminar planes or skin to core boundaries. These cracks modified the deformation behaviour and caused early fibre failure.

(9) Acoustic emissions which occurred at low loads tended to be generated in short bursts which corresponded to bursts of crack growth. Crack growth steps caused redistribution of strain concentration which led to temporary arrests until higher load levels were imposed. Results in vibration tests suggest that cracks stabilise at particular stress levels and further cycling does not lead to further growth in the short term. This does not give an indication of long term stability however.

(10) Testing of a specimen cut at 45° to the fibre directions confirmed that the low energy emissions were due to resin cracking rather than fibre failure.

(11) During vibration testing low level acoustic emissions were continually detected from the test equipment. When

failure mechanisms in the dishes occurred, the emissions from these emerged very clearly, in terms of amplitude and frequency of occurrence, from the background level.

(12) During vibration testing 1 dish failed by growth of cracks initiated at defects, and 3 failed by debonding of attached components (rim masses, centre support-plates, transducers). Whilst these were not the intended failure modes they all involved failure of adhesive bonds or resin failure. Defect growth and gradual failure of centre plate adhesive bonds caused emissions at load levels well below failure load whilst failure of Hottinger adhesive bond only caused emissions immediately before failure. This indicates differing rates of damage development in the two types.

(13) No single non-destructive testing method has been successful in identifying all the defects considered.

(14) On thin skins it is possible to detect prepreg gaps or splits, overlap joints and butt joints by visual examination if they are in the outer plies. If they are not in the outer plies they are not detected visually. When interply contamination causes a debond this may be detected visually. On integrated panels regions of crushed core skin to core debonds caused by contamination may be detected visually but debonds due to holes in the film adhesive are not. Thus visual examination alone is a valuable test but is not completely adequate.

(15) The second easiest test is the coin tapping test applied to an integrated panel. This detects debonding reliably if the debonded area is tapped. The Fokker bond tester operates on the same principle as coin tapping, it is successful in detecting debonds, it is easy to apply systematically but it causes contamination of the panels.

(16) The most reliable method for detecting and identifying all defects in skins is low energy X-radiography. This identified all defects except vapour contamination in single skins. It is easy to apply to flat skins but difficult to apply

if they are curved. It has a major disadvantage in that skins need to be handled in order to be tested. The method is not suitable for application to integrated panels but higher energy X-radiography will detect damage in the aluminium core.

(17) Roller probe ultrasonic examination is easy to apply to skins and to panels. It detects all defects but skill is required in interpretation of the defect type. It has the advantage that it may be carried out on skins before they are removed from the mould after curing and that it causes no damage or contamination. It is therefore to be preferred to any other ultrasonic method.

(18) In order to obtain highest confidence from presently available methods it is recommended that complete examination using the roller probe method supported by X-radiography of doubtful areas should be employed.

(19) Thermography is an attractive method because it offers the possibility of examining very large areas in a short time, however its theoretical resolution is limited to defects larger than 6 mm and it has been found to be very difficult to apply in practice due to the difficulty of obtaining a uniform surface temperature. It cannot be recommended for routine use at present.

(20) Holographic interferometry does not have the limitations on resolution of thermography and it also has the promise of enabling large areas to be examined. The specimen stability which is required is beyond that which may be reliably produced in a normal test situation.

(21) Laser speckle pattern interferometry and air coupled ultrasonics are promising techniques which overcome problems which appear in holographic interferometry and direct coupled ultrasonics respectively. They are not yet developed to a stage where they may be fully evaluated.

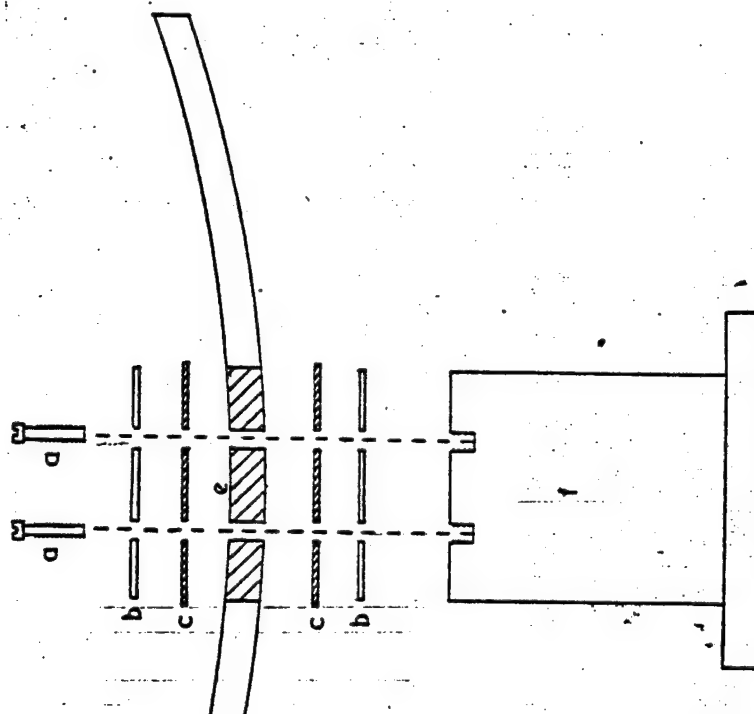
(22) No NDT method has been successful in detecting contamination by vapour and solvent. The mechanical test results indicate that effects due to these defects may be significant. It is essential therefore that maximum care should be exercised to avoid these defects by attention to good housekeeping in the manufacturing areas.

RLC/WHB/MB

1. Tsai, S.W. Mechanics of Composite Materials Part II, Theoretical Aspects AFML-TR-66-149 (Nov. 1966).
2. Chiao, T.T., Hamstad M.A., Proc. 1975 Int. Conf. on Comp. Mat., Geneva, 2, 885 (1976).
3. Fuwa, M., Harris, B. and Bunsell, A.R., J. Phys. D: Appl. Phys., Vol. 8, (1975).
4. Beaumont, P.W.R., Harris, B., Carbon Fibres, their Composites and Applications: Plastics Inst., (1972).

KEY

- a - fixing screws  
(2 not shown)
- b - aluminium alloy  
load spreaders
- c - adhesive fillet
- d - bi-curve  
CFRP\AL dish
- e - encapsulating  
compound
- f - aluminium alloy  
mounting bracket



scale  
1:2

FIG.1 Vibrational testing rig

82

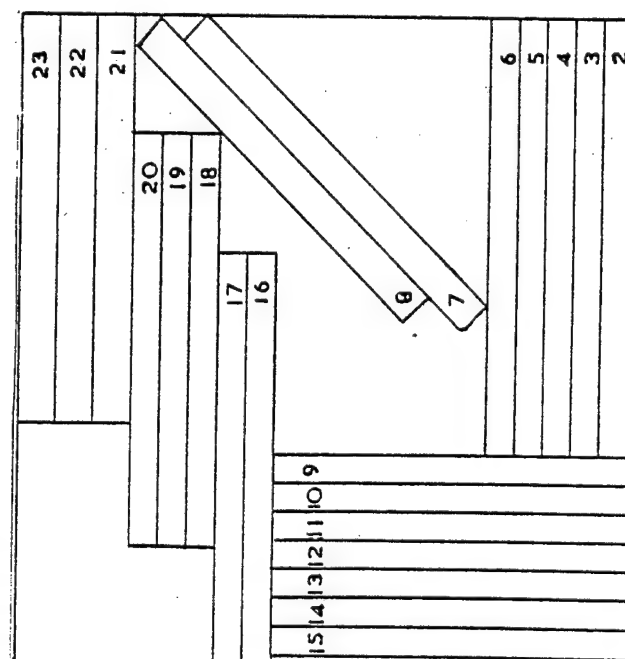
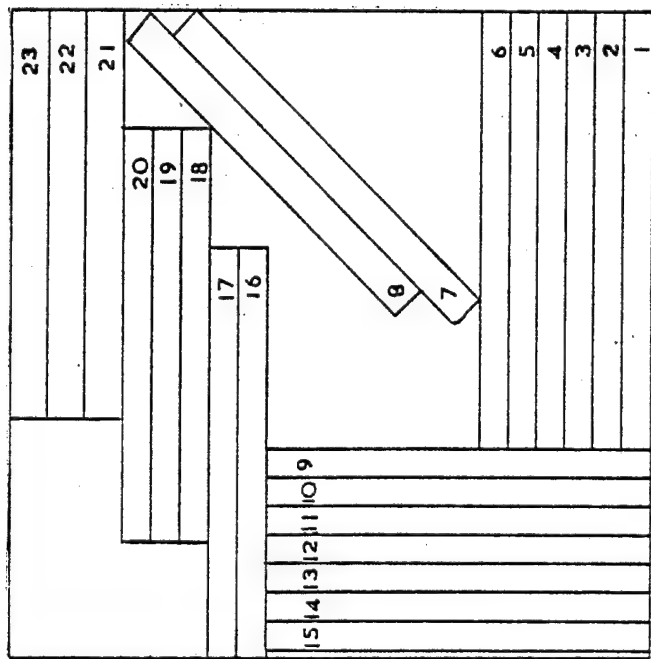
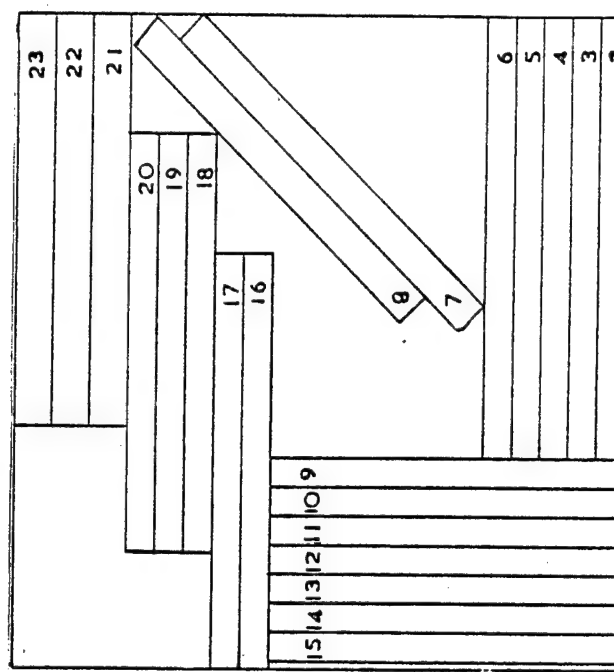
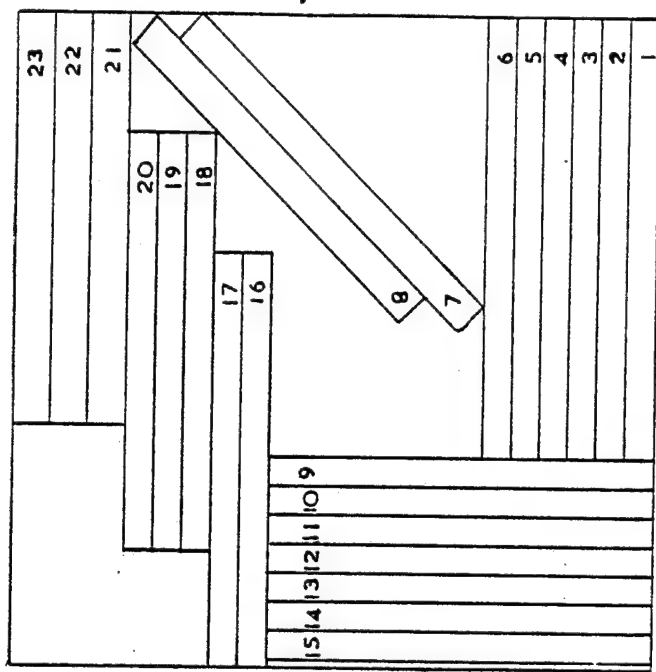
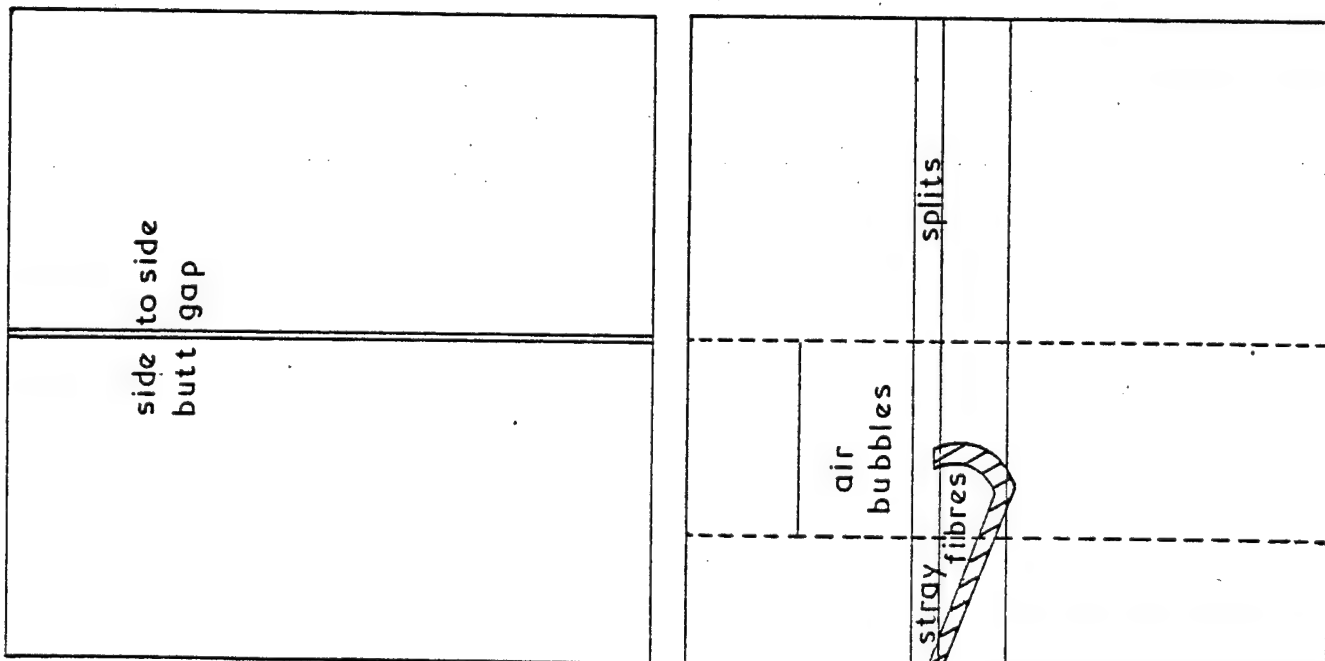
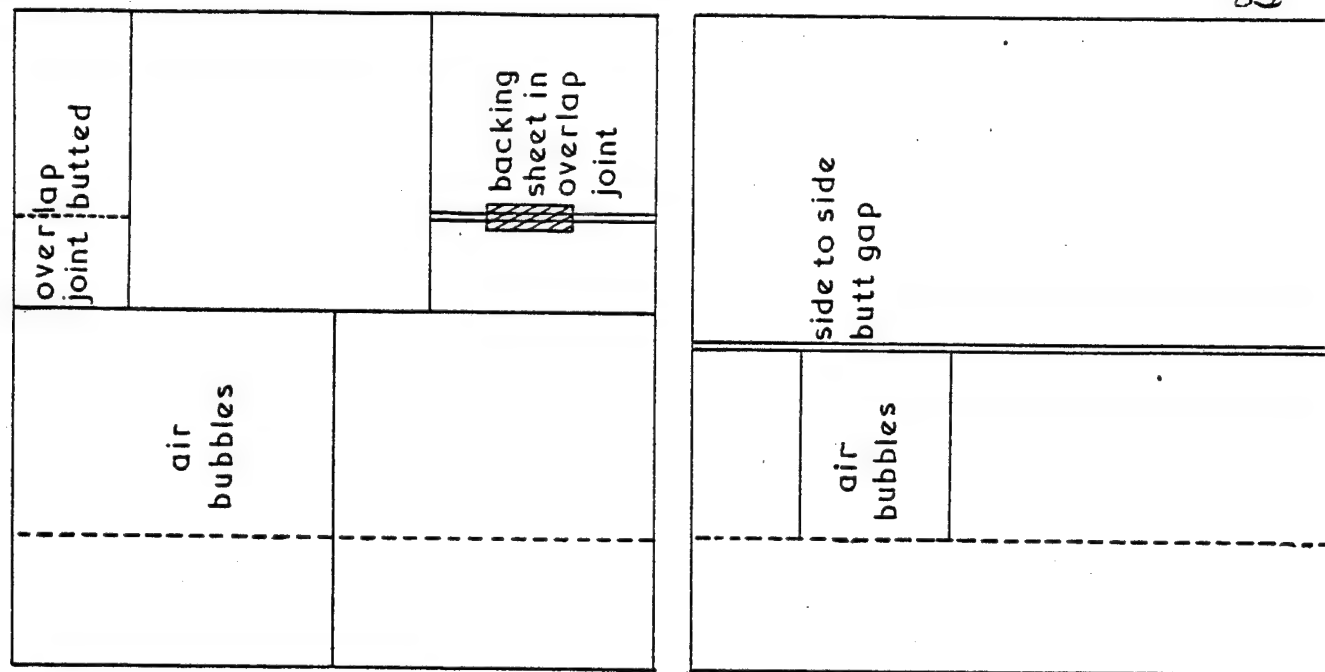


FIG. 2



Layer 1  
0° ↑

Layer 2  
90° →

FIG. 3

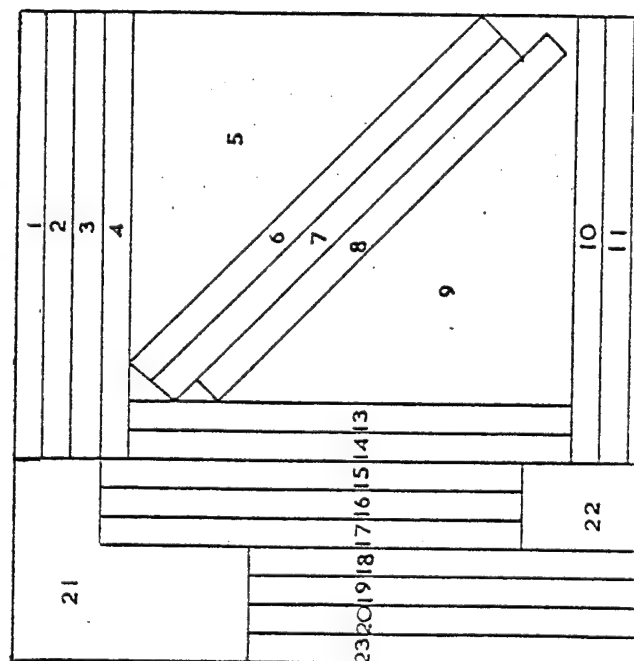
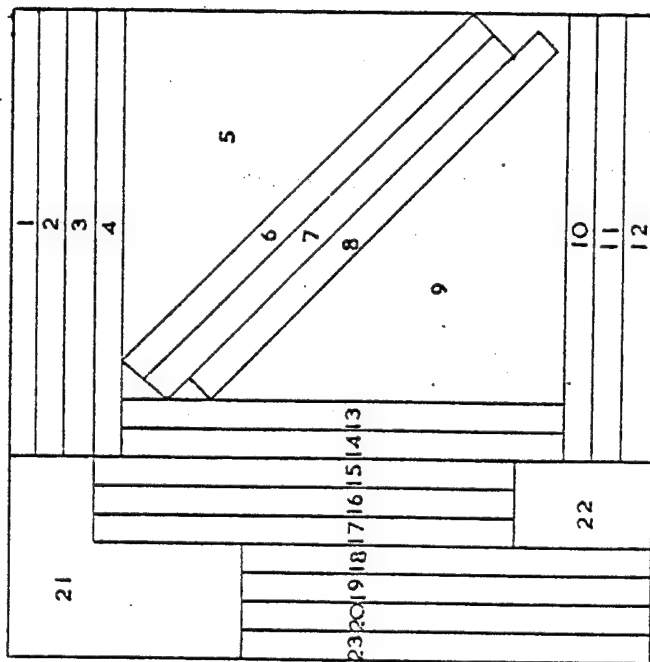
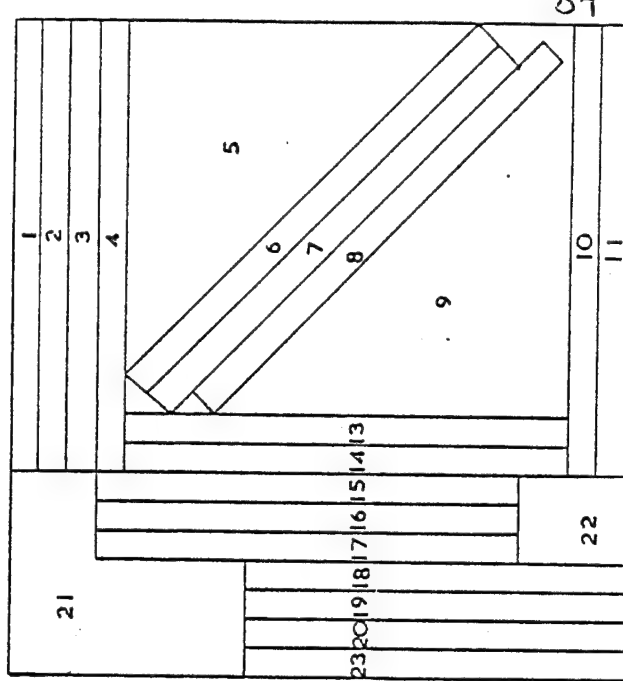
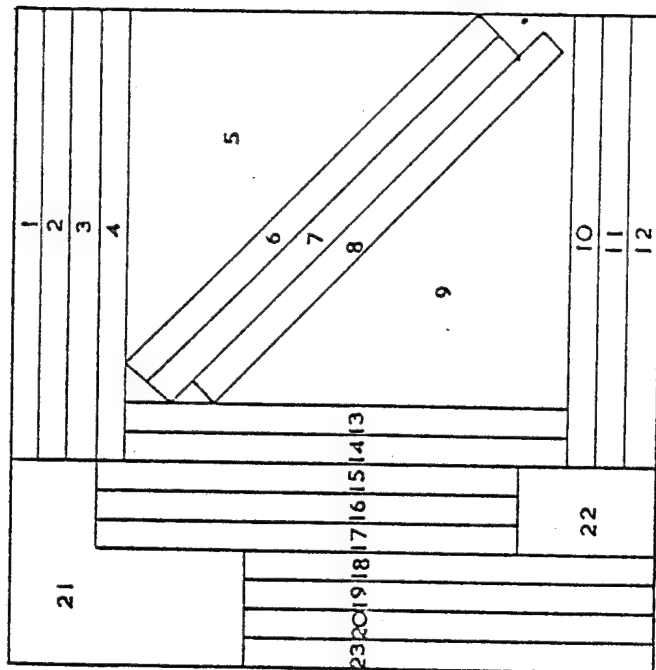
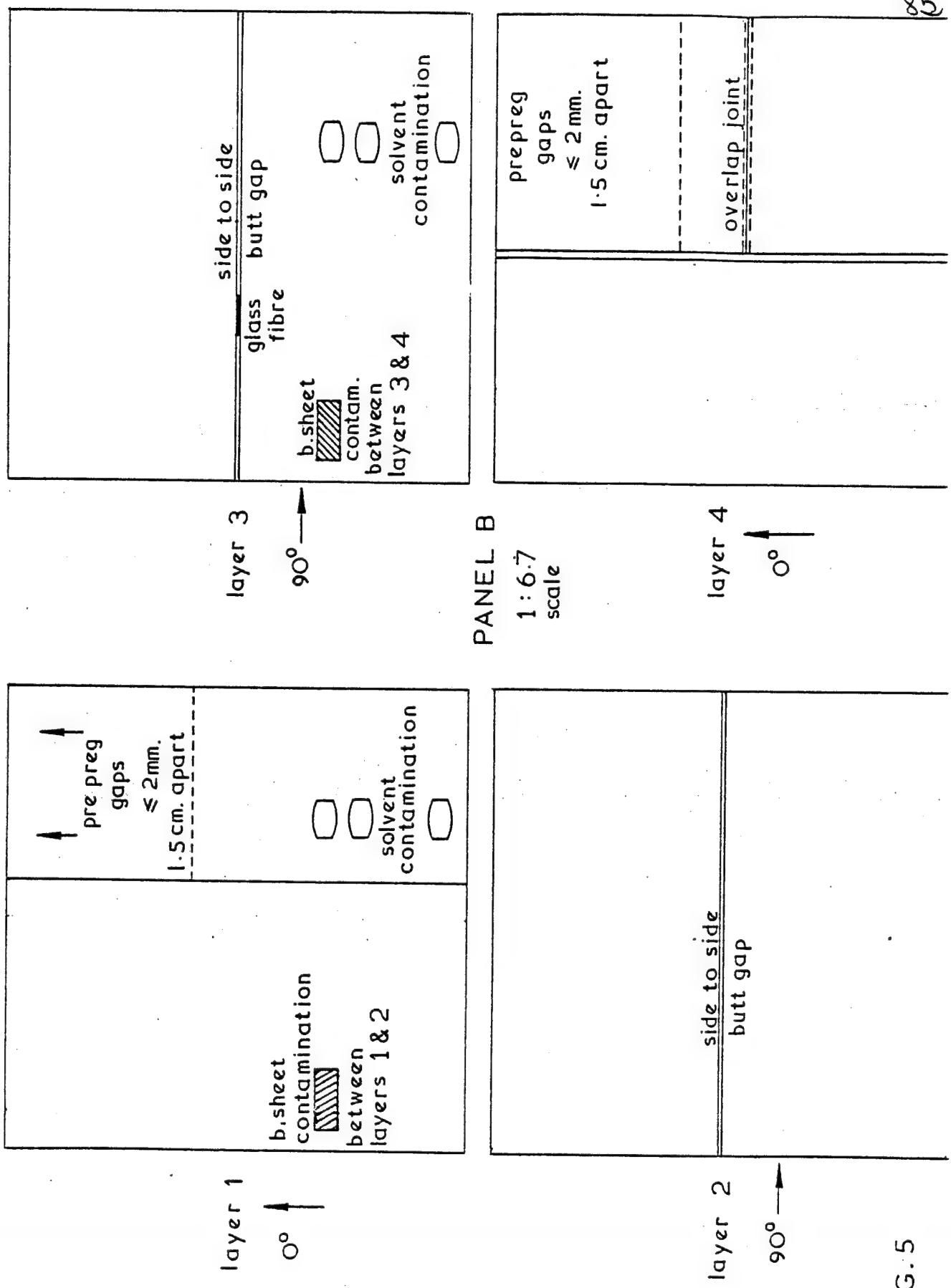


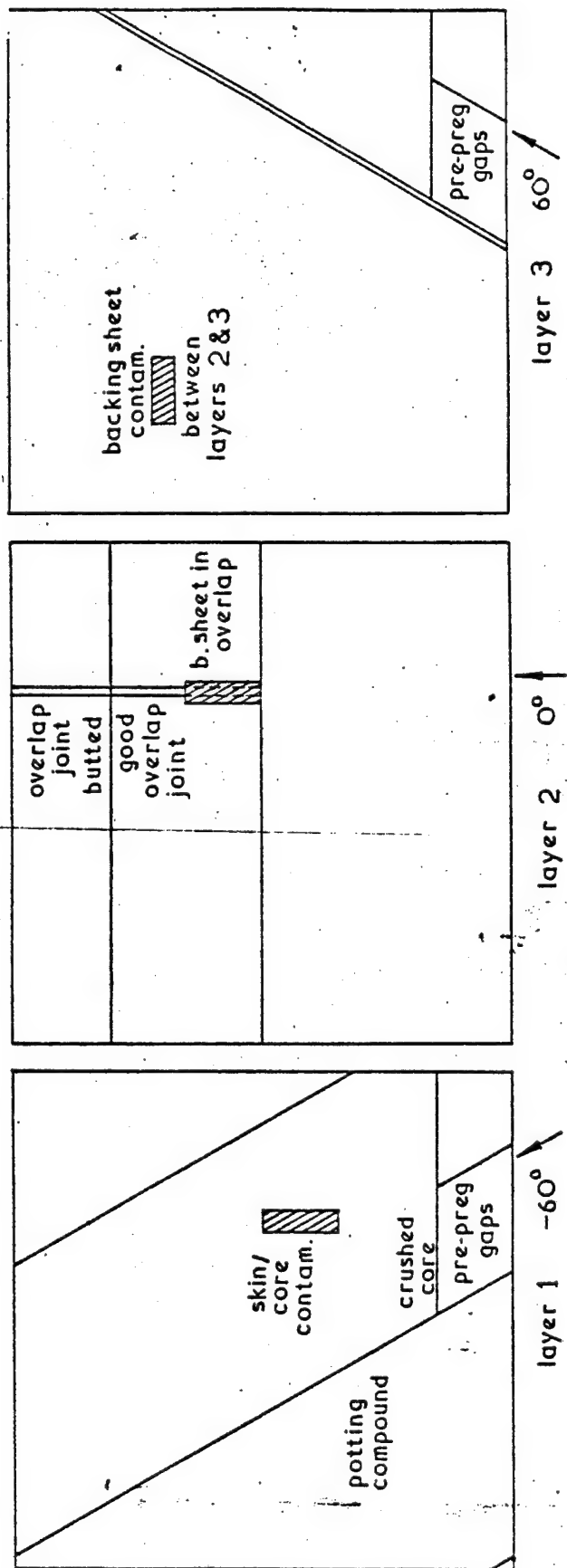
FIG. 4



• 86

<b>Unusable</b>	1	13
	2	14
	3	15
	4	16
	5	
	6	
	7	
	8	
	9	
	10	
	11	
	12	
<b>20</b>	19	13
<b>21</b>	18	
<b>22</b>		
<b>23</b>		
<b>24</b>		
<b>25</b>		
<b>26</b>		

FIG. 6



PANEL C

scale 1 : 6.7

FIG. 7

87

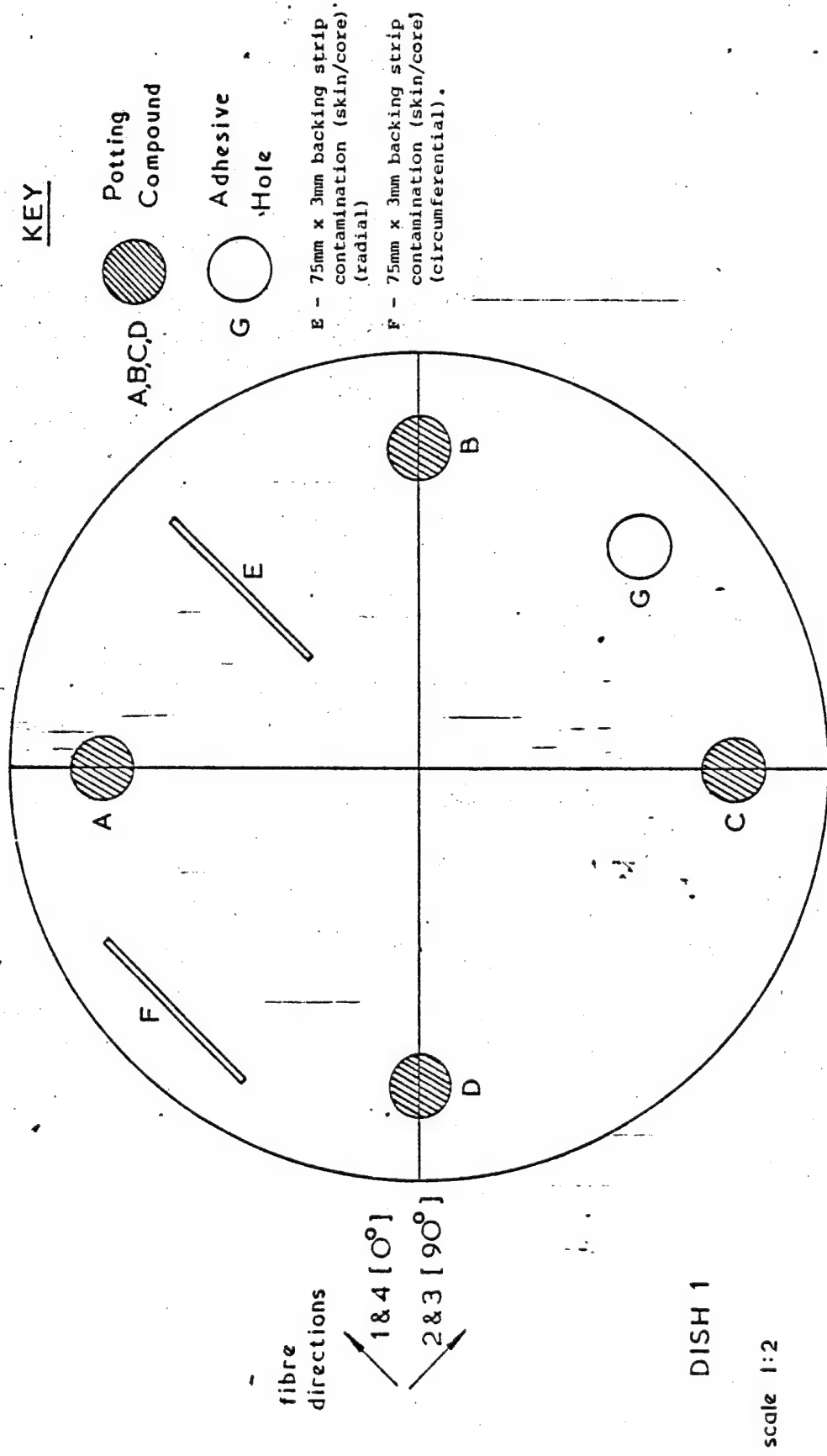


FIG. 8 Plan of Laminate/Core Defects (layer 1 is nearest to the core).

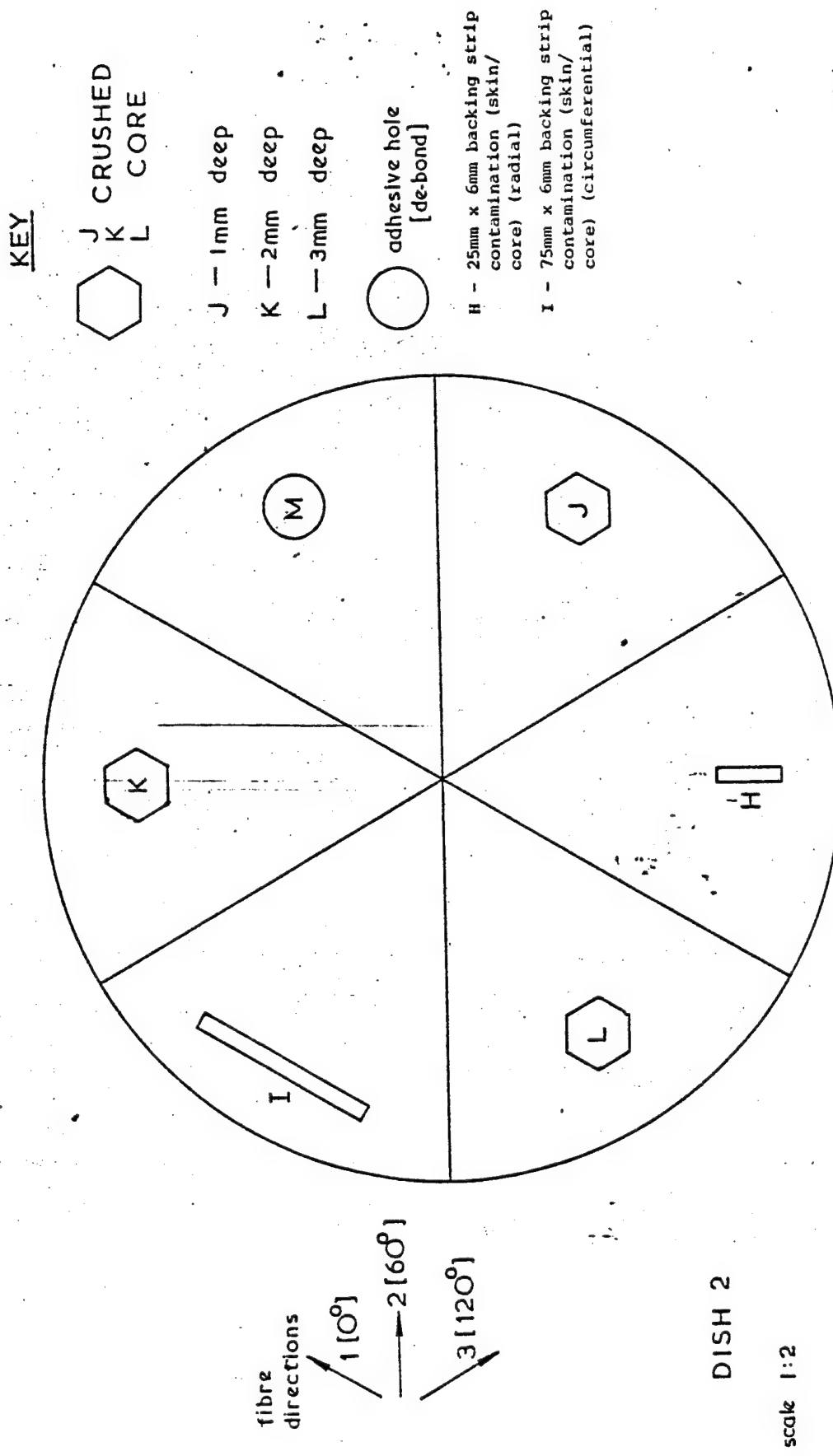


FIG. 9 Plan of core and laminate/core defects (layer 1 is nearest to the core).

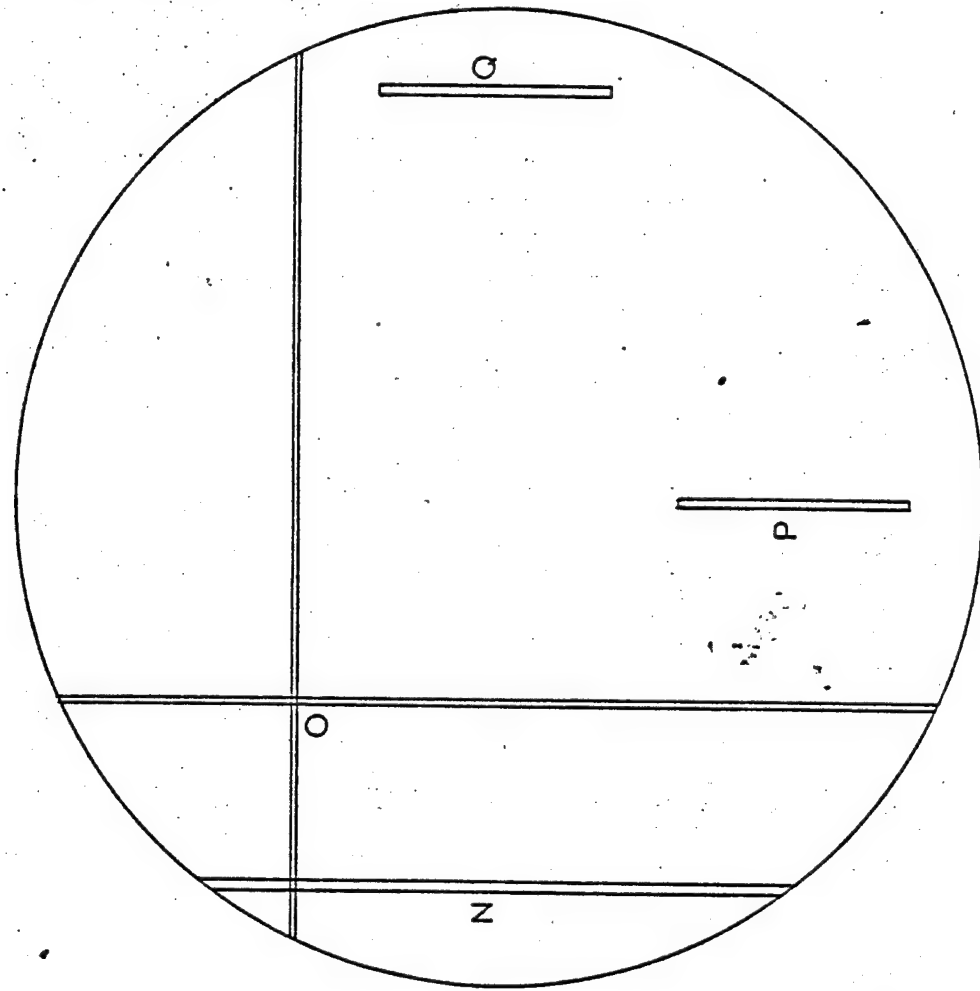
KEY

N - 3mm side to side overlap  
Joint in layer 1

O - Resin rich area

P - 75mm x 3mm backing strip  
contamination between  
layers 1 & 2 and 3 & 4  
(radial)

Q - 75mm x 3mm backing strip  
contamination between  
layers 1 & 2 and 3 & 4  
(circumferential).



Fibre  
Directions  
1 & 4  $[\theta]$   
2 & 3  $[-90^\circ]$

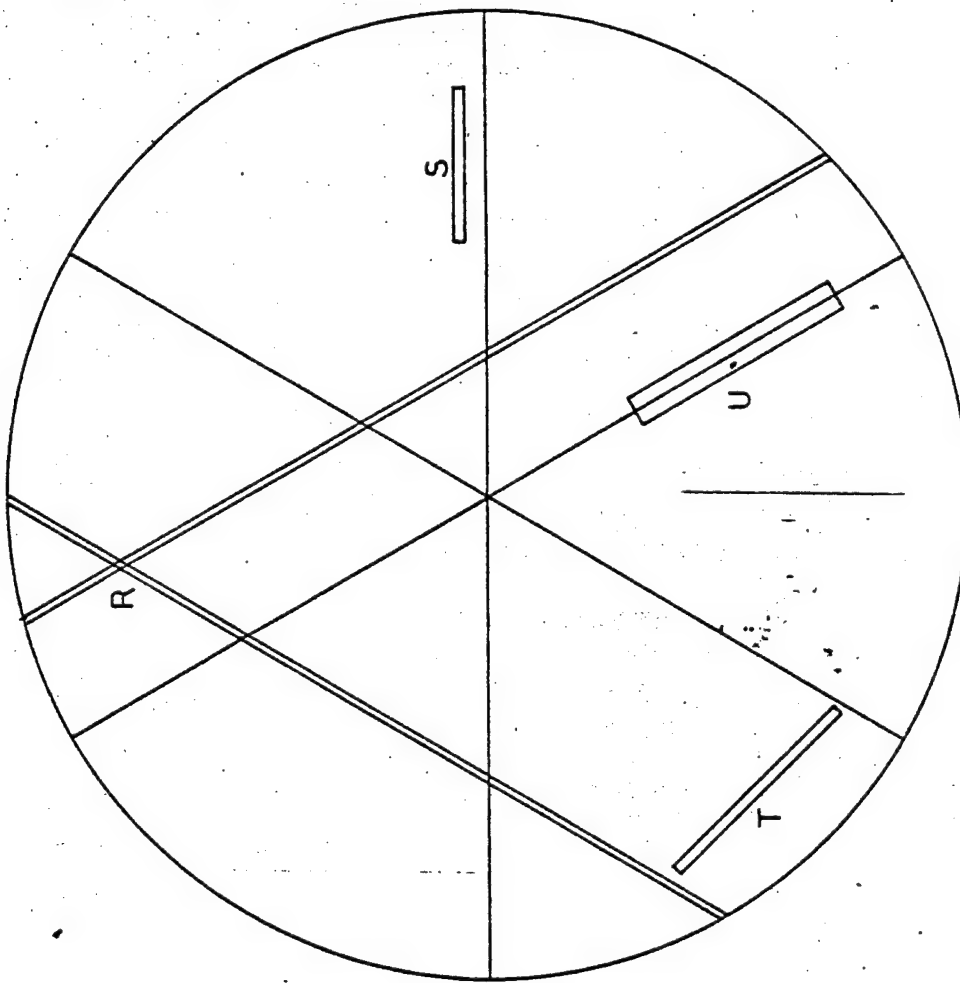
DISH 3

scale 1:2

FIG.10 Plan of laminate defects (layer 1 is nearest to the core). 20

KEY

R - Resin-rich area  
S - 50mm x 4mm backing strip  
contamination between  
layers 1 & 2 and 2 & 3  
(radial)  
T - 75mm x 4mm backing strip  
contamination between  
layers 1 & 2 and 2 & 3  
(circumferential)  
U - 75mm x 5mm backing strip  
contamination between  
layers 2 and 3 (radial).



fibre  
directions  
1 [ $0^\circ$ ]  
2 [ $60^\circ$ ]  
3 [ $120^\circ$ ]

DISH 4

scale 1:2

FIG. 11

Plan of laminate defects (layer 1 is nearest to the core).

2

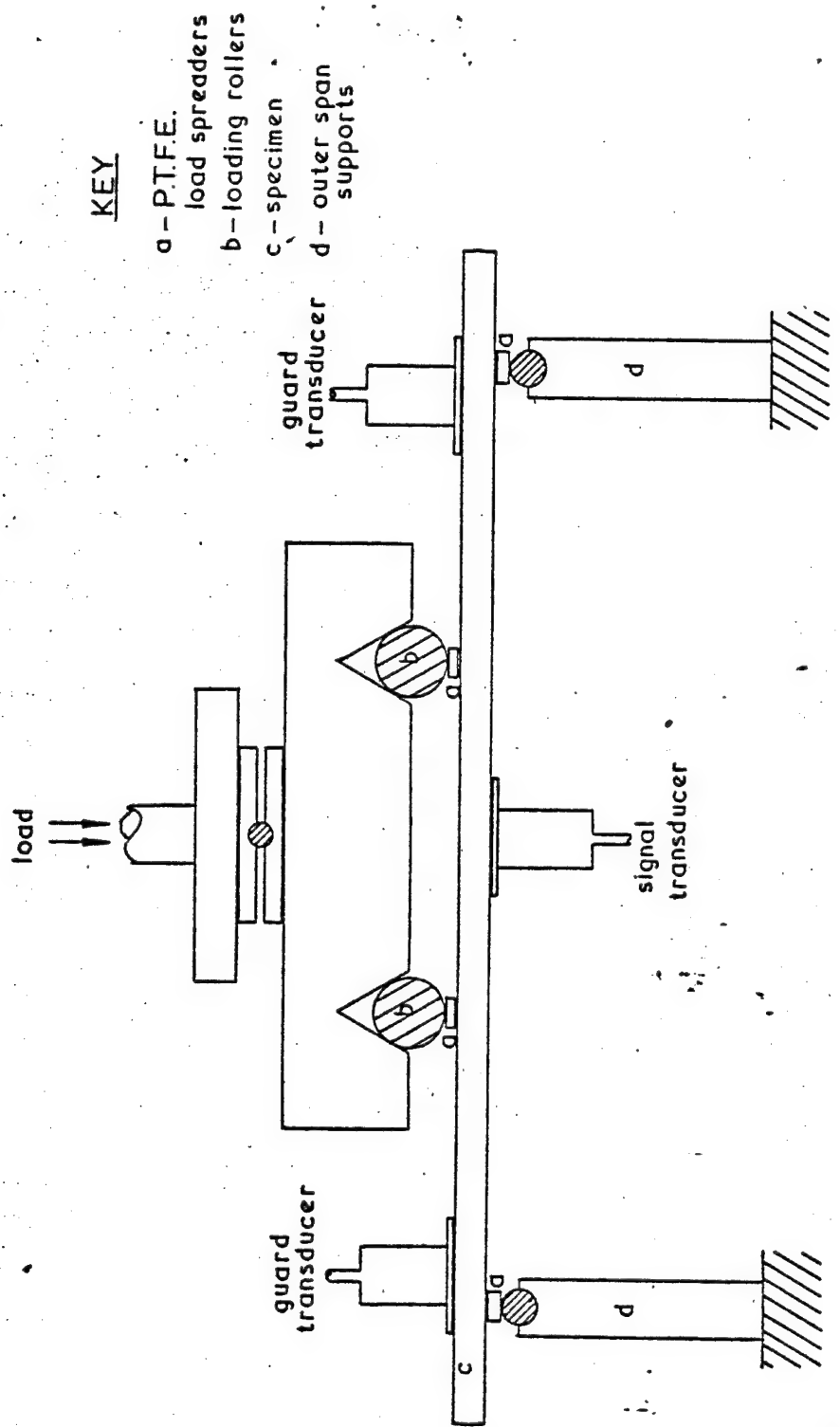


FIG. 12

scale 1:2

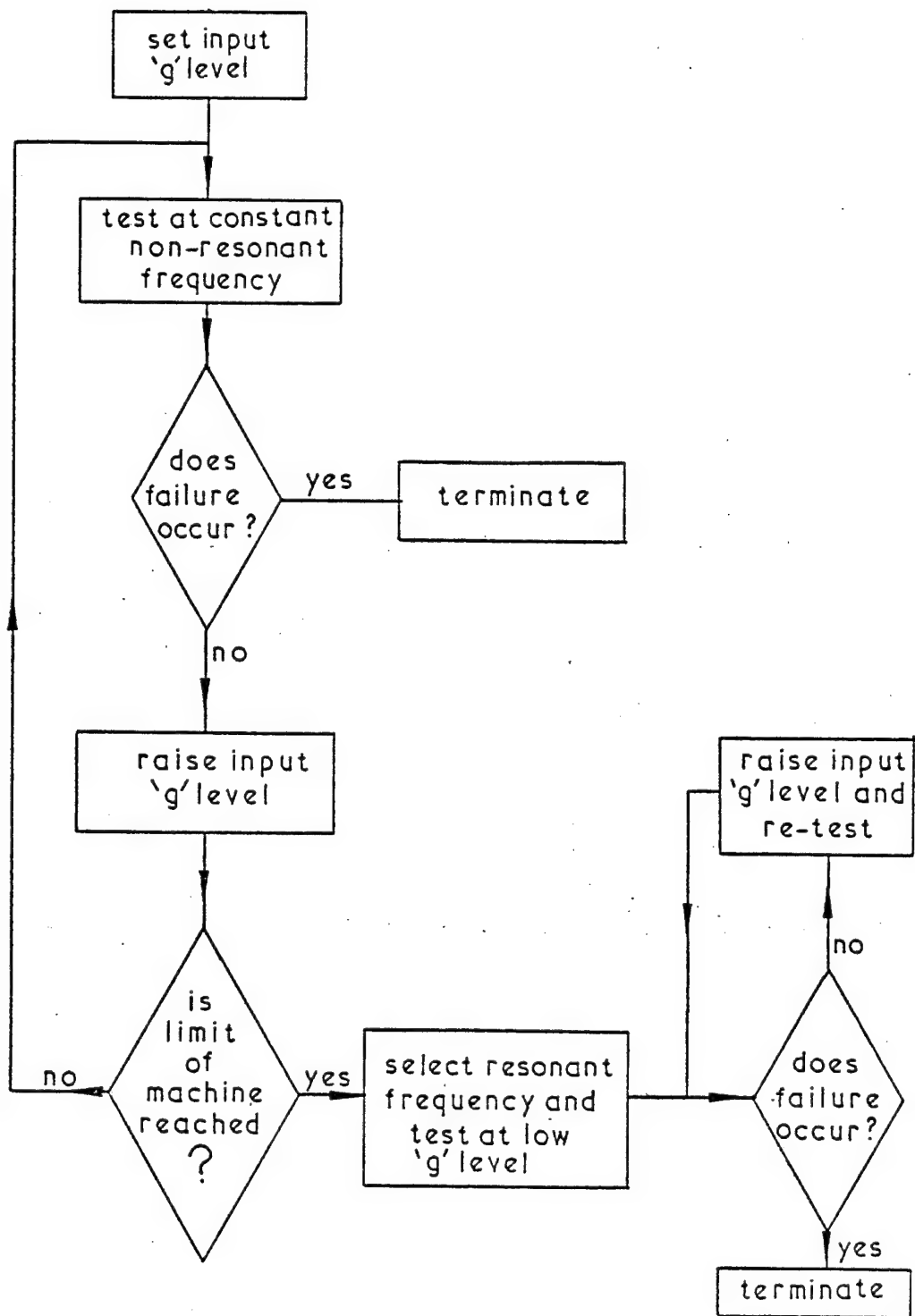


FIG.13 Phase 1 vibration test programme

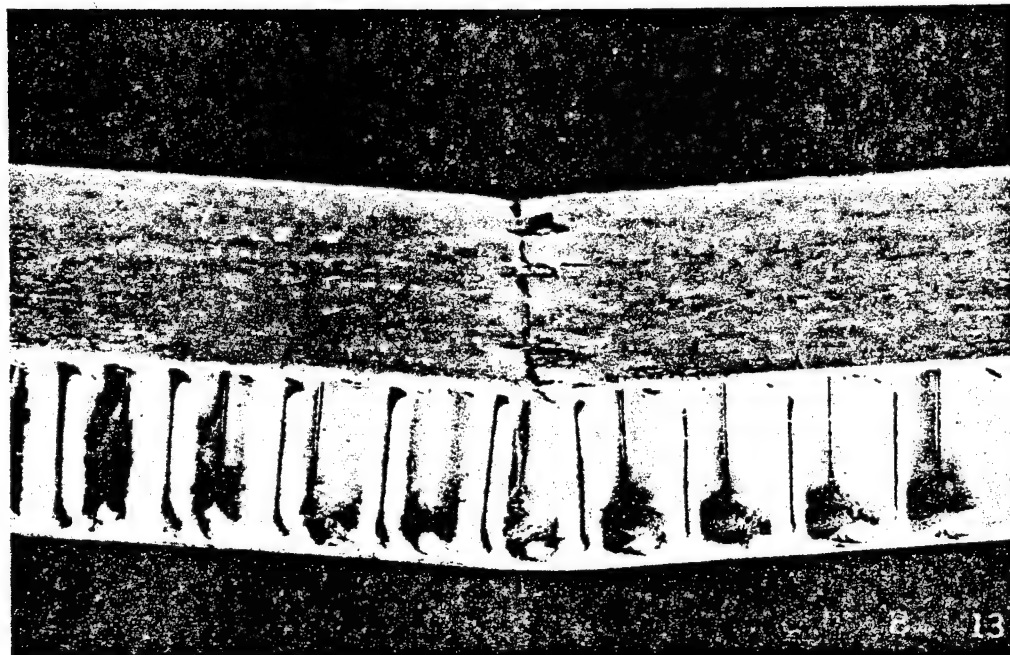


Figure 14 0/90/0 flexural test specimen with fibre directions  $\parallel$  and  $\perp$  to beam axis showing compressive failure of upper face skin and undamaged honeycomb core.  
(Specimen 13B)

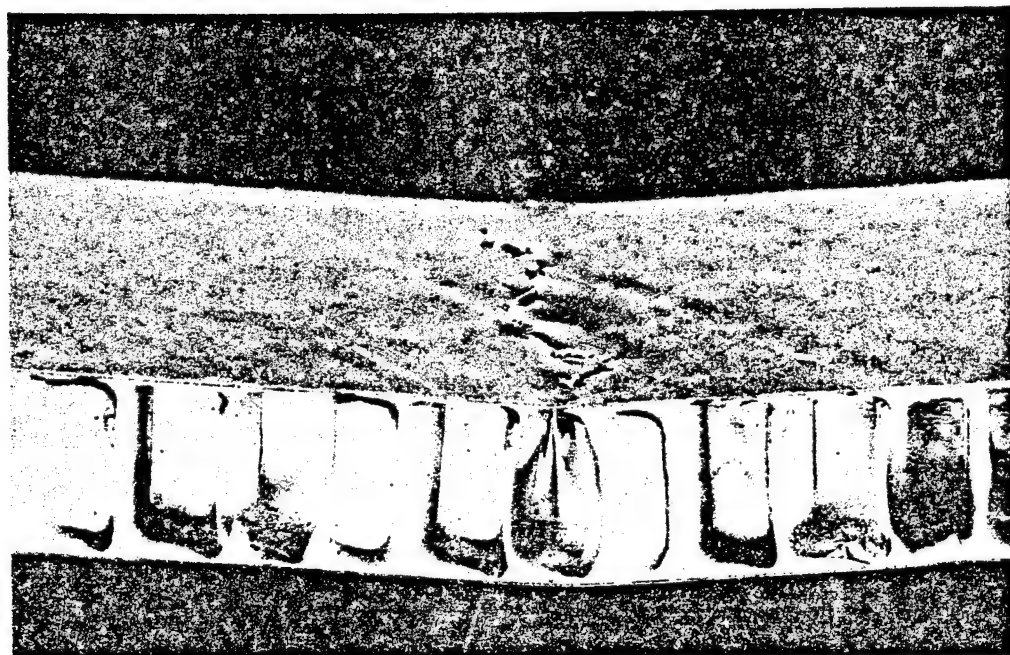


Figure 15 0/90/0 flexural test specimen with fibre directions at  $45^\circ$  to beam axis showing compressive failure of upper face skin.

R736/4

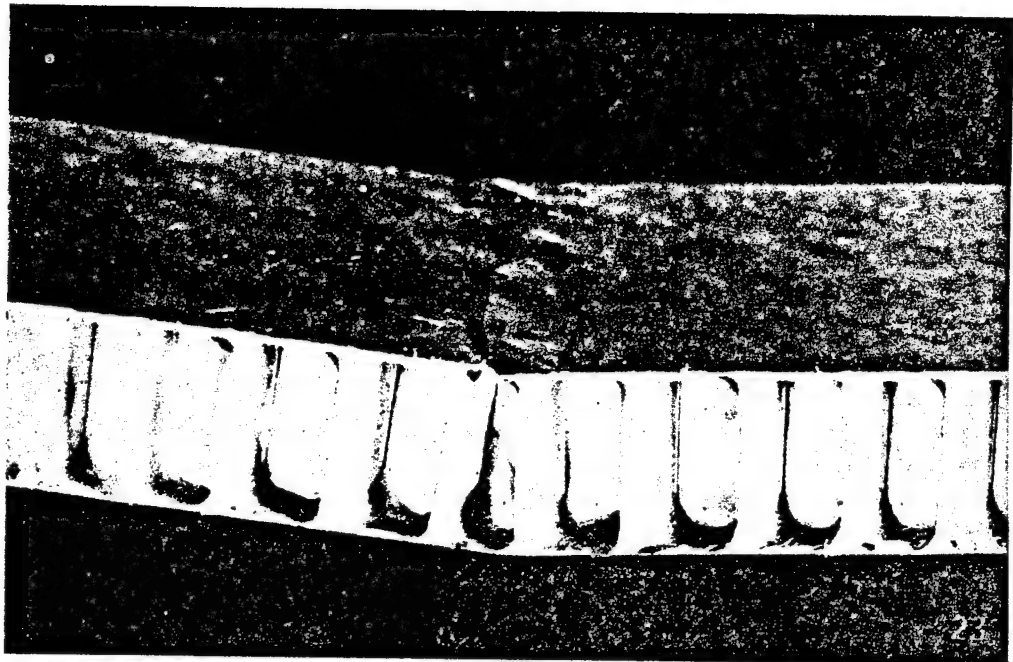


Figure 16 0/60/120 flexural test specimen showing compressive failure of upper face skin and undamaged honeycomb core.  
(Specimen 23C)

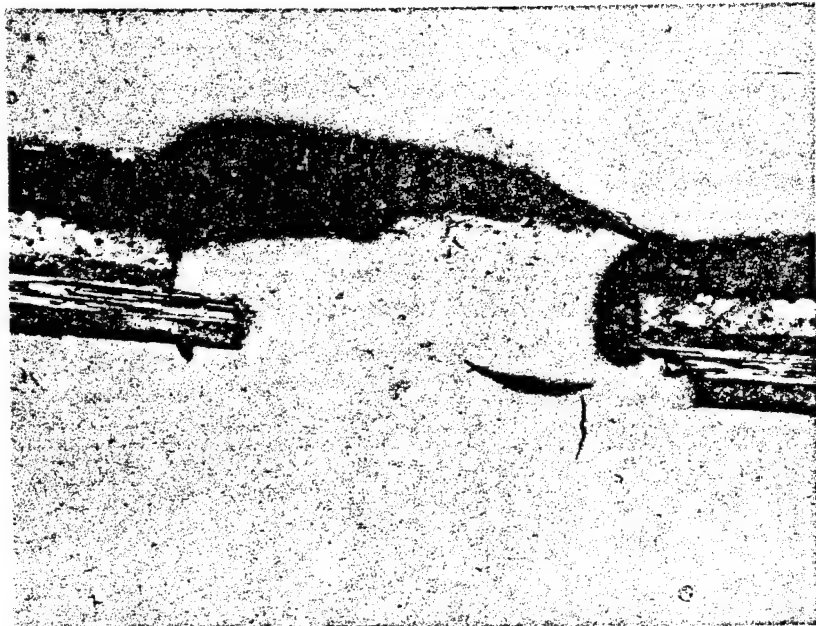
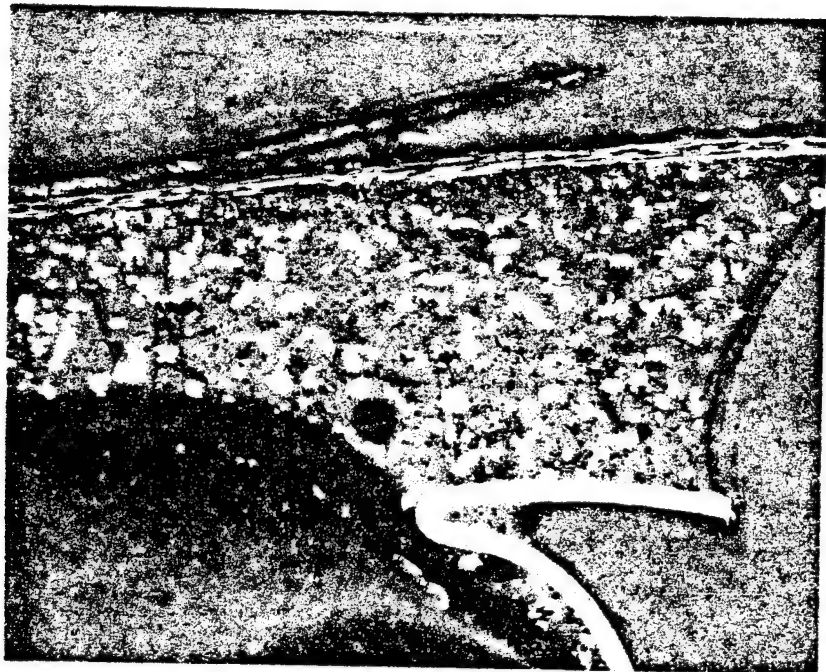


Figure 17 Micrograph of section of fracture area in the face skin showing fracture of both the plies and the adhesive layer.  
(Specimen 2B x 50)



96

Figure 18 Micrograph of fracture showing delamination of face skin and adhesive and deformation of the honeycomb core.  
(Specimen 13C x 50)

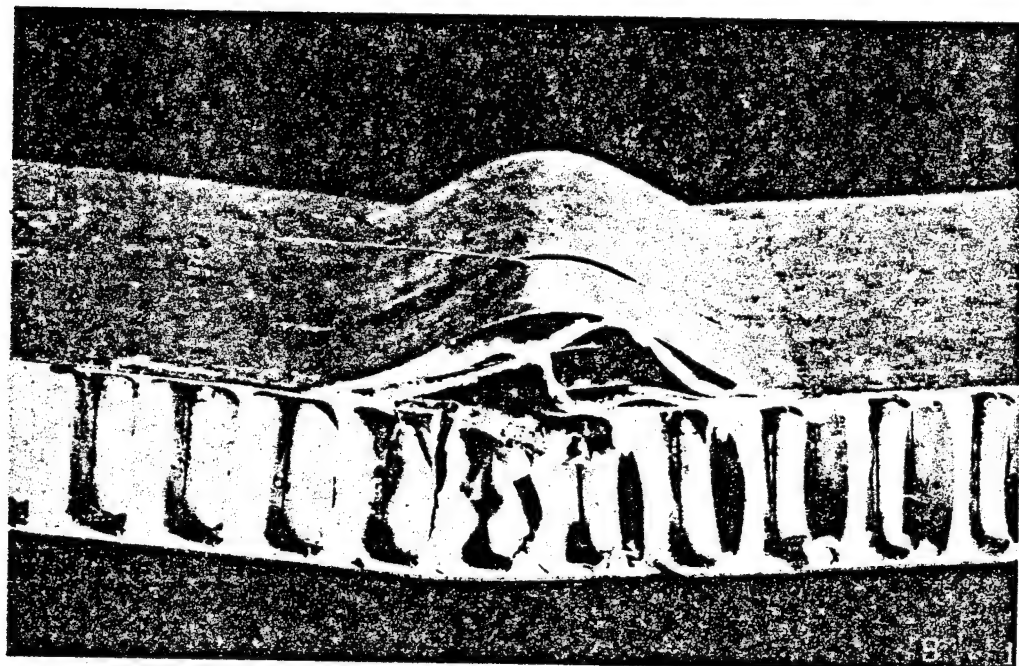


Figure 19 Fractured beam containing a backing sheet contamination defect showing delamination but not fracture of the face skin and local collapse of the honeycomb core.



Figure 20 Radial crack passing through a severe defect which resulted in failure of Dish 2.

Figure 21 Acoustic Emission from Flexural Tests on CFRP/Al Honeycomb Beams Containing Deliberate Defects.

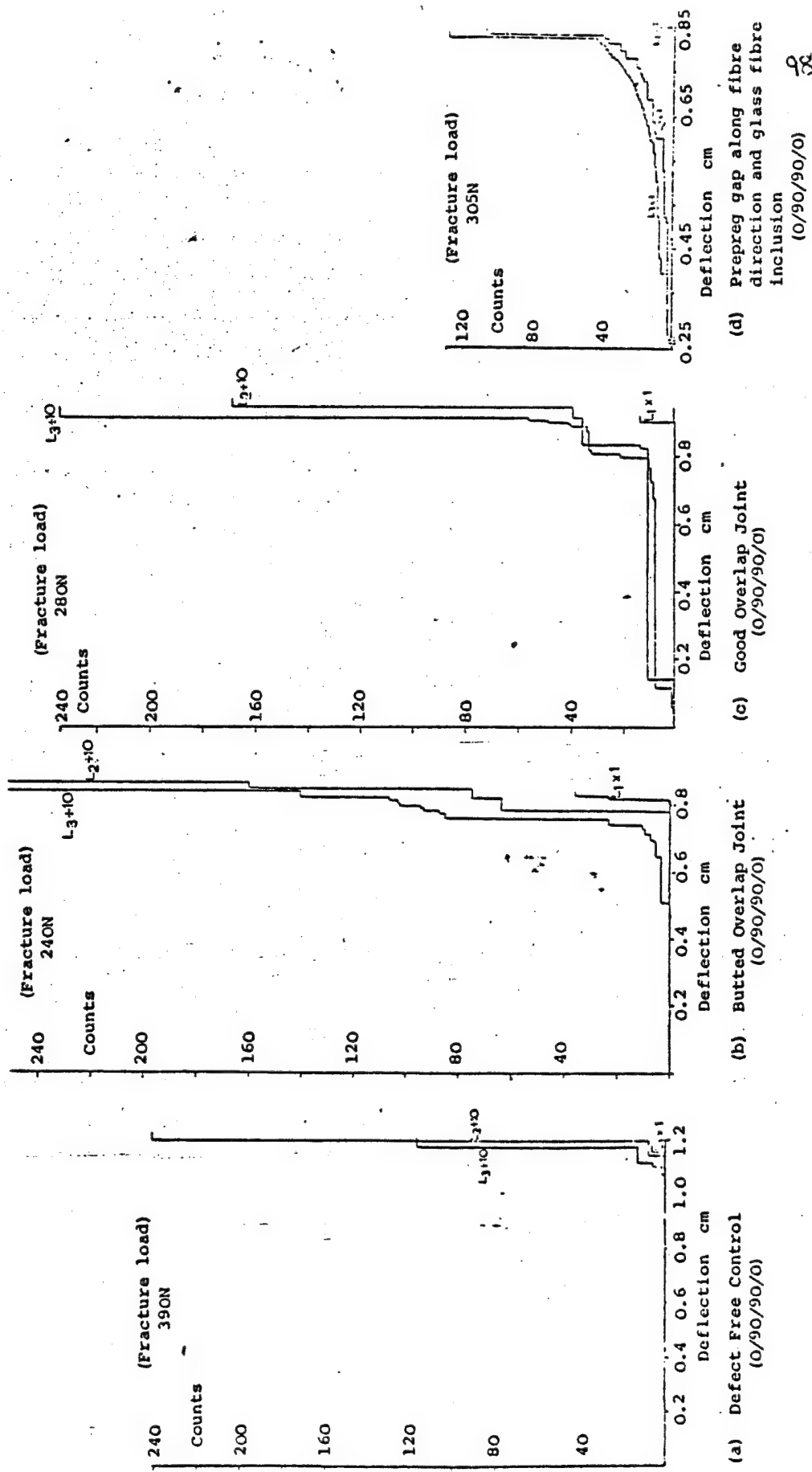


Fig. 21 (Cont'd).

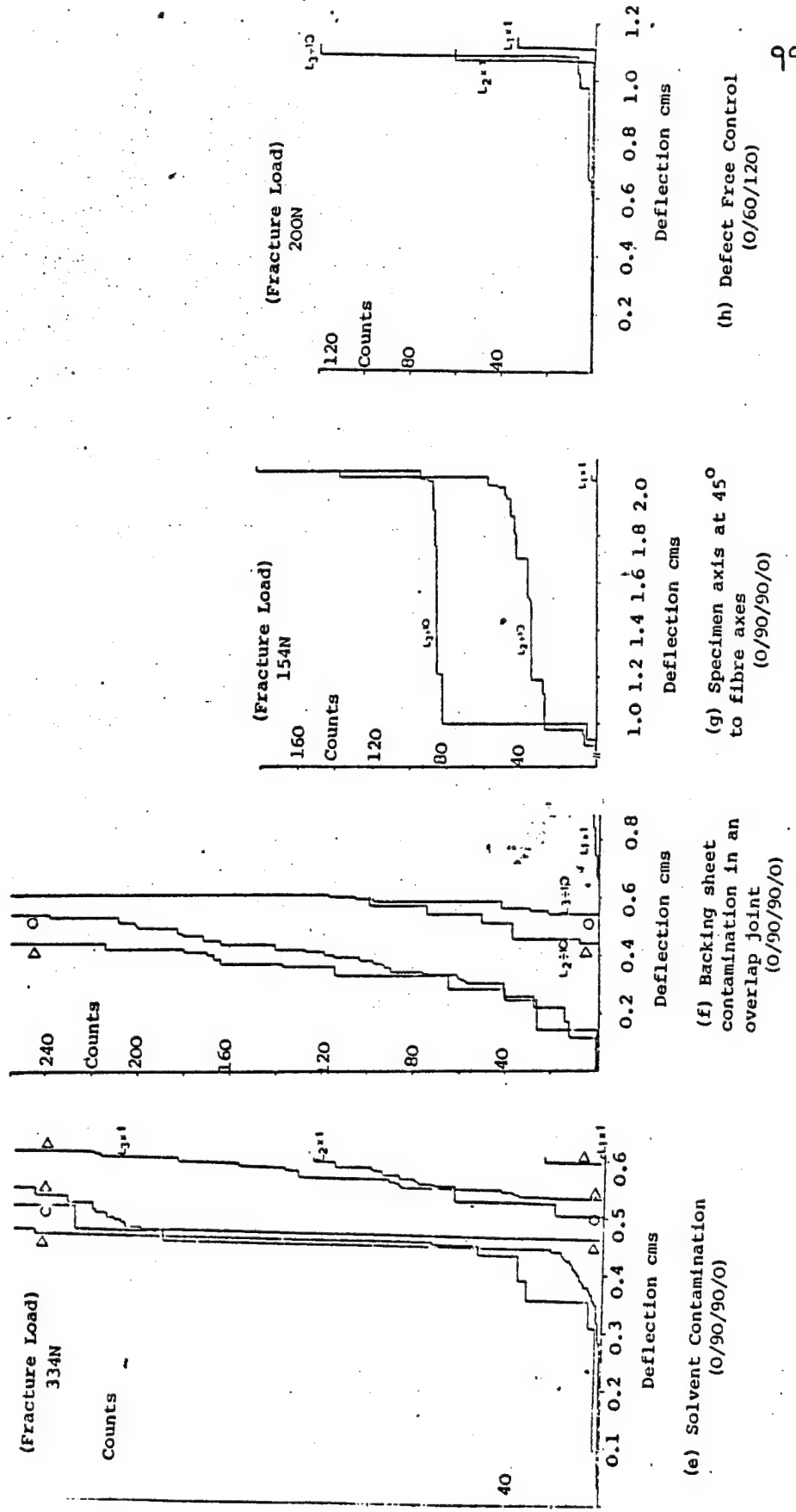
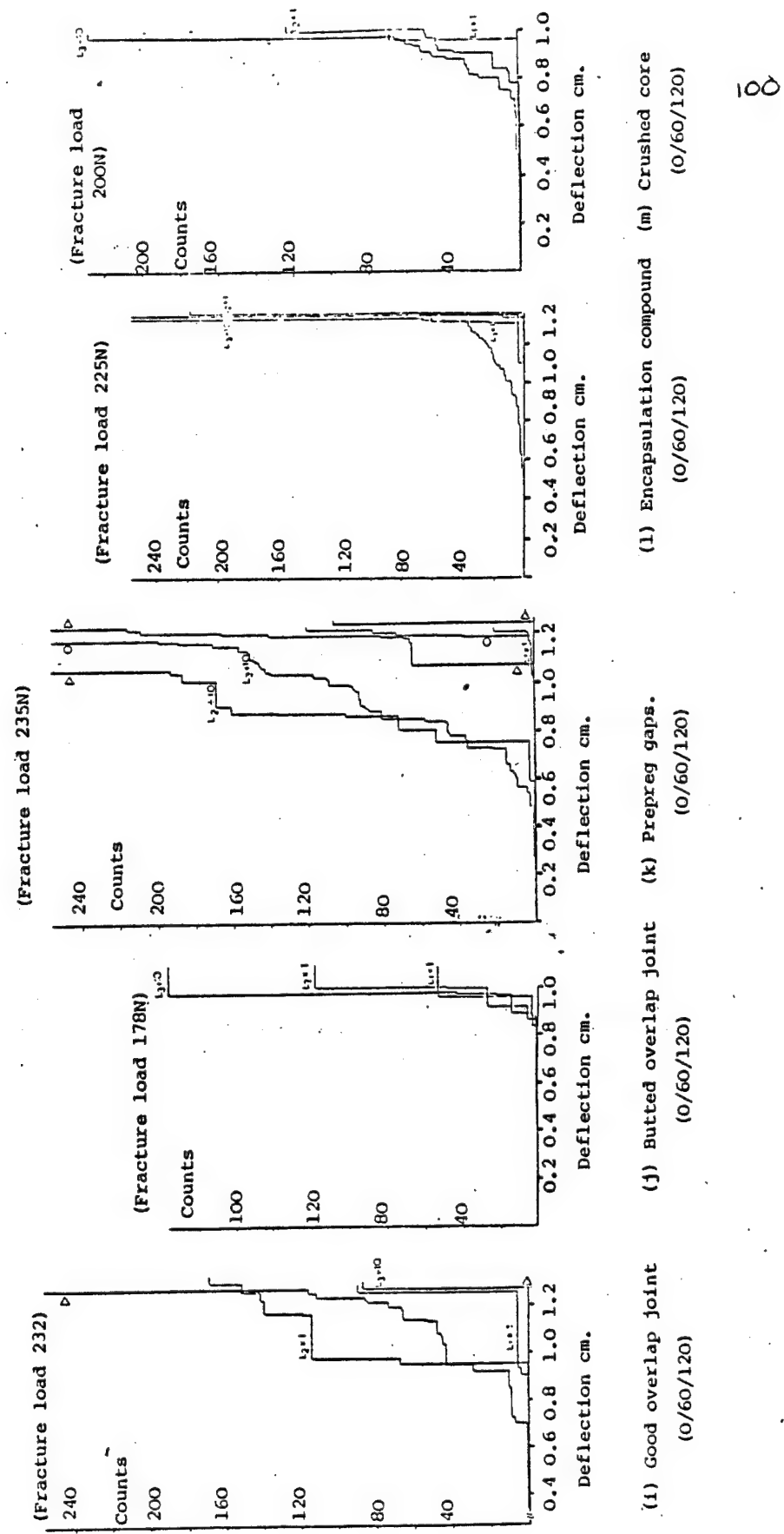
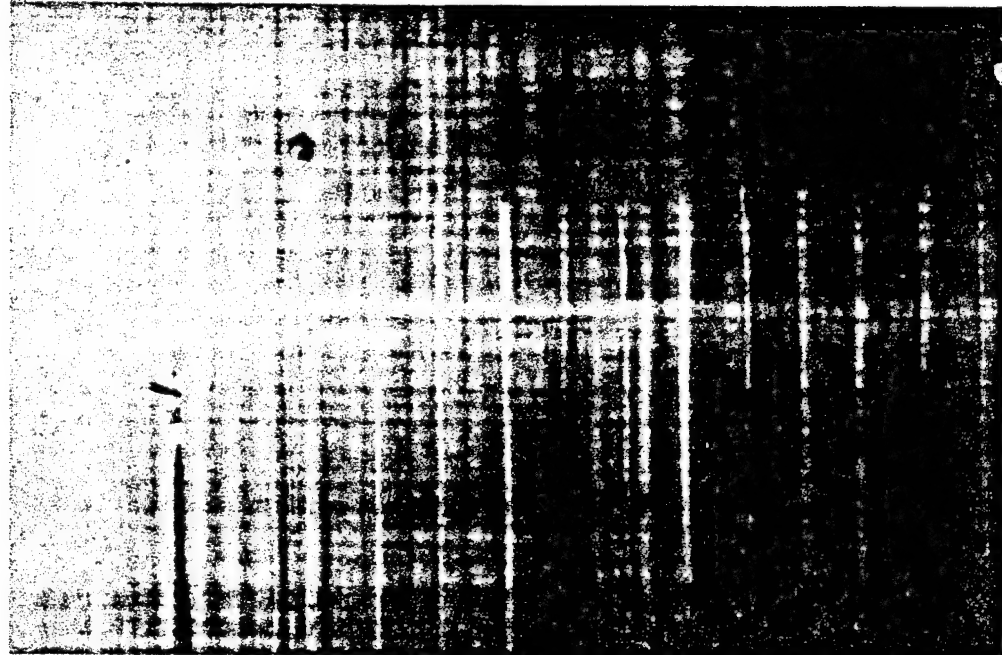


Fig. 21 (Cont'd.).





101

Figure 22 Low energy (7kV) x-radiograph of a 4 ply laminated CFRP skin before bonding to a honeycomb core. The prominent light strips running from the lower edge to three-quarters height are due to prepreg splits, the less pronounced light and dark stripes running vertically and horizontally indicate uneven fibre distribution in the prepreg. (Sections 3.3. and 5.1.4)

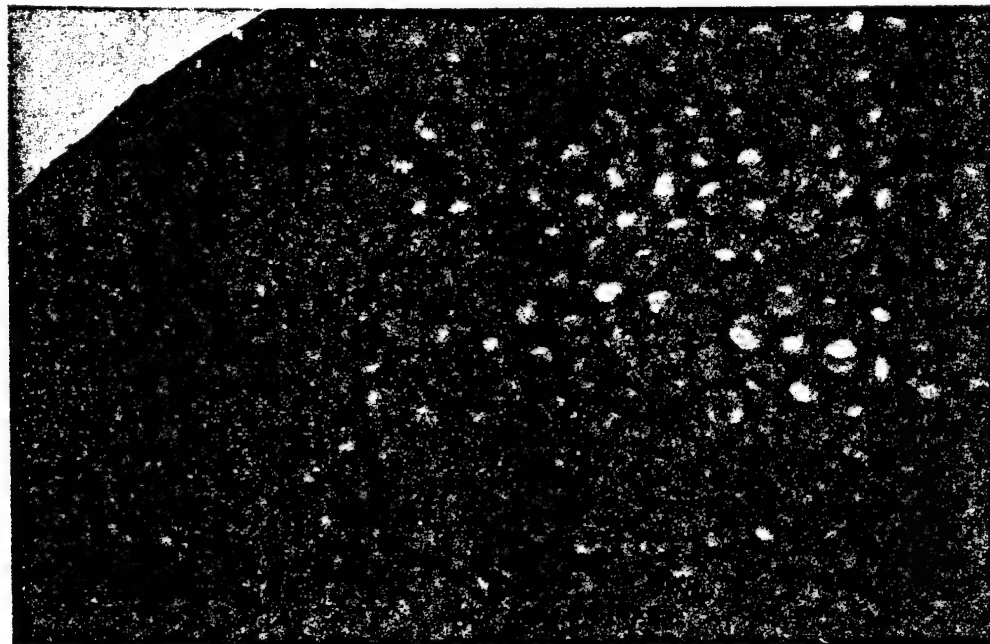


Figure 23 Low energy (7kV) x-radiograph of part of a dish specimen. The outer edge of the dish is seen at top left. The honeycomb core is clearly visualised and at the upper right the cell centers reveal some texture attributable to the CFRP skins but no detail can be resolved. (Sections 3.3. & 5.1.4)

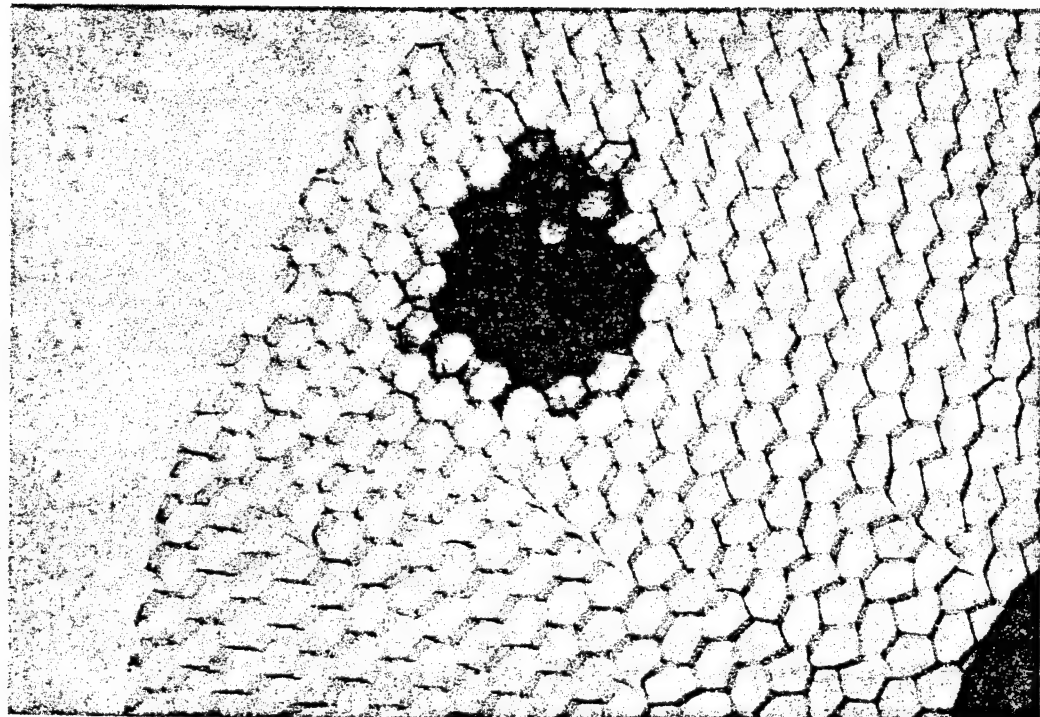


Figure 24 Conventional x-radiograph using a contact technique and 50kV x-rays showing clear visualisation of the aluminium honeycomb and encapsulation compound. Some local damage to the core is seen above the dark area of encapsulation compound. (Section 3.3. & 5.1.4)

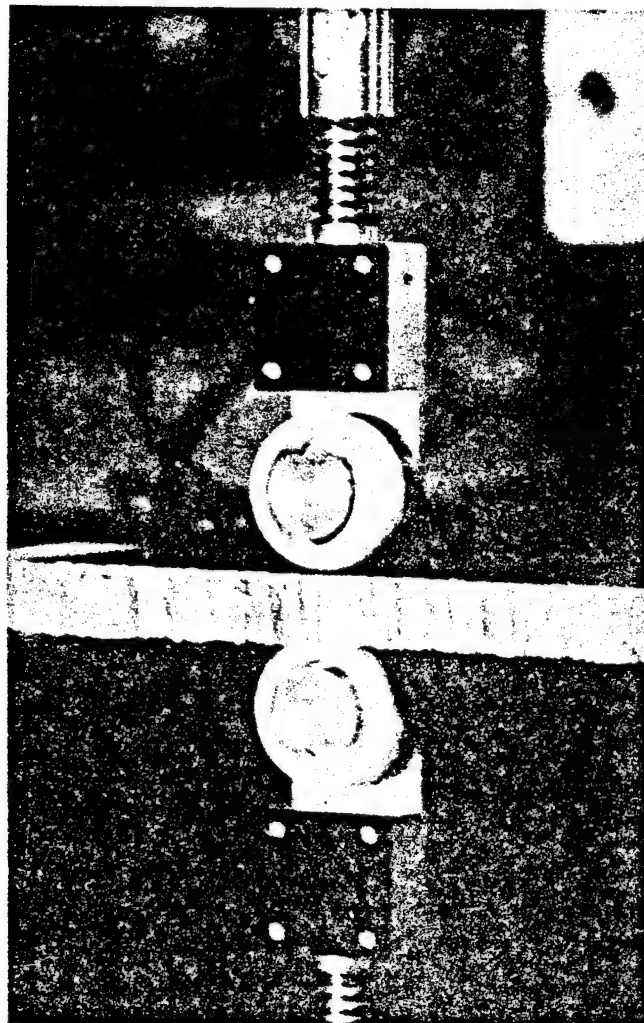


Figure 25 The roller probes mounted in the through transmission mode on a flat CFRP/Al bonded panel. The rubber tyres are spring loaded onto the specimen and the probes kept in direct opposition with a jig. The transducing crystals are mounted on the non-rotating axle of the wheels, oriented perpendicular to the specimen. (Sections 3.4.5. and 5.1.5.4.).

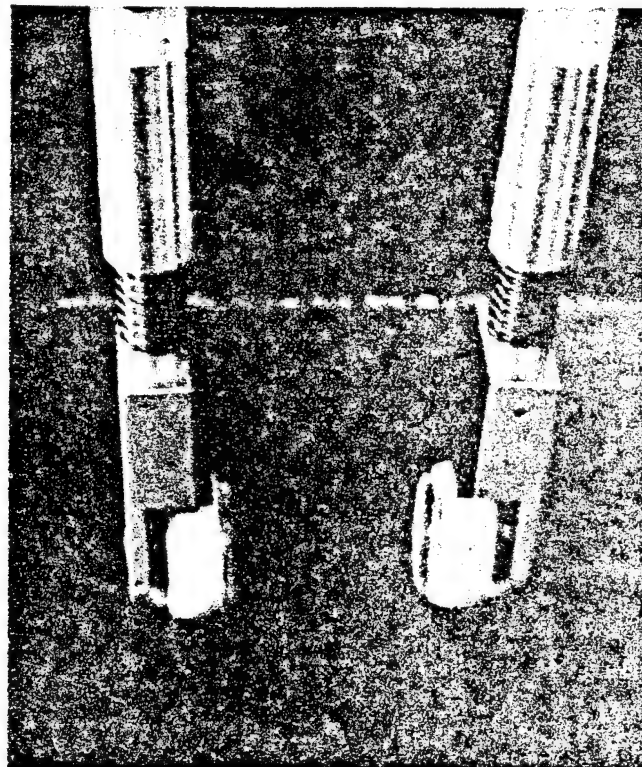


Figure 26 The roller probes mounted in the transverse transmission  
xl Mag. mode. Note the probes are now mounted at an angle to  
(approx.) the perpendicular to the specimen to enable transverse  
transmission of ultrasound through the specimen.  
(Sections 3.4.5. & 5.1.5.4)

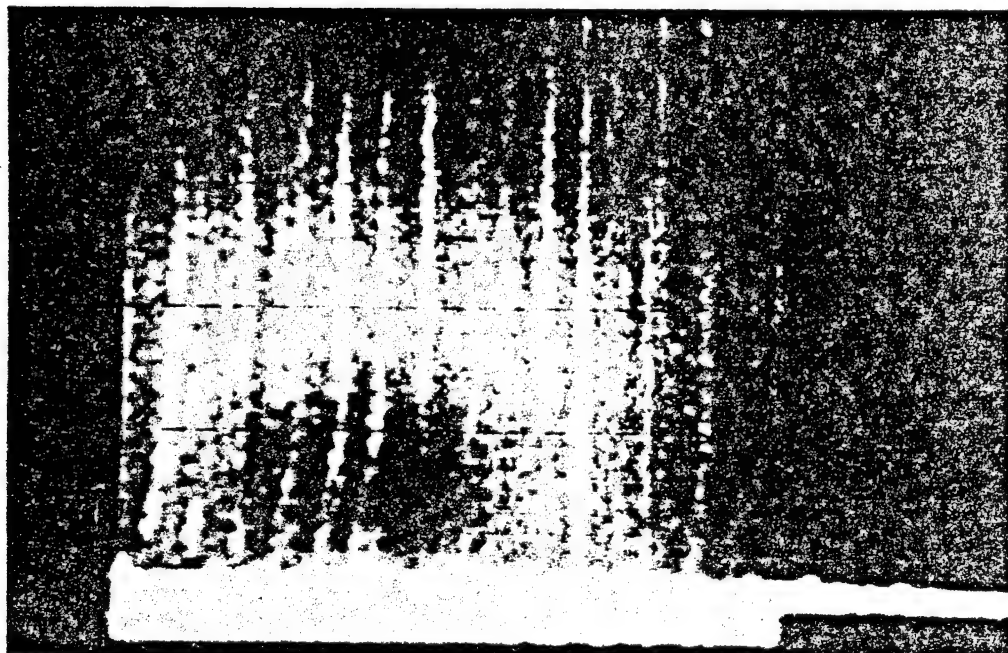


Figure 27 Prepreg gaps and splits revealed by thermography.  
xl Mag. Resolution on screen is better than in photographic  
reproduction but this figure is representative of the  
results achieved with this technique. (Sections 3.5 & 5.1.6)

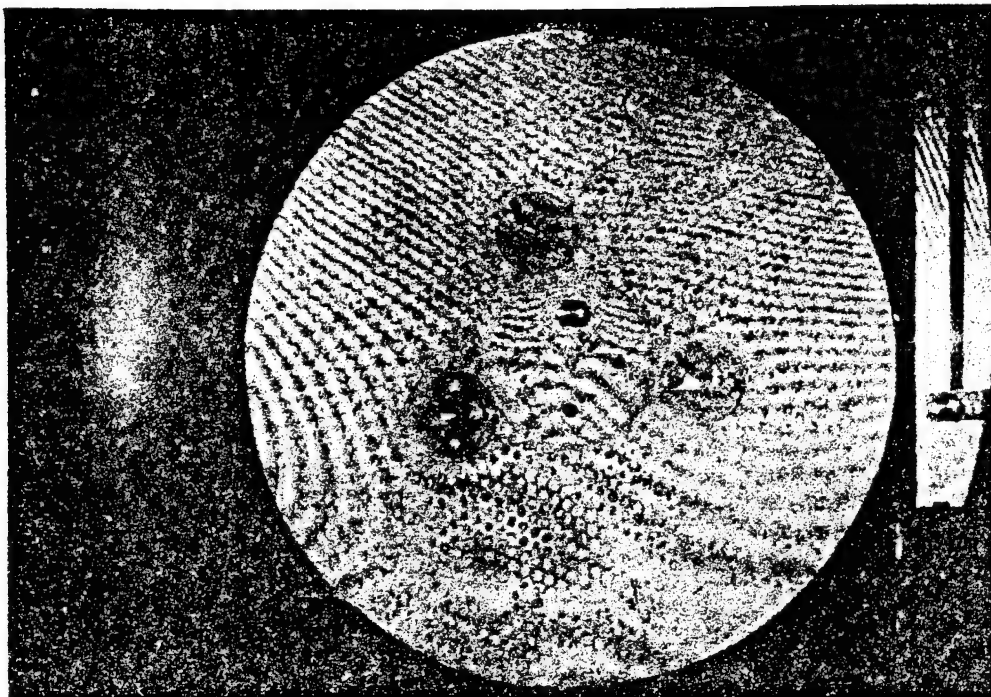


Figure 28 An interferogram of a CFRP/Al honeycomb dish specimen and its superimposed holographic image. Four circular areas of perturbed fringe pattern can be seen and right of centre towards the lower edge of the dish, the fringe pattern caused by hole cut in the skin/core film adhesive is visible.

Note the visualisation of the honeycomb cells, and also the regular fringe pattern on the stand to the right of the dish. Closely spaced fringes around the central fixing bolt indicate an area of high strain. (Sections 3.6 and 5.1.7.)

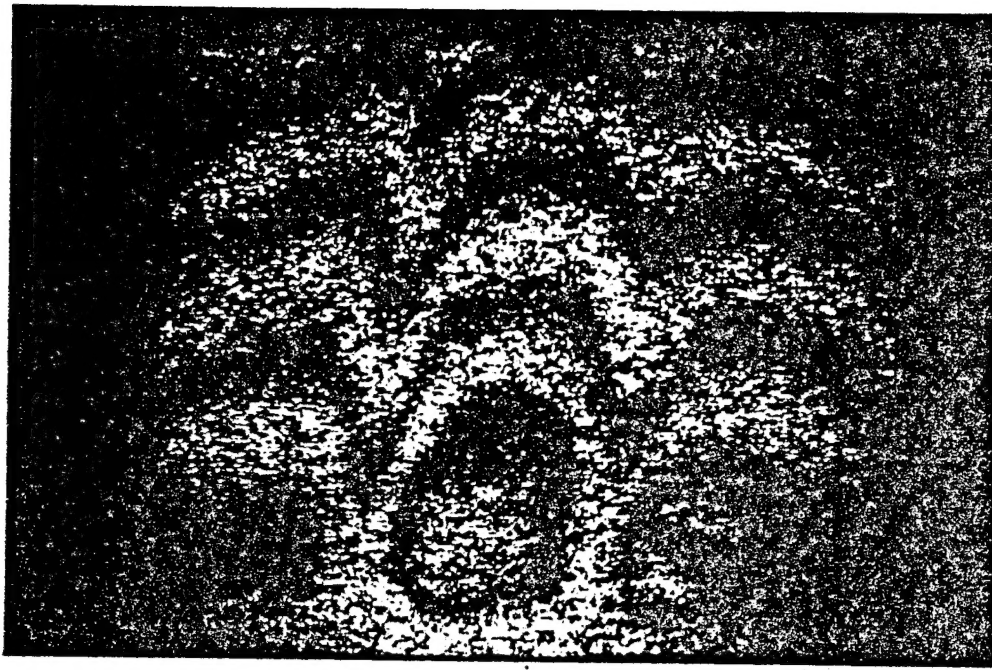


Figure 29 A laser speckle interferogram. The fringes illustrated result from the differential strain caused on the front face of a CFRP/Al bonded panel when a finger tip was placed momentarily on the rear face. (Sections 3.7 & 5.1.8)

Details of equipment and techniques described in Sections 3 and 5 are available from the manufacturers and development organisations listed below. Illustrations of the various techniques are presented where available.

Radiography (Sections 3.3 and 5.1.4)

Low voltage radiography :-

A.Q.D.  
Harefield  
Middlesex

Tel: Harefield 3757

and

Fulmer Research Institute Ltd.  
Stoke Poges, Slough  
Bucks. SL2 4 QD

Tel: 02816 2181

See figures 22 and 23

High voltage radiography :-

Balteau Sonatest Ltd.  
Old Wolverton Road  
Wolverton, Milton Keynes  
Bucks. MK12 5QQ

Tel: 0908 316345

See Figure 24

Ultrasonics (Sections 3.4 and 5.1.5)

Direct contact (Sections 3.4.2 and 5.1.5.1)

Inspection Instruments (NDT) Ltd.  
32 Duncan Terrace  
London N1 8BS

Tel: 01 278 6825

The Inspection Instruments model Ultrasonoscope Mk 10 was used in this project.

Soft tipped probes (Sections 3.4.3 and 5.1.5.2)

Air coupled resonance (Sections 3.4.4 and 5.1.5.3)

Roller probe/Discriminator (Sections 3.4.5 and 5.1.5.4)

The equipment used in these techniques was supplied by Balteau-Sonatest Limited, address as in "Radiography" above.

See Figures 25, 26

APPENDIX (continued)

103

### Fokker bond tester (Sections 3.4.6 and 5.1.5.5)

Manufacturer and distributor :-

Space Division  
Fokker V.F.W.B.V.  
Schipol-Oost  
Netherlands

Tel: 020 544 9111

U.K. Supplier :-

Bonded Structures Division  
Ciba Geigy U.K.  
Duxford  
Cambridge CB2 4QD

Tel: 0223 833141

### Acoustic Flow Detector (Sections 3.4.7 and 5.1.5.6)

## Apparatus manufactured by Inspection Instruments.

Address as in Direct Contact Ultrasonics above.

## Thermography (Sections 3.5 and 5.1.6)

The equipment used in this project was supplied by:-

E.M.I. Electronics Ltd.,  
Victoria Road  
Feltham Road  
Middlesex

Tel: 01 890 3600

See Figure 27

## Holographic Interferometry (Sections 3.6 and 5.1.7)

The facilities for this study were kindly made available by:-

Instrumentation & Trials Dept.  
Royal Aircraft Establishment  
Farnborough  
Hants. Tenn.

Tel: 0252 24461

See Figure 28

## Laser Speckle Interferometry (Sections 3.7 and 5.1-8)

This system is being developed by :-

Loughborough Consultants Ltd.  
Loughborough University of Technology  
Loughborough

Tel: 0509 30426

See Figure 29

10<sup>c</sup>

APPENDIX (continued)

Acoustic Emission Monitoring (Sections 3.8 and 5.1.9)

The two sets of equipment used in this project were manufactured and supplied by:

Dunegan Endevco  
Melbourn  
Royston  
Herts.

Tel: 0763 61311

and

Department of Electronic and Electrical Engineering  
University of Surrey  
Guildford  
Surrey.

Tel: 0483 71281